Universidade de Aveiro Departamento de Eletrónica, Telecomunicações e Informática
2018

Ricardo Simões de Simões

Esquemas de Pré-codificação e Equalização para Arquiteturas Híbridas Sub-Conectadas na Banda de Ondas Milimétricas

Pre-codification and Equalization Schemes for Hybrid Sub-Connected Architectures in the Millimeter Wave Band

Dissertação apresentada à Universidade de Aveiro para cumprimento dos requisitos necessários à obtenção do grau de Mestre em Engenharia Eletrónica e Telecomunicações, realizada sob a orientação científica do Professor Doutor Adão Silva (orientador), Professor Auxiliar do Departamento de Eletrónica, Telecomunicações e Informática da Universidade de Aveiro e do Doutor Daniel Castanheira (co-orientador), investigador no Instituto de Telecomunicações de Aveiro.

This work is supported by the European Regional Development Fund (FEDER), through the Competitiveness and Internationalization Operational Program (COMPETE 2020) of the Portugal 2020 framework, Regional OP Centro (CENTRO 2020), Regional OP Lisboa (LISBOA 14-20) and by FCT/MEC through national funds, under Project MASSIVE5G (AAC nº 02/SAICT/2017).

O júri / The jury

Presidente / President

Professor Doutor Atílio Manuel da Silva Gameiro
Professor Associado, Universidade de Aveiro

Vogais / Examiners committee

Professor Doutor Paulo Jorge Coelho Marques
Professor Adjunto, Instituto Politécnico de Castelo Branco

Professor Doutor Adão Paulo Soares da Silva
Professor Auxiliar, Universidade de Aveiro

Agradecimentos / Acknowledgments

Primeiramente gostaria de agradecer pela excelente orientação e coordenação ao Prof. Doutor Adão Silva (orientador) e ao Doutor Daniel Castanheira (co-orientador).

Em segundo, a toda a minha família pelo apoio incondicional e paciência, nomeadamente aos meus pais, irmão, avós, padrinhos e namorada.

A todos os professores pelos ensinamentos e paciência durante toda a minha formação.

A todos os amigos e colegas de curso com os quais fui trabalhando, aprendendo e partilhando saberes.

Por fim, mas não menos importante, agradeço a todos que, direta ou indiretamente, contribuíram para a realização desta dissertação.

Palavras-chave

MIMO Massivo, Banda das Ondas Milimétricas, Pré-codificador Analógico, Equalizador Híbrido Analógico/Digital Multi-utilizador, Arquiteturas Sub-conectadas.

Resumo

Nos últimos anos, a necessidade por elevadas taxas de transmissão de dados tem vindo a aumentar substancialmente uma vez que as comunicações móveis assumem cada vez mais um papel fundamental na sociedade atual. Por isso, o número de utilizadores que acedem a serviços e aplicações interativas tem vindo a aumentar. A próxima geração de comunicações móveis (5G) é esperada que seja lançada em 2020 e é projetada para fornecer elevadas taxas de transmissão de dados aos seus utilizadores. A comunicação na banda das ondas milimétricas e o MIMO massivo são duas tecnologias promissoras para alcançar os multi Gb/s para as comunicações móveis futuras, em particular o 5G. Conjugando essas duas tecnologias, permite-nos colocar um maior número de antenas no mesmo volume comparativamente às frequências atuais, aumentando assim a eficiência espectral. No entanto, quanto se tem um grande número de antenas, não é viável ter uma arquitetura totalmente digital devido às restrições de *hardware*. Por outro lado, não é viável ter um sistema que trabalhe apenas no domínio analógico. Assim sendo, é necessária uma arquitetura híbrida analógica-digital de modo a remover a complexidade geral do sistema. É esperado que os sistemas de comunicação baseados em ondas milimétricas sejam de banda larga, no entanto, a maioria dos trabalhos feitos para arquiteturas híbridas são focados em canais de banda estreita. Dois exemplos de soluções híbridas são as arquiteturas completamente conectada e sub-conectada. Na primeira, todas as cadeias RF estão ligadas a todas as antenas enquanto na arquitetura sub-conectada cada cadeia RF é ligada apenas a um grupo de antenas. Consequentemente, a arquitetura sub-conectada é mais interessante do ponto de vista prático devido à sua menor complexidade quando comparada à arquitetura completamente conectada.

Nesta dissertação é projetado um pré-codificador analógico de baixa complexidade no terminal móvel, combinado com um equalizador multiutilizador desenhado para uma arquitetura híbrida sub-conectada, implementado na estação base. O pré-codificador no transmissor assume um conhecimento parcial da informação do canal e, de modo a remover eficientemente a interferência multiutilizador, é proposta também uma arquitetura híbrida sub-conectada que minimiza a taxa média de erro. Os resultados de desempenho mostram que o esquema híbrido sub-conectado proposto está próximo da arquitetura híbrida completamente conectada. No entanto, devido ao grande número de conexões, a arquitetura híbrida completamente conectada é ligeiramente melhor que a arquitetura sub-conectada proposta à custa de uma maior complexidade. Assim sendo, o pré-codificador analógico e o equalizador sub-conectado híbrido proposto são mais viáveis para aplicações práticas devido ao compromisso entre o desempenho e a complexidade.

Keywords massive MIMO, millimeter wave communications, analog precoder, hybrid analog/digital multi-user equalizer, sub-connected architectures.

Abstract

In the last years, the demand for high data rates increased substantially and the mobile communications are currently a necessity for our society. Thus, the number of users to access interactive services and applications has increased. The next generation of wireless communications (5G) is expected to be released in 2020 and it is projected to provide extremely high data rates for the users. The millimeter wave communications band and the massive MIMO are two promising keys technologies to achieve the multi Gbps for the future generations of mobile communications, in particular the 5G. The conjugation of these two technologies, allows packing a large number of antennas in the same volume than in the current frequencies and increase the spectral efficiency. However, when we have a large number of antennas, it is not reasonable to have a fully digital architecture due to the hardware constrains. On the other hand, it is not feasible to have a system that works only in the analog domain by employing a full analog beamforming since the performance is poor. Therefore, it is required a design of hybrid analog/digital architectures to reduce the complexity and achieve a good performance. Fully connected and sub-connected schemes are two examples of hybrid architectures. In the fully connected one, all RF chain connect to all antenna elements while in the sub-connected architecture, each RF chain is connected to a group of antennas. Consequently, the sub-connected architecture is more attractive due to the low complexity when compared to the fully connected one. Also, it is expected that millimeter waves be wideband, however, most of the works developed in last years for hybrid architectures are mainly focused in narrowband channels.

Therefore, in this dissertation it is designed a low complex analog precoder at the user terminals and a hybrid analog-digital multi-user linear equalizer for broadband sub-connected millimeter wave massive MIMO at the base station. The analog precoder at the transmitter considers a quantized version of the average angle of departure of each cluster for its computation. In order to remove the multi-user interference, it is considered a hybrid sub-connected approach that minimizes the bit error rate (BER). The performance results show that the proposed hybrid sub-connected scheme is close to the hybrid full-connected design. However, due to the large number of connections, the full-connected scheme is slightly better than the proposed sub-connected scheme but with higher complexity. Therefore, the proposed analog precoder and hybrid sub-connected equalizer are more feasible to practical applications due to the good trade-off between performance and complexity.

Contents

List of Figures

List of Tables

Acronyms

1G First Generation

2G Second Generation

3G Third Generation

3GPP 3rd Generation Partnership Project

4G Fourth Generation

5G Fifth Generation

5GNow 5th Generation Non-Orthogonal Waveforms for Asynchronous Signalling

5GPPP 5G Infrastructure Public Private Partnership

ADC Analog-to-Digital Converter

AGC Automatic Gain Control

AMPS Advanced Mobile Phone Systems

AoD Angles of Departure

AS Antenna Selection

AWGN Additive White Gaussian Noise

BD Block Diagonalization

BER Bit Error Rate

BF Beamforming

BS Base Station

CDMA Code Division Multiple Access

CDMA2000 Code Division Multiple Access 2000

CE-OFDM Constant Envelope OFDM

CP Cyclic Prefix

CSI Channel State Information

DAC Digital-to-Analog Converter

D-AMPS Digital Advanced Mobile Phone System

D-BLAST Diagonal Bell Labs Space-Time Architecture

DFT Discrete Fourier Transform

DL Downlink

DoF Degree of Freedom

EDGE Enhanced Data Rates for GSM Evolution

EE Energy Efficiency

EGC Equal Gain Combining

EHF Extremely High Frequency

ELF Extremely Low Frequency

EU European Union

FDD Frequency Division Duplex

FDMA Frequency Division Multiple Access

GPRS General Packet Radio Service

GS Gram-Schmidt

GSM Global System for Mobile Communications

HF High Frequency

HSPA High Speed Packet Access

ICI Inter Carrier Interference

IDFT Inverse Discrete Fourier Transform

IEEE Institute of Electrical and Electronics Engineers

IMD-HBF Iterative Matrix Decomposition Hybrid Beamforming

IoT Internet of Things

ISI Inter-Symbol Interference

JTACS Japanese TACS

LF Low Frequency

LoS Line of Sight

LSAS Large Scale Antenna Systems

LSTC Layered Space-Time Codes

LTE Long Term Evolution

MA Multiple Access

MAA Massive Antenna Array

MC-CDMA Multi-Carrier Code-Division Multiple Access

METIS Mobile and Wireless Communications Enablers for Twenty-twenty Information Society

MF Medium Frequency

MIMO Multiple-Input Multiple-Output

MISO Multiple-Input Single-Output

mMIMO Massive Multiple-Input Multiple-Output

MMS Multi-Media Messages

MMSEC Minimum Mean Square Error Combining

mmW Millimeter Wave

MRC Maximal Ratio Combining

MSE Mean-Squared Error

MU-MIMO Multi-User MIMO

NAMPS Narrowband AMPS

NLoS Non-Line of Sight

NMT Nordic Mobile Telephone

NTACS Narrowband TACS

NTT Nippon Telegraph and Telephone

OFDM Orthogonal Frequency Division Multiplexing

OFDMA Orthogonal Frequency Division Multiple Access

PA Power Amplifier

PAPR Peak to Average Power Ratio

PDC Pacific Digital Cellular

PM Phase Modulate

PSD Power Spectral Density

QAM Quadrature Amplitude Modulation

QoS Quality of Service

QPSK Quadrature Phase Shift Keying

RF Radio Frequency

SC Selection Combining

SC-FDMA Single Carrier Frequency Division Multiple Access

SE Spectral Efficiency

SFBC Space Frequency Block Coding

SHF Super High Frequency

SIC Successive Interference Cancellation

SIMO Single-Input Multiple-Output

SIR Signal-To-Interference Ratio

SISO Single-Input Single-Output

SM Spatial Modulation

SMS Short Message Service

SNR Signal-To-Noise Ratio

STBC Space Time Block Coding

STTC Space-Time Trellis Code

SU-MIMO Single-User MIMO

SVD Singular Value Decomposition

TACS Total Access Communications Systems

TDD Time Division Duplex

TDMA Time Division Multiple Access

TD-SCDMA Time Division Synchronous CDMA

UHF Ultra High Frequency

UL Uplink

ULA Uniform Linear Array

UMTS Universal Mobile Telecommunication System

UT User Terminal

V-BLAST Vertical Bell Labs Space-Time Architecture

VHF Very High Frequency

VLF Very Low Frequency

W-CDMA Wideband CDMA

WF Water Filling

WiMAX World Wide Interoperability for Microwave Access

ZFC Zero Forcing Combining

1. Introduction

In this chapter we start by presenting the historical evolution of the telecommunications systems since 150 years ago toward the most recent generation of the telecommunications systems 5G, in order to be easier to understand the proposed work. Then, we will give an overview, motivations and contents of this dissertation. At last, the structure of the dissertation is shown followed by the used notation.

1.1 Evolution of Cellular Communications Systems: 1G to 4G

Currently, people have the necessity to communicate each other not only for voice calls or Short message Service (SMS) but also, to use the internet access to read news, make business, can be helpful in case of an emergency, use the GPS tracking system to find people way, and also, people can share information, photographs with other people, and very others functionalities of communication tools. However, it was not always possible to have these benefits for all the users.

The history of the mobile communications started about 150 years ago, in 1865, with the Maxwell equations developed by James Maxwell. In 1887, Heinrich Hertz create the oscillator and radios waves and, with these radio waves, Guglielmo Marconi in 1895 develop a transmitter with radiotelegraph signals that have a long wavelength and a high power transmission. In 1907, Lee De Forest create the vacuum tube that allow to transmit signals at a higher frequency, until 1.5 MHz, however this higher frequency still small. The analog radio communications emerged in 1907 with the voice transmission and eight years later it was made the first wireless voice transmission in New York. In the early 1920s, happen a high increase the radio communications systems for broadband where the Titanic disaster had a great impact. With the arrival of the Second World War, the radio systems become essential. Pierce and Kompfner do a transatlantic communications trough satellite in 1959. In 1947 emerged the cellular network concept where basically a base station (BS) covers a given transmission area called cell. This cellular concept has mainly two key aspects that are the division of geographical space in cells that allows the reuse of resources in sufficiently apart cells and the handover that allows the continuity in the communication. With this structure it is possible

to define some advantages such as the possibility to reuse the spectrum, needs a lower transmission power, more robust and it is possible to adapt each base station to the local where is placed. Nonetheless, this technology has some limitations comparatively to cable connections, such as the lower velocity transmission, the requirement of infrastructures to connect the BSs and the intercell interference [1]. After this concept of cellular network, arrive the new paradigm of generations used until nowadays. Figure 1.1 shows the evolution of the mobile communications since the first generation until the fourth generation that are described below.

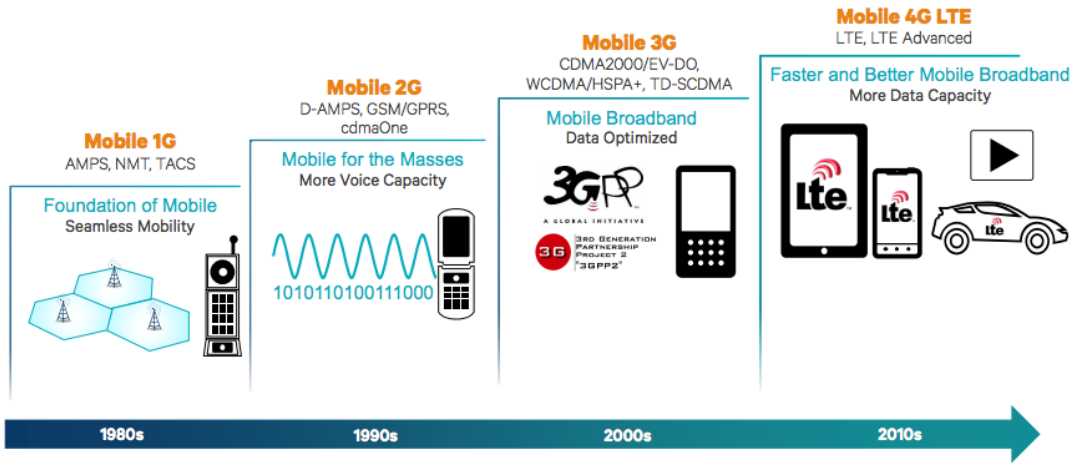

Figure 1.1: Evolution of the Mobile Communication Systems [2].

The first commercial generation (1G) of cellular systems born in the 80s and was characterized by the use of analog signals and the only service provided was voice with poor quality. This first generation has been introduced in Japan by Nippon Telegraph and Telephone (NTT), in U.S. by the Advanced Mobile Phone Systems (AMPS) and in Europe for the Nordic Mobile Telephone (NMT). Some other systems are developed as well Total Access Communications Systems (TACS) and extended TACS that are similar to AMPS and appear in U.K. In finals of the 80s, to improve capacity, appear in North America the narrowband AMPS (NAMPS) and appear in Japan the Japanese TACS (JTACS) and the narrowband TACS (NTACS) systems. All of these presented systems are incompatible with each other due to the way that they are developed in each country [3][4].

Second generation (2G) systems emerged in 1991 and brought the digital era with more coverage and capacity than the last version. Comparatively to 1G, in 2G it was possible to send SMS, multi-media messages (MMS) and this second generation brought the first data services. In this generation, the following techniques are deployed: Global System for Mobile Communications (GSM) in Europe, Digital Advanced Mobile Phone System (D-AMPS) IS-54 in the U.S.A., Code Division Multiple Access (CDMA) IS-95 by Qualcomm in U.S.A. and Pacific Digital Cellular (PDC) in Japan [4][5].

The GSM system is the most dominant system used and nowadays is implanted in more than 200 countries in worldwide. This system support transfer data rates up to 22.8 kb/s [6] and operates in the 900 MHz / 1800 MHz and 850 MHz / 1900 MHz band, depending on the part of the world considered as seen in Figure 1.2 [7]. This system uses two multiple access (MA) technologies to accommodate multiple users on the same frequency: Frequency Division Multiple Access (FDMA) and Time Division Multiple Access (TDMA) where FDMA divides the spectrum in sub bands and TDMA divides the partition time in disjoints time slots [1].

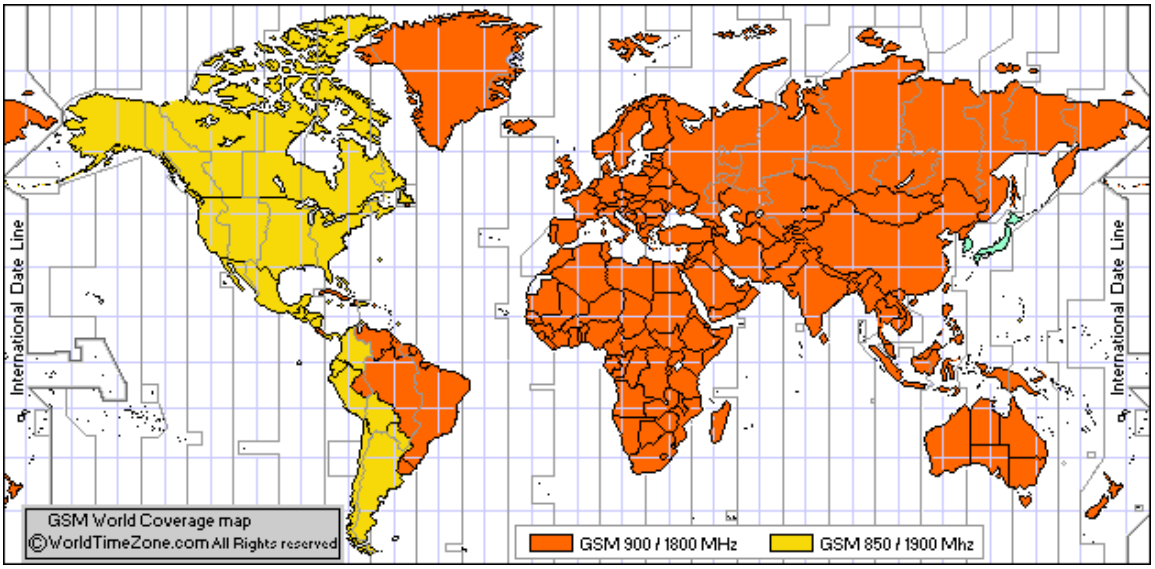

Figure 1.2: GSM Bands Information by Country Currently [7].

Toward third generation (3G), General Packet Radio Service (GPRS) has been created, in 2001, to upgrade GSM with the main objective to allow a higher data rate via packet switching. With this improvement, theoretically, the data rates increase until 171.2 kb/s when is used a perfect channel. In practice, the data rates vary between 10 to 115 kb/s with an average of 40 kb/s. Another improvement system of the GSM is the Enhanced Data Rates for GSM Evolution (EDGE) with data rates between 8 and 60 kb/s [4].

With the increase of the mobile data services demand, emerged the necessity to develop another generation of mobile communications. As a result, in 2000 was introduced the third generation with the following main objectives: achieve high data rates until 2 Mb/s, low latency, better quality of service (QoS), simplicity and scalability [8]. Nonetheless, 3G don't repeat the success of the previous generation 2G. Initially, two services have been created that accomplish that requirements: Universal Mobile Telecommunication System (UMTS) in Europe and Japan and Code Division Multiple Access 2000 (CDMA2000) in U.S.A. UMTS support both Time Division Duplex (TDD) and Frequency Division Duplex (FDD) and include two standards: Wideband CDMA (W-CDMA) and

High Speed Packet Access (HSPA). Another approach is Time Division Synchronous CDMA (TD-SCDMA) developed also in Europe [9]. The 3rd Generation Partnership Project (3GPP) is a corporation of 6 regional standards groups with the aim of control the evolution and migration of GSM systems, 3G systems and LTE systems presented below [1]. The World Wide Interoperability for Microwave Access (WiMAX) forum has been created based on an Institute of Electrical and Electronics Engineers (IEEE) 802.16 standards and it is an alternative to the transmissions with cable once it has a range of 40 to 50 km [9]. An example of WiMAX technology from point-to-point and point-to-multipoint to portable and static cellular are presented in Figure 1.3.

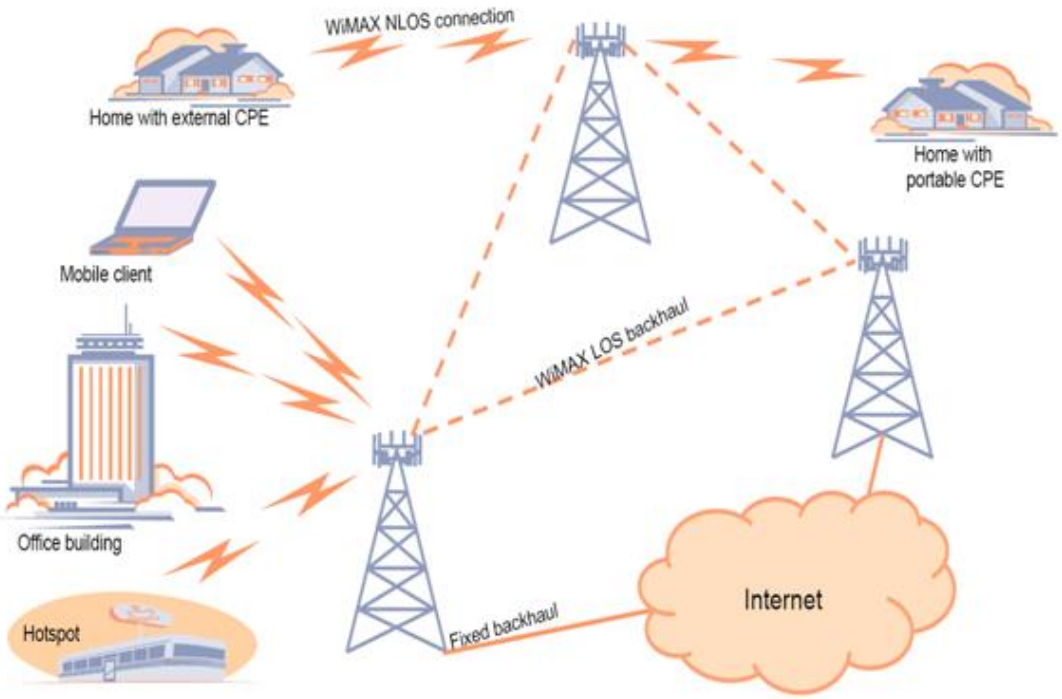

Figure 1.3: WiMAX Wireless Telecommunication Protocol [10].

The successor of 3G is the fourth generation (4G) that appeared in 2009 being marketed as Long Term Evolution (LTE) with the aim of give more data capacity with data rates more than 100 Mb/s and a low latency. This generation did not bring as principal objective the increase of the bit rate but the increase of the system capacity. The speed of the peak rate increase over the years where in 2009 was 50 Mb/s, in 2010 was 150 Mb/s and in 2015 was 1000 Mb/s [1]. Nowadays, 4G LTE represents a generation in expansion that has 2.8 Billion of connections, more 0.1 Billion of connection than GSM that is the second system most used [11].

Contrary to WiMAX, that uses Orthogonal Frequency Division Multiple Access (OFDMA) at both downlink (DL) and uplink (UL), LTE uses OFDMA at DL and Single Carrier Frequency Division Multiple Access (SC-FDMA) at UL [8]. OFDMA and SC-FDMA are discussed in Chapter

2 where we see that SC-FDMA is in general equal to the OFDMA but with a lower Peak to Average Power Ratio (PAPR) [1].

Comparing for example W-CDMA with LTE, in W-CDMA the radio frequency (RF) specifications for FDD and TDD are different, and with LTE it is possible to operate with the same specifications the two different duplex modes, FDD and TDD [12]. For the FDD, the signals of UL and DL transmissions are separated by different frequencies and for the TDD, the signals of UL and DL transmissions operate at the same band, but in separated time domain [13]. A comparison of these two modes are represented in Figure 1.4.

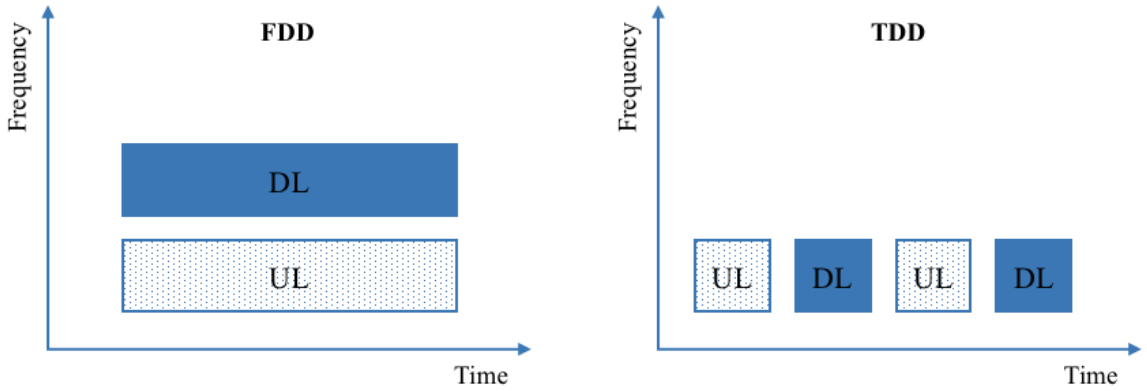

Figure 1.4: FDD versus TDD.

In order to develop the LTE, the 3GPP started looking to the future and built the LTE Advanced, specified as LTE Release 10 and beyond with a peak data rate of 1 Gb/s for DL and 500 Mb/s for UL. Some features are added to LTE Advanced such as: carrier aggregation, improvement of DL and UL multiple antenna transmission, relaying and support for heterogeneous network [12]. Concluding, the LTE and LTE Advanced are two keys for the development of the future mobile telecommunications systems. The actual global statistics show that LTE was a big weight (32.5%) in the worldwide connection market, as show in Figure 1.5 and the perspective is to increase their influence, like in the last few years, up to approximately 2020, when the next generation 5G will start expanding [11].

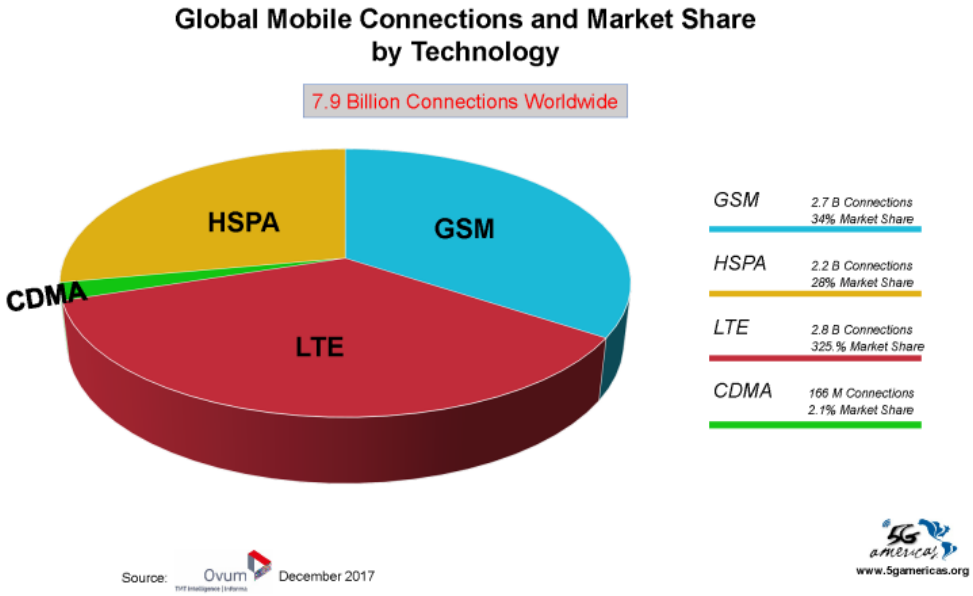

Figure 1.5: Global Statistics of Mobile Systems [11].

1.2 5G Systems

The number of wireless network users are increasing day by day due to the services such as video, music, social networking, gaming and other interactive applications. As a result, the mobile data traffic has increased over the years and is required a new mobile system. Currently, wireless multimedia systems require dozens of Mb/s to have a reasonable quality of service (QoS). The next fifth generation (5G) it is designed to interconnect billions of objects and can be a suitable candidate to respond at this demand of high capacity and data rates [14][15]. An example of this demand for data rates and capacity is sport events with many people that share their experience instantly with video or images. It is expected that 5G should be available by 2020 and will achieve a minimum data rate of 1Gb/s, 5Gb/s for high mobility users and 50 Gb/s for pedestrian users [16][17]. These rise of number connections devices like smartphones, notebooks, tablets, smart TV's, etc., make a high consumption on energy that has a great impact in CO2 in the planet as see in [18]. The 5G is a new cellular network concept comparatively to the previous versions of mobile systems and due to this, are necessary to apply new technologies. Therefore, some key technologies for the 5G are being developed such as millimeter wave (mmW) systems, Massive Multiple-Input Multiple-Output (mMIMO), Spatial Modulation (SM), Mobile Femtocell (MF) and separating of indoor-outdoor scenarios [19]. In this master dissertation we mainly focus in the mmW and mMIMO systems. Numerous benefits will come with 5G, however this this new technology includes some challenges that need to be solved.

The frequency spectrum used nowadays by the mobile communications is currently saturated, so it is necessary to find another spectrum band for mobile applications. In this context, the mmW band, with its huge available bandwidth [20], with wavelengths from 1 to 10 millimeters [21], can be an interesting solution. The mMIMO systems, that includes both transmitter and receiver sides, are another key technology for the future generation 5G to support more users, achieve higher capacity and data rates, obtain a better Energy Efficiency (EE) and a Spectral Efficiency (SE) gain when compared to the previous generation of mobile telecommunications, 4G-LTE [22][23]. These two technologies, mMIMO and mmW, are discussed in Chapter 3 and Chapter 4, respectively. Nonetheless, with the application of these two key technologies, it is necessary to develop an architecture that reduces the overall complexity and the costs of the system. So, hybrid architectures that work in both analog and digital domains, have been designed to accomplish these 5G requirements and simultaneously maintain the EE design.

In Figure 1.6 is depicted the main concepts of 5G such as a bigger autonomy of the mobile devices, wider coverage, high data rates and mobility (up to 500 km/h), low latency (below 1 ms), etc.

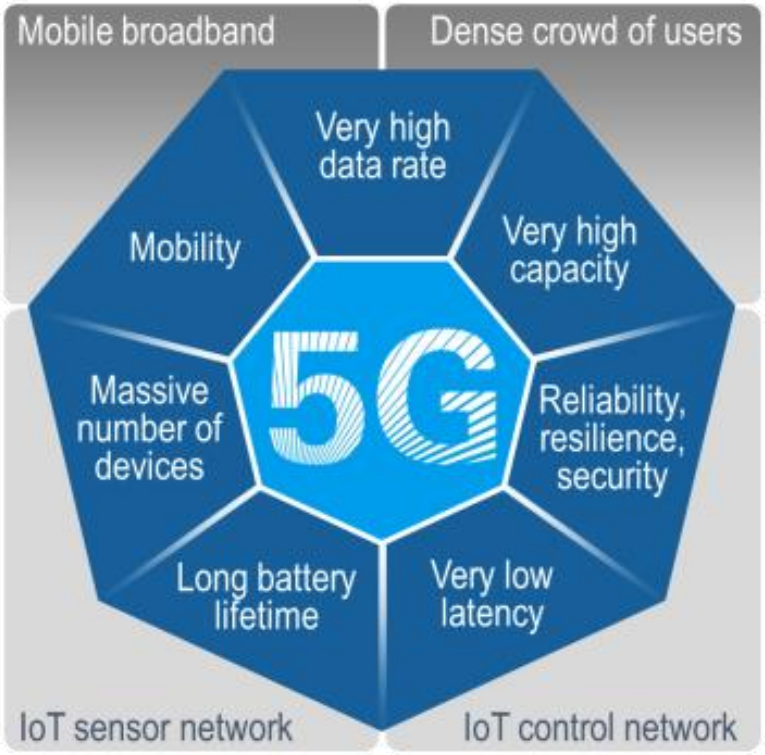

Figure 1.6: 5G Concepts [24].

Some projects supported by European Union (EU) are being developed in the last few years such as: the 5th Generation Non-Orthogonal Waveforms for Asynchronous Signalling (5GNow), Mobile

and Wireless Communications Enablers for Twenty-twenty Information Society (METIS), Horizon 2020 and 5G Infrastructure Public Private Partnership (5GPPP) [24].

In Figure 1.7 we can see the possible evolution of the systems since 2G until 5G for the next years. 2G and 3G will lose their influence and, as seen before, the 4G-LTE will have a big weight in the next years in the market of mobile telecommunications. Meanwhile, the 5G will have a fast adhesion after its release in 2020 [25].

Concluding, the 2G is design for voice, 3G for data, 4G for large data stream applications such as music and video and 5G needs to be more efficient to handle not necessarily with a huge amount of data but with a huge number of connected devices.

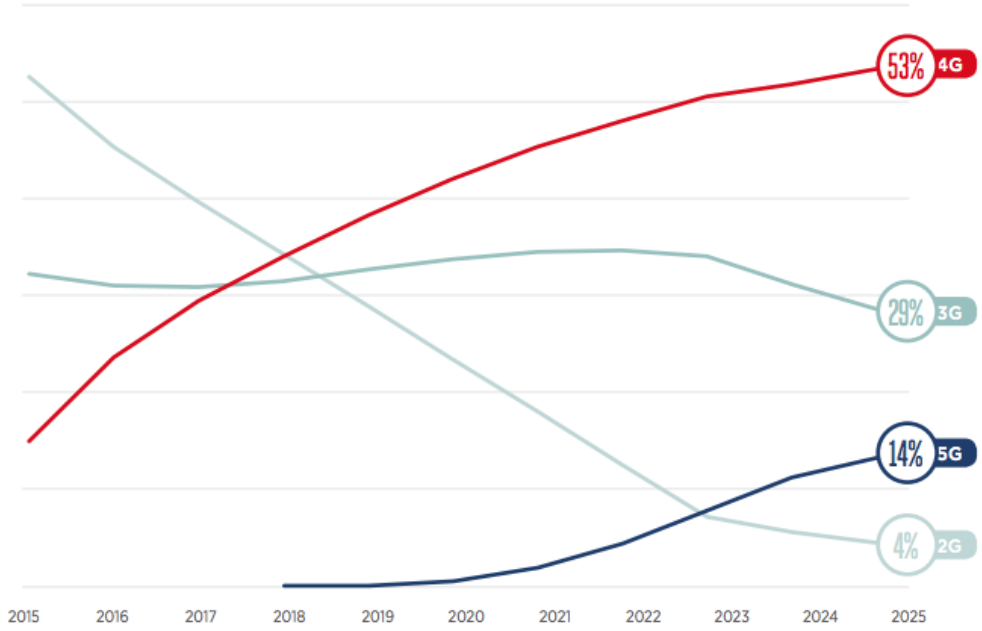

Figure 1.7: Global Mobile Adoption by Technology [25].

1.3 Overview and Motivations

The mobile data traffic has increased over the years and the next generation (5G) arise to respond at this demand for higher data rates [14][15]. The frequency spectrum used by the mobile communications is currently saturated, so it is necessary to find another spectrum band for mobile applications. In this context the mmW band, with its huge available bandwidth, can be an interesting solution. Other key technology for future generation communications is mMIMO, allowing to achieve higher data rates and EE [22].

The combination of mmW with mMIMO systems enables the use of a large antenna array at the BS and in the user terminal (UT) due the mmW has a smaller wavelength than the frequency bands

used by the current cellular systems [26]. Massive MIMO beyond of improving EE, can also improve the SE of the mobile communications systems [23]. SE is independent of the number of antennas employed at the BS and grows with the increase of the number of RF chains as discussed in [27]. When we have a large number of antennas it is not feasible to have one dedicated RF chain per antenna and consequently, a fully digital beamforming (BF) architecture is not realistic due to the higher costs and power consumption [23]. On the other hand, a system that works in the analog domain employing a full analog BF is not feasible due to the availability of only quantized phase shifters and the constraints on the amplitudes of these analog phase shifters [28]. One possible solution to overcome these limitations is to consider hybrid digital and analog BF where the signal is processed at both analog and digital levels.

Some fully connected hybrid beamforming architectures for narrowband single-user systems were discussed in [29]-[31]. The work presented in [29] considered a transmit precoding and a receiver combining scheme for mmW mMIMO. In this work the spatial structure of the mmW channels is exploited to design the precoding/combining schemes as a sparse reconstruction problem. In [30] was proposed an iterative turbo-like algorithm that finds the near-optimal pair of analog precoder/combiner. A matrix decomposition method that can convert any existing precoder/combining design for the full digital scheme into an analog-digital precoder/combining for the hybrid architecture is addressed in [31]. Approaches for narrowband multi-user systems have been also considered in [32]-[36]. A limited feedback hybrid analog-digital precoding/combining scheme for multi-user systems was addressed in [32]. A heuristic hybrid BF is addressed in [33], where the proposed design can achieve a performance close to the fully digital BF with low-resolution phase shifters. A hybrid analog-digital precoding/combining multi-user system based on the mean-squared error (MSE) was proposed in [34]. The authors of [35] designed an iterative hybrid analog-digital equalizer that efficiently removes the multi-user interferences. In [36], was proposed an iterative precoder and combiner design by exploiting the duality of the uplink and downlink multi-user MIMO channels. The hybrid architecture for either single or multi-user the mmW mMIMO broadband systems is considered in [37][38]. Precoding solutions with codebook design for limited feedback spatial multiplexing in single user broadband mmW were developed in [37]. A hybrid multi-user linear equalizer for the uplink of mmW massive MIMO SC-FDMA systems was proposed in [38].

The previous works have mainly focused on fully connected architectures. However, sub-connected architectures, where each RF chain is only connected to a subset of the available antennas, is more suited for practical applications due to its lower complexity. Narrowband fixed sub-connected hybrid architectures for single user systems were addressed in [39][40]. The authors of [39] proposed a two-layer optimization method jointly exploiting the interference alignment and

fractional programming principles. First, the analog precoder and combiner are optimized via the alternating-direction optimization method and then the precoder and combiner are optimized based on an effective MIMO channel coefficient. In [40] two analog precoder schemes for high and low signal-to-noise ratio (SNR) condition were developed. For multi-user sub-connected narrowband architecture, some approaches have been also proposed in [41]-[44]. In [41], the total achievable rate optimization problem with nonconvex constraints is decomposed into a series of sub-rate optimization problems for each subantenna array, and then it was proposed a successive interference cancelation (SIC) based hybrid precoder. A low-complexity hybrid precoding and combining design was discussed in [42], where it is performed a virtual path to maximize the channel gain and then, based on the effective channel, is applied a zero-forcing precoding to manage the interference. The scheme proposed in [43] efficiently control the multi-user interference by sequentially computing the analog part of the equalizer over the RF chains, using a dictionary obtained from the array response vectors. In [44], the Gram-Schmidt (GS) based antenna selection (AS) algorithm was used to obtain an appropriate antenna subset for the overlapped, interlaced and dynamically architectures. Recently, solutions for broadband mmW multi-user downlink massive MIMO-OFDM systems were proposed in [45]. A unified heuristic design for both fully connected and sub-connected hybrid structures was developed by maximizing the overall spectral efficiency.

The previous works considered mainly a sub-connected hybrid architecture for single and multi-user narrowband systems. Therefore, in this dissertation we design and evaluate an efficient hybrid multi-user equalizer combined with a pure analog precoder for sub-connected uplink mmW massive MIMO SC-FDMA systems. We consider single RF UTs employing a low complexity, yet efficient, analog precoder approach based on the knowledge of partial channel state information (CSI), i.e., only a quantized version of the average angle of departure (AoD) of each cluster is considered. The hybrid multi-user linear equalizer employed at the BS is optimized by using the BER as a metric over all the subcarriers. We assume that the digital part of the equalizer is computed on a per subcarrier basis while the analog part is constant over the subcarriers. The analog domain hardware constraints considerably increase the complexity of the corresponding optimization problem. To simplify it, the merit function is first upper bounded, and by leveraging the specific properties of the resulting problem, we show that the analog equalizer may be computed iteratively over the RF chains by assigning the users in an interleaved fashion to the RF chains, using a dictionary built from the array response vectors. The results show that the performance penalty of the sub-connected multi-user equalizer approach to the fully connected counterpart decreases as the number of RF chains increases.

1.4 Contributions

The main contributions of the research performed in this dissertation are: the study of two promising techniques for future mobile communications (millimeter waves and massive MIMO) and the development of an analog precoder and a sub-connected hybrid analog-digital multi-user equalizer that has originated the following article:

Ricardo Simões, Daniel Castanheira, Adão Silva and Atílio Gameiro, "Multi-User Linear Equalizer and Precoder Scheme for Hybrid Sub-connected Broadband Millimeter Wave Systems", submitted to *Physical Communications*, Elsevier, June 2018.

1.5 Structure

This dissertation is organized as follows: In this first Chapter, we made an overview of the historical evolution of the mobile communications and the corresponding technologies adopted until the next generation of mobile communications (5G). After it was described the overview and motivations followed by the notations used.

In Chapter 2, we first make a description of the single and multi-carrier techniques and after it is discussed some common multiple access techniques. After the OFDM, OFDMA and SC-FDMA systems followed by a promising modulation technique, CE-OFDMA, are presented.

In Chapter 3, we first introduce the concept of diversity and multiple antennas systems and then, we presented the spatial diversity and multiplexing techniques. After that it is described the concept of massive MIMO and its opportunities and limitations.

In Chapter 4, we present the millimeter waves systems with their respective advantages and disadvantages. Lastly, the conjugation of massive MIMO and millimeter waves are discussed as well as hybrid and low-resolution ADCs architectures.

In Chapter 5, we describe the overall system proposed. We start by describing the transmitter, after the channel and the receiver system model. Then, the analog precoder employed at each UT is described. After, the sub-connected hybrid analog-digital multi-user equalizer is derived. In the end, the main performance results are presented.

Finally, in Chapter 6, we conclude this dissertation and provide some possible guidelines for future research.

1.6 Notations

The following notation is used in this dissertation: boldface uppercase letters, boldface lowercase letters and italic letters denote matrices, vectors and scalars, respectively. The operations $(.)^T$, $(.)^H$, $(.)^*$ and $tr(.)$ represent the transpose, the Hermitian, the conjugate and the trace of a matrix, respectively. The operator diag($\mathbf{A}$) corresponds to the diagonal entries of matrix $\mathbf{A}$. The identity matrix of size $N \times N$ is denoted $\mathbf{I}_N$. $\mathbb{E}[.]$ and $\{\alpha_l\}_{l=1}^{L}$ represents the expectation operator and an L length sequence, respectively. $[\mathbf{A}]_{n,l}$ represents the entry of the *n*th row and *l*th column of the matrix $\mathbf{A}$. The indices, t, k and u represent the time domain, subcarrier in frequency domain, and UT, respectively.

2. Modulation and Multiple Access in Cellular Networks

In this Chapter is introduced some modulation schemes and multiple access techniques that are considered in cellular systems. Basically, the process called modulation consists in the addition of the information transmitted to the electromagnetic waves. In the receiver, we have the opposite process that is demodulation. This bring us some advantages such as more flexibility, more electromagnetic energy efficiency, more bandwidth available and more efficiency in the utilization of the transmission channel. So, we will give an overview of the OFDM that can be easily extended to multiple access OFDMA and SC-FDMA modulations. Finally, we present an example of new modulation that can be used in future systems, such as, constant envelop OFDM (CE-OFDM).

2.1 Single and Multi-Carrier Approaches

The single carrier approach, depicted in Figure 2.1, means that information is modulated only to one single carrier and, for high data rates solutions, needs a complex equalizer to reduce the intersymbol interference (ISI). With the FDMA scheme, it is possible to have different users using different carriers or subcarriers as represented in Figure 2.2. Nonetheless, to avoid inter carrier interference (ICI), the FDMA scheme needs a guard band that wastes a lot of spectrum. In order to solve the problem described above, for broadband communications, is the use parallel transmission. In a multicarrier approach with N subcarriers, we have B/N Hz of bandwidth per sub-carrier, where B is the total bandwidth. An example of multi-carrier is showed in Figure 2.3, where the subcarriers are overlapped and have a better spectral efficiency. However, it is necessary to ensure that sub-carriers do not interfere with each other even with the spectrum overlapped. A solution is achieved with the orthogonality between the different transmissions addressed below with the Orthogonal Frequency Division Multiplexing (OFDM) principle [46].

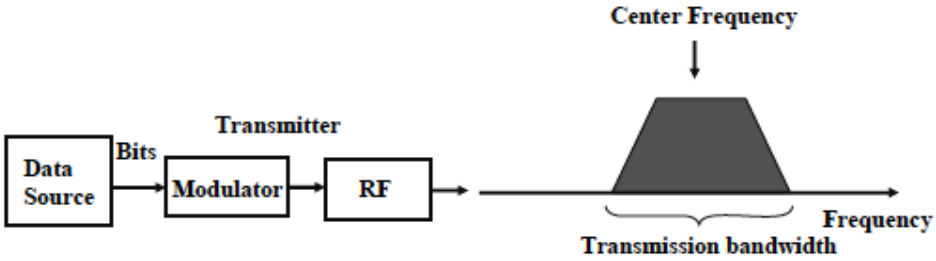

Figure 2.1: Single carrier scheme [46].

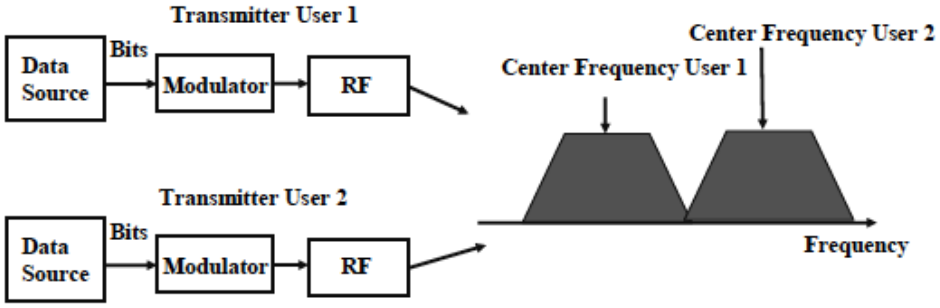

Figure 2.2: FDMA scheme [46].

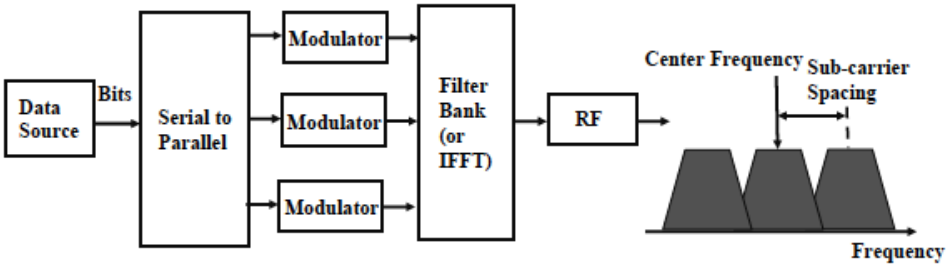

Figure 2.3: Multicarrier scheme [46].

2.2 Frequency Multiplexing

The frequency division multiplexing is a principle where the spectrum allocated is divided in smaller slots of bands like represented in Figure 2.4. So, a determinate channel uses a given band of the corresponding spectrum. FDMA is an example of a method that uses frequency multiplexing.

This type of multiplexing has some advantages such as:

- Dynamic coordination not required
- Adapted to work with analog signals
- No ISI due to narrowband channels
- Moderate complexity

However, has some disadvantages like the waste of bandwidth with asymmetric traffic, difficult to allocate several channels at the same user and needs a guard band between the bands in the spectrum.

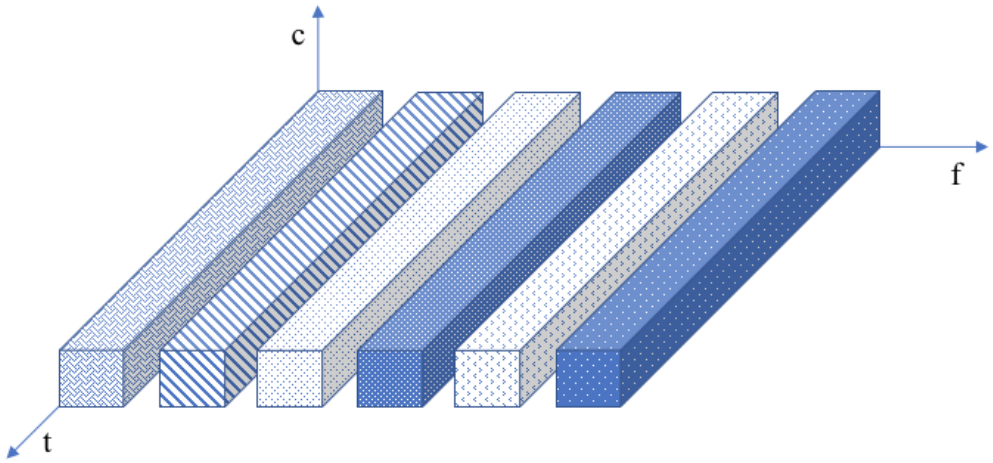

Figure 2.4: Frequency Division Multiplexing.

2.3 Time Multiplexing

Time division multiplexing is a digital technology that has the principle which a channel uses all the spectrum during a given time, that is, the time is divided in time slots for the different channel as represented in Figure 2.5. In this case, the time is used to separate the different data streams. TDMA is an example of the time multiplexing technique that has been used in 2G.

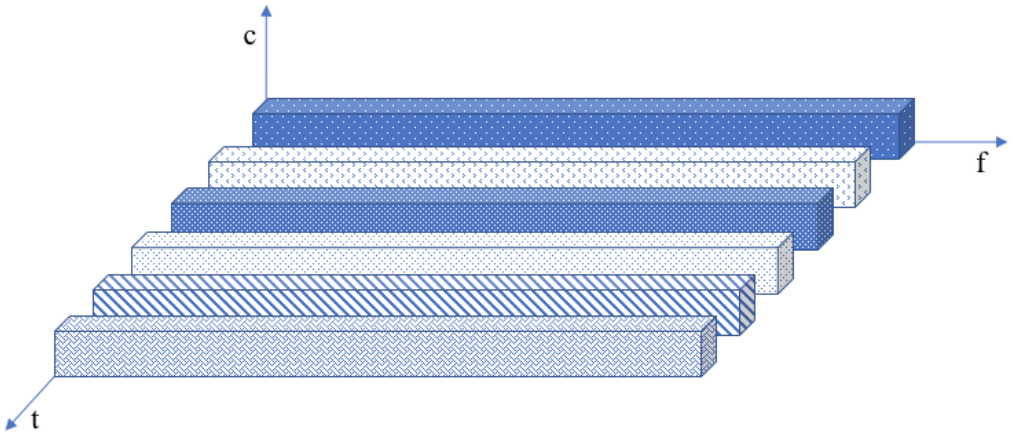

Figure 2.5: Time Division Multiplexing.

With this technique, the efficiency is typically higher than in frequency multiplexing, it is possible to have a single carrier at any time and is easier to allocate multiple channels for a given user.

Nonetheless, it is necessary a synchronization and need ISI elimination which leads us to complex equalizers.

2.4 Frequency and Time Multiplexing

Conjugating the time and frequency multiplexing, we obtain the method depicted in Figure 2.6 where a channel uses, at a given band, a time interval. This bring a protection against frequency selective interference but still needs a precise synchronization. At the TDMA seen before, if add frequency hopping, we obtain an example of frequency and time multiplexing.

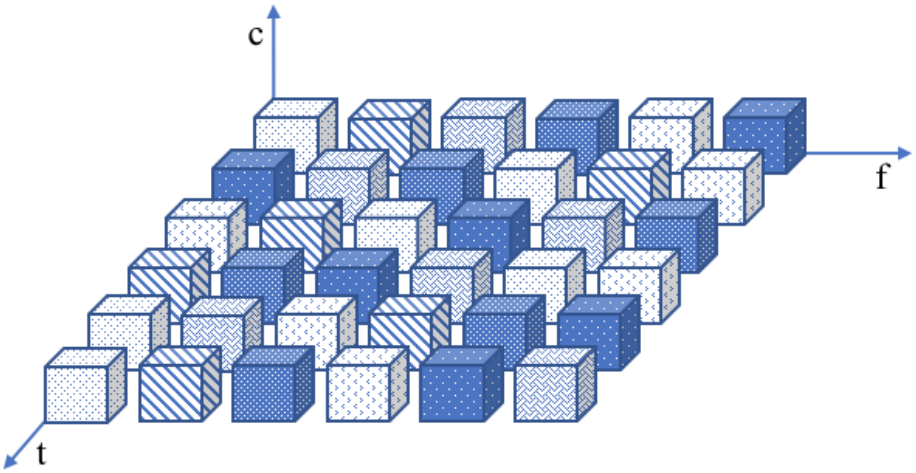

Figure 2.6: Time and Frequency Division Multiplexing.

2.5 Code Multiplexing

In the code multiplexing, represented in Figure 2.7, all channels use all spectrum at the same time and have a code that allows the separation in the code domain. With this technique it is possible to choose of simultaneous voice, data, FAX and SMS with a lower capital cost, however, with a more complex receiver. CDMA is an example of code multiplexing and has been used in 3G. With the increase of users, the performance of CDMA decreases smoothly, contrary to FDMA and TDMA, where the system works well until all slots, in frequency or time, are fulfilled.

The main advantages of this principle are:

- Simplification of the coordination requirements (time or frequency)
- Good protection against interference
- No strict limit on the number of users

- Possible to allocate multiple channels to a single user

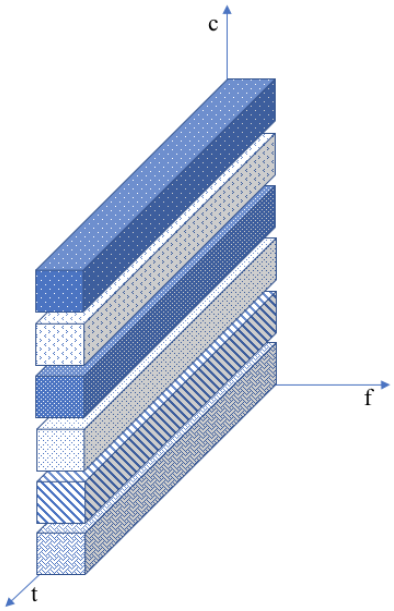

Figure 2.7: Code Division Multiplexing.

2.6 Orthogonal Frequency Division Multiplexing

OFDM is an extension of the concept of modulation in multi carriers that allow us to separate the symbols transmitted in a set of frequency subcarriers. The carries of OFDM are orthogonal and thus they overlap without the ICI problem. This overlapping does not interfere with the capacity to recover the original signal once that each subcarrier corresponds to a *sinc* function. In Figure 2.8 it is possible to see that, where a peak of a subcarrier aligns with the nulls of the other subcarriers. So, if we have a different information in two sub-carries in the receiver, it is possible to separate the information transmitted in each sub-carrier easier [47]. Hence, we can separate a single high data rate stream in a multiple lower data rate streams that can be transmitted simultaneously in parallel subcarriers.

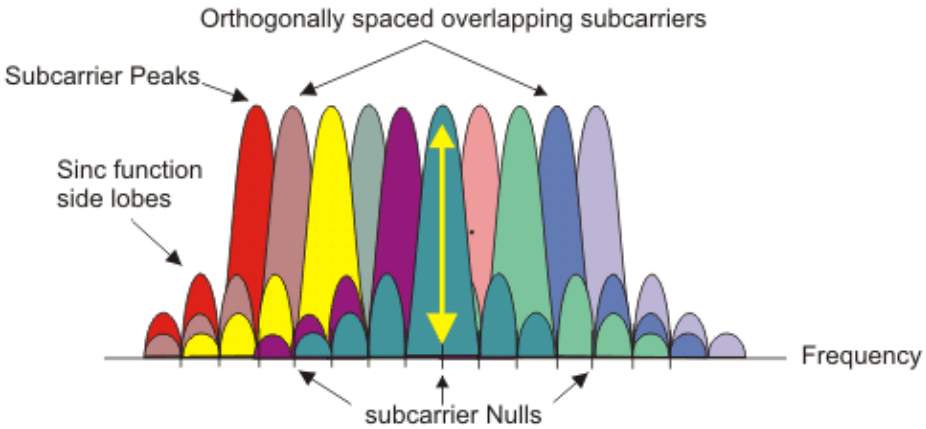

Figure 2.8: OFDM signal frequency spectrum [47].

This concept is represented in Figure 2.9 where this modulation divides the high bit rate stream into a d_k parallel low bit rate, with N_c subcarriers, where $k = 0,...,N_c - 1$.

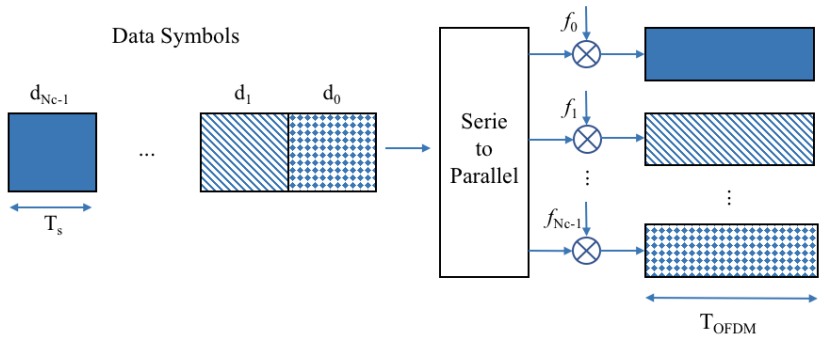

Figure 2.9: OFDM modulation principle.

The duration of each OFDM symbol is the following,

$$T = \frac{1}{\Delta f_c} \text{ with } T = T_s N_c . \tag{2.1}$$

To avoid the ISI, the OFDM principle has a space between the subcarriers with bandwidth B given by

$$\Delta f_c = \frac{B}{N_c} . \tag{2.2}$$

At the receiver, the corresponding signal is

$$r(t) = \mathrm{Re}\left\{ \sum_{k=0}^{N_c-1} d_k \, rect(t/T) e^{j2\pi t f_k} e^{j2\pi t f_c} \right\} . \tag{2.3}$$

The corresponding signal after removing the RF carrier, for a time slot of duration T, is given by

$$s(t) = r(t) e^{-j2\pi f_c t} = \sum_{k=0}^{N_c-1} d_k e^{\frac{j2\pi kt}{T}} \text{ with } f_k = \frac{k}{T} . \tag{2.4}$$

If we sample the sequence at a rate N_c / T, we obtain the following set of N_c samples

$$s_n = s(nT/N_c) = \sum_{k=0}^{N_c-1} d_k e^{\frac{j2\pi kn}{N_c}} \text{ with } n = 0,1,...,N_c - 1 . \tag{2.5}$$

That means

$$\{s_n\} = IFFT\{d_k\} \Rightarrow \{d_k\} = FFT\{s_n\}. \tag{2.6}$$

Consequently, the original sequence can be simply recovered by sampling at a rate N_c / T and taking the FFT over the N_c samples from one slot of duration T.

Now, at the transmitter we have over a period T the following signal,

$$s(t) = \sum_{k=0}^{N_c-1} d_k e^{\frac{j2\pi kt}{T}} rect(t/T), \tag{2.7}$$

that is formed by all the N_c subcarriers.

If we sample the sequence at a rate N_c / T, we obtain the following sequence

$$s_n = s(nT/N_c) = \sum_{k=0}^{N_c-1} d_k e^{\frac{j2\pi kn}{N_c}} \text{ with } n = 0,1,...,N_c - 1. \tag{2.8}$$

This means that the implementation of the multicarrier modulation can be done by replacing the bank of modulators by an IFFT [1].

When the signal passes through a time-dispersive channel, the orthogonality of the signal can be concerned. At the transmitter, the initial solution has a guard interval that consists as an empty space between two OFDM symbols, which serves as a buffer for the multipath reflection. This solution leads us to the ICI problem that means they are no longer orthogonal to each other. The cyclic prefix (CP) is a better solution than the guard interval where instead of the empty spaces, it is used a copy of the last OFDM symbol added in front of the transmitted OFDM symbol that allow a zero ICI. These two solutions, represented in Figure 2.10, occupies the same time interval but the CP ensures that a delayed OFDM symbol have a complete symbol in the FFT interval that helps to maintain the orthogonality between subsequent subcarriers. At the receiver, the CP is first removed and after the process continues. The orthogonality is lost when the delay spread $\tau_{\max}$ is larger than the length of CP interval. With the insertion of the CP interval we lose, but is not too significant, part of signal energy since it does not carry information that is represented as

$$SNR_{CP_{loss}} = -10\log_{10}\left(1 - \frac{T_{CP}}{T_{sym}}\right), \tag{2.9}$$

where T_{CP} and T_{sym} are the interval length of the CP and the OFDM symbol duration, respectively [48].

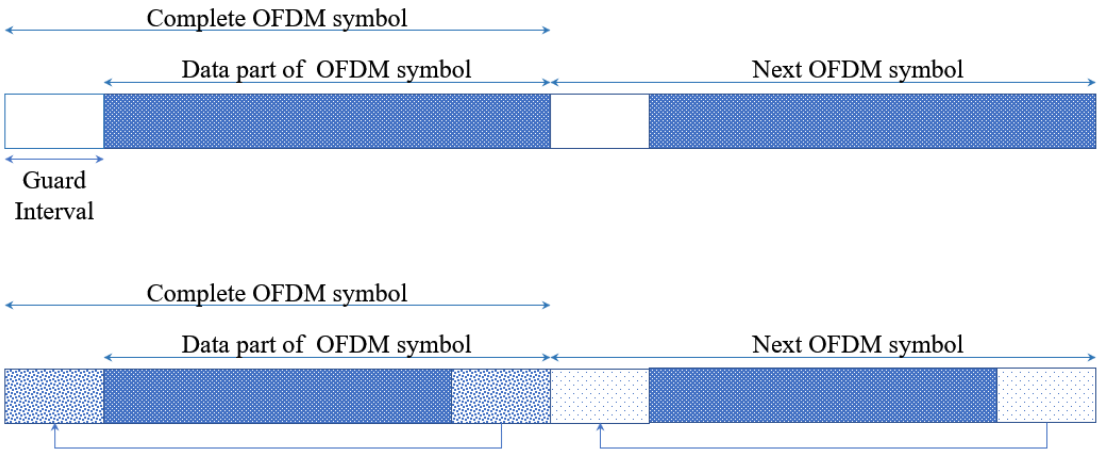

Figure 2.10: Guard interval and CP to OFDM systems [48].

Concluding, OFDM modulation ensures that the ISI caused by the high data rates is minimized, adapts to severe channel conditions, has a high SE that allow an overlap of the power spectral density (PSD) and has a low sensitivity to time synchronization errors like represented in Figure 2.11. So, we can say that approach turns the channel into a flat fading channel that is easy to estimate.

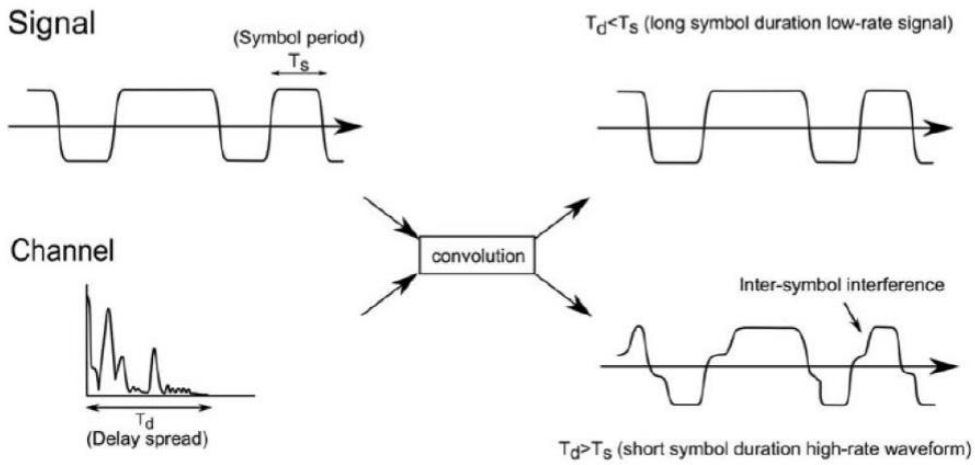

Figure 2.11: Effect of the multipath channel [1].

Nonetheless, OFDM is sensitive to frequency synchronization problems because of the multipath fading, the efficiency decreases due the CP interval and has a high Peak to Average Power Ratio (PAPR) that is proportional to the number of subcarriers used in OFDM systems [49][50]. With a large PAPR makes that the implementation of digital-to-analog converters (DAC), analog-to-digital converters (ADC) and RF amplifiers extremely difficult. Clipping windowing and linear peak cancelation are two techniques used to reduce the PAPR discussed in [48].

The OFDM system, at the transmitter and receiver, is represented in Figure 2.12. Initially, the data bits are modulated into symbols with a data modulation schemes for example, Quadrature Amplitude Modulation (QAM) or Quadrature Phase Shift Keying (QPSK). These symbols pass through an IFFT to convert the frequency domain signal into the time domain. In the end, the CP is added and passes by a DAC. At the receiver, the signal passes by an ADC and the CP is removed. After that the signal passes by a FFT to convert the received time domain signal into a frequency domain and is applied an equalizer (based on the channel state information knowledge) to remove the channel effects. Finally, the signal is demodulated and then the data bits are recovered [48].

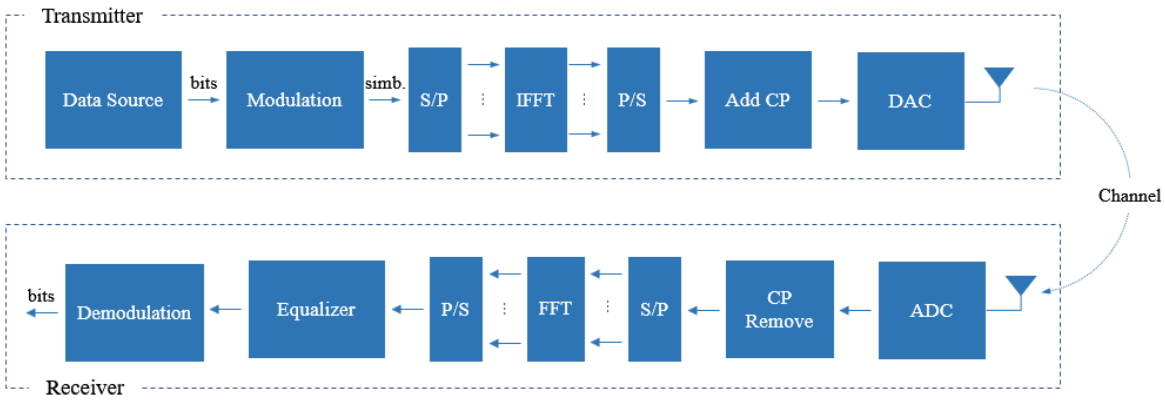

Figure 2.12: Block diagram of an OFDM system.

2.7 Orthogonal Frequency Division Multiple Access

OFDMA, distinguished by its simplicity, is an extension of OFDM to multi-user communication systems that distributes the subcarriers among all the users at the same time [48]. A comparison between OFDM and OFDMA for different users is showed in Figure 2.13.

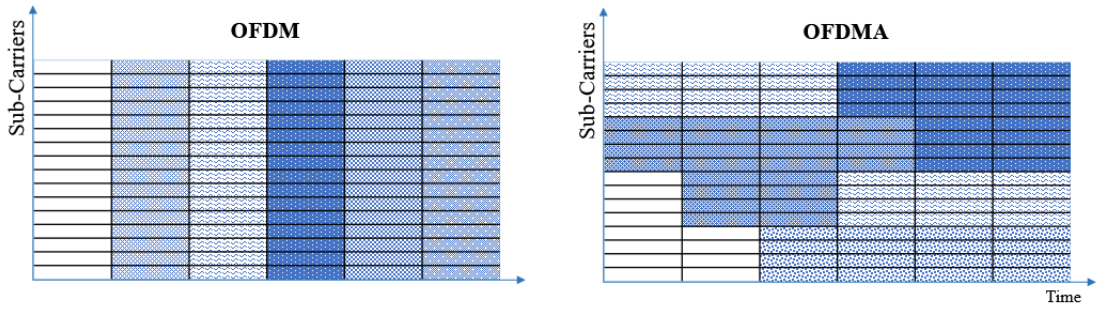

Figure 2.13: Differences between OFDM and OFDMA.

Some techniques can be implemented with OFDMA such as the interleaved and localized mapping techniques. When is interleaved OFDMA it is known as IOFDMA and when is localized OFDMA is known as LOFDMA. In the IOFDMA, the symbols are a repetition of the original inputs

with a systematic phase rotation and in LOFDMA, the subcarriers are mapped side by side. These two techniques are represented in Figure 2.14. In [51] is demonstrated that the performance of IOFDMA is slightly better than the LOFDMA technique.

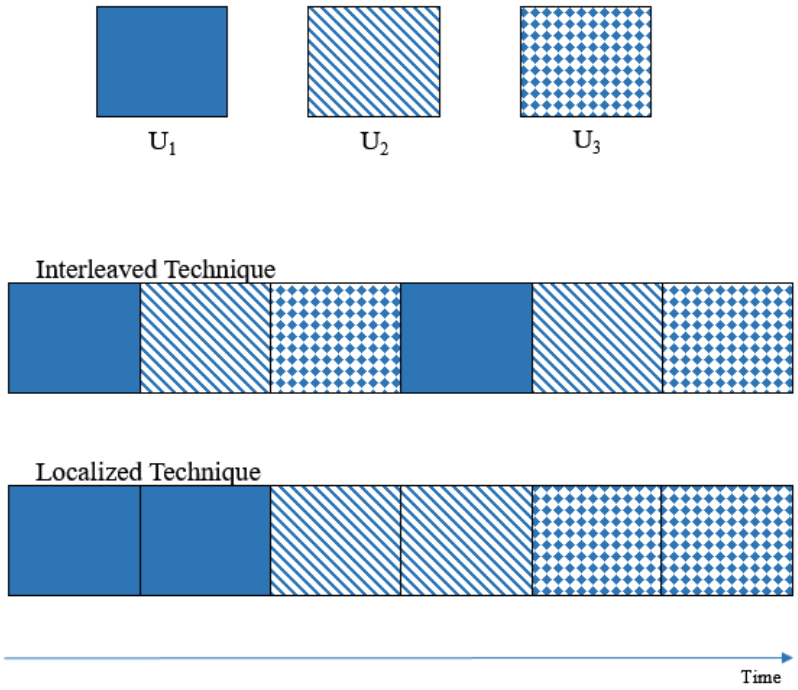

Figure 2.14: Comparison between IOFDMA and LOFDMA.

The main advantages for OFDMA are, a good performance in frequency selective fading channels, low complexity of base band receiver, good spectral properties and handling of multiple bandwidths, link adaptation and frequency domain scheduling and compatibility with advanced receiver and antenna technologies. However, OFDMA has some drawbacks such as the high PAPR, due the constructively or destructively overlap of the various transmitted signals, which requires high linearity in the transmitter and the non-constant envelope of the modulated signal that reduces the efficiency of the RF power amplifier (PA). In LTE, OFDMA is used in the downlink multiple access and SC-FDMA is used in uplink multiple access to achieve a better PA efficiency [1][46].

2.8 Single Carrier Frequency Division Multiple Access

SC-FDMA is a multiple access hybrid modulation scheme developed specifically to the uplink in LTE that combines the low PAPR of the single-carrier technique with the robust multipath resistance and flexible subcarrier achieved by OFDMA. This low PAPR achieved is also a good opportunity to the uplink due the constrain of the mobile battery [52]. Figure 2.15 shows a SC-FDMA block diagram. In the transmitter, first the signal is modulated into symbols using for example a QPSK or QAM schemes, like in OFDMA. Then, the signal passes by a N-point FFT to convert the data

symbols into frequency domain. Finally, is the subcarrier mapping and the signal passes by an N_c-point IFFT that converts the frequency to time domain and after the CP is added.

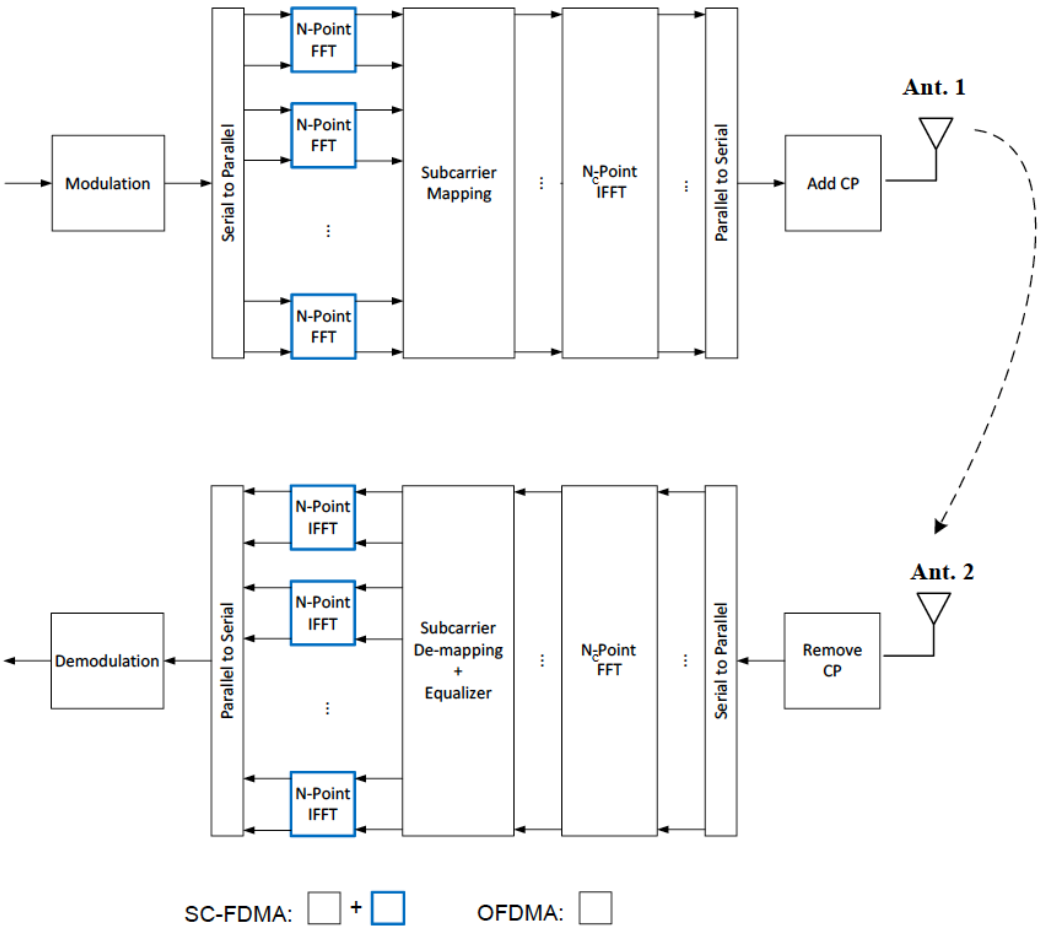

Figure 2.15: SC-FDMA receiver and transmitter scheme [1].

At the receiver, firstly the CP is removed and then the signal passes by an N_c-point FFT that convert the time domain into frequency domain. After, the subcarriers are de-mapped and the equalization in the frequency domain is done. In the end, the equalized symbols in frequency domain are converted in time domain by an N-point IFFT and the symbols are converted into the original signal due to demodulation. The main difference between the SC-FDMA and the OFDMA schemes in the transmitter and receiver are the N-point FFT and N-point IFFT operations, respectively, for the N data symbols represented in Figure 2.15 [1].

The most common single-user equalizer coefficients used in SC-FDMA systems are the following:

Maximal Ratio Combining (MRC)

The main objective of MRC is to maximize the instantaneous SNR at the receiver. The expression of this equalizer is obtained doing the conjugate transpose of the frequency response of the channel h_l of each subcarrier [53][54]. So, this equalizer is given by:

$$g_l = h_l^* \text{ with } l = 1,...,N. \tag{2.10}$$

Equal Gain Combining (EGC)

The EGC technique basically rotates the phases of the arrived signals in each antenna in order to compensate the phase rotation by the channel, and for this, all the subcarriers arrive in phase at the receiver. This technique only needs the phase information of the channel coefficients, thus is less complex [53][54]. This equalizer is given by:

$$g_l = \frac{h_l^*}{\left|h_l^*\right|} \text{ with } l = 1,...,N. \tag{2.11}$$

Zero Forcing Combining (ZFC)

ZFC equalizer symbolizes the inverse of the channel frequency response and recover the orthogonality among the distinct users and therefore, the ISI goes to zero. However, this scheme amplifies the noise particularly to the channel coefficients with low amplitude. The coefficients can be obtained by flipping the channel [53][54].

$$g_l = \frac{h_l^*}{\left|h_l^*\right|^2} \text{ with } l = 1,...,N. \tag{2.12}$$

Minimum Mean Square Error Combining (MMSEC)

This algorithm is what presents better results comparatively to the others MRC, EGC and ZFC. With this algorithm, the coefficients are acquired by minimizing the mean square error among the transmitted signal before OFDM modulation and the signal to the equalizer on each subcarrier [53][54].

$$g_l = \frac{h_l^*}{\left|h_l^*\right|^2 + \sigma^2} \text{ with } l = 1,...,N. \tag{2.13}$$

where σ^2 is the noise variance. When the noise variance tends to zero, it is easy to see that MMSEC algorithm is equal to the ZFC algorithm.

A transmission of four QPSK data symbols with OFDMA is showed in Figure 2.16 where the transmission of the data symbols, one per subcarrier, is made in parallel and in SC-FDMA system, the transmission of the data symbols is made in series, at four times the rate. The high PAPR is achieved due these parallel transmissions in OFDMA. In the SC-FDMA, the N transmitted data symbols in series at N times the rate occupy the same bandwidth as a multi-carrier OFDMA but with a lower PAPR. The use of SC-FDMA is restricted to uplink due to the increase of time domain processing that be a problem in the BS [55]. So, like in LTE, the SC-FDMA can also be used in the 5G uplink transmission [56].

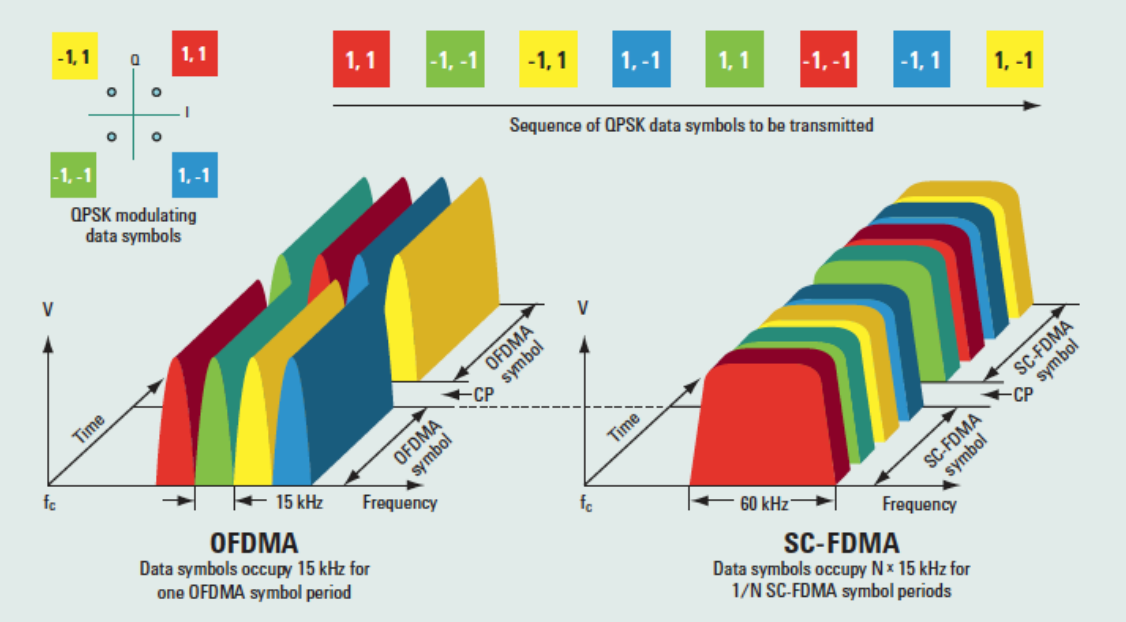

Figure 2.16: Comparison between OFDMA and SC-FDMA [55].

2.9 Constant Envelop Orthogonal Frequency Division Multiplexing

As seen before, the OFDM as a high PAPR that increases with the rise of the number of subcarriers. Therefore, are necessary highly linear PA for OFDM systems that makes a system with low power efficiency and decrease the battery life of the mobile device [57]. To overcome these problems, in past years some techniques have been developed such as the Constant Envelope OFDM (CE-OFDM) and the SC-FDMA presented above. Contrary to OFDM that amplitude modulates the carrier, the CE-OFDM, at the transmitter, uses the OFDM signal to phase modulate (PM) the carrier and the inverse transform, phase demodulator, it is made in the receiver previous to the OFDM demodulator [58][59]. So, CE-OFDM is a promising modulation technique for the future wireless communications systems where basically converts the high PAPR OFDM signal into a constant envelop signal, i.e., with a PAPR of 0dB [60]. This comparison is showed in Figure 2.17 where we

can observe that high PAPR of OFDM is converted in a constant envelop signal with a PAPR value of 0dB. Nevertheless, the CE-OFDM systems requires more bandwidth than OFDM that results in a lower spectral efficiency comparatively to OFDM [58].

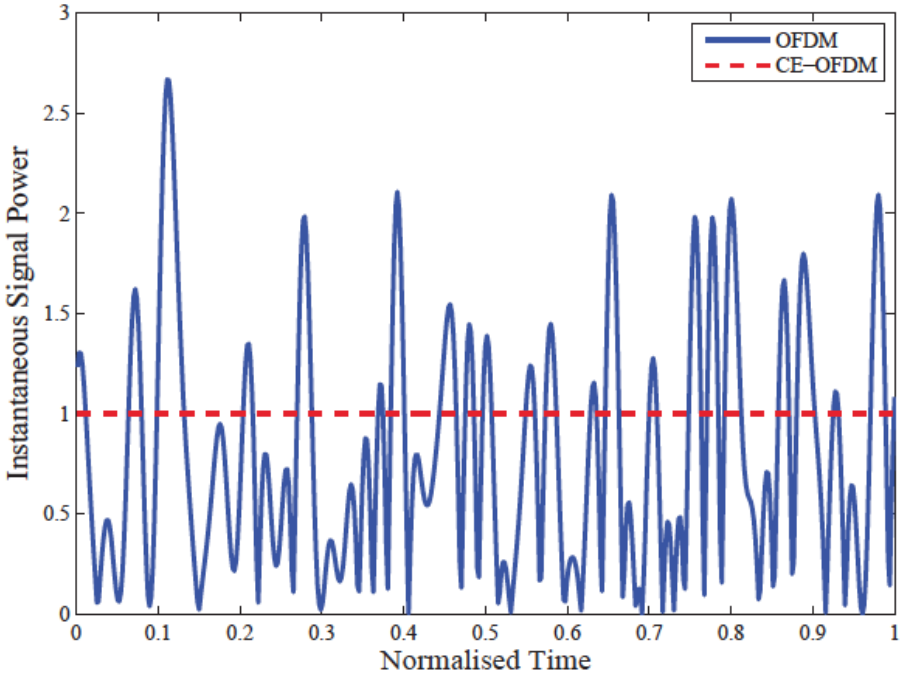

Figure 2.17: Comparison between OFDMA and CE-OFDM PAPR [58].

The CE-OFDM system, as depicted in Figure 2.18, shares many blocks with the same functionality of OFDM system [61]. In this figure, the shaded blocks represent the exclusive blocks of CE-OFDM and the unshaded blocks represent the common blocks of OFDM and CE-PFDM.

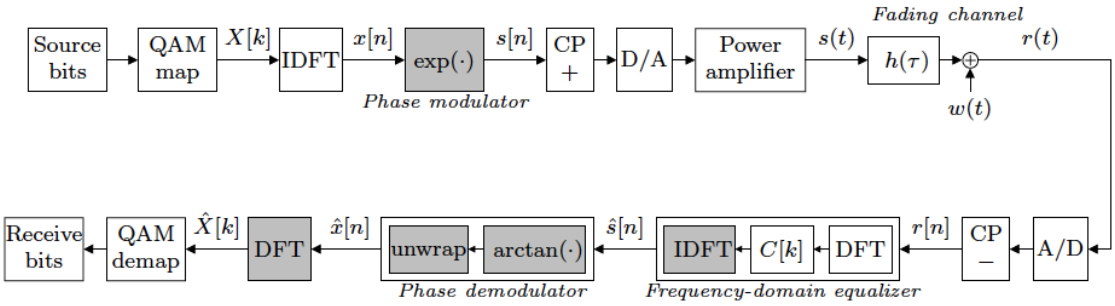

Figure 2.18: Example of CE-OFDM system proposed in [61].

3. Multiple Antenna Systems

In order to accommodate the increasing demand of high data rates for the wireless services, the cellular systems tend to be developed with multi antenna terminals. So, it is possible to improve the capacity and the throughput of the systems with the application of multiple antennas.

In this chapter we introduce the diversity principle. After that, we present the antennas configurations and the receive and transmit diversity techniques. Then, some spatial diversity approaches that be implemented in multiple antenna systems are presented. Finally, we discuss the techniques used in SU/MU Multiple-Input Multiple-Output (MIMO) and, in the end, the massive MIMO systems are described.

3.1 Diversity - Fading Problem

One of the main problems in the wireless communications are the fading effect and diversity is one way to overcome this problem. This principle consists in transmitting the same information through different independent fading paths. By doing that, the probability of all the replicas of the signal fade is reduced, that represents an important advantage for wireless communications. A flat fading can be in good states if the SNR is high enough to achieve the required reliability or in bad states if the SNR is too low to guarantee the required reliability. The overall system performance is imposed by the bad state channels and therefore the performance is worse as compared with Additive White Gaussian Noise (AWGN) channels. By providing diversity to the system it is possible to bring the performance curve to close one achieved by the AWGN channel as depicted in Figure 3.1, where L represents the order of diversity (that can be in time, frequency or space as we will see) [1][62]. In this Figure, the overall performance of the system increases (toward AWGN curve) as the diversity order L increases.

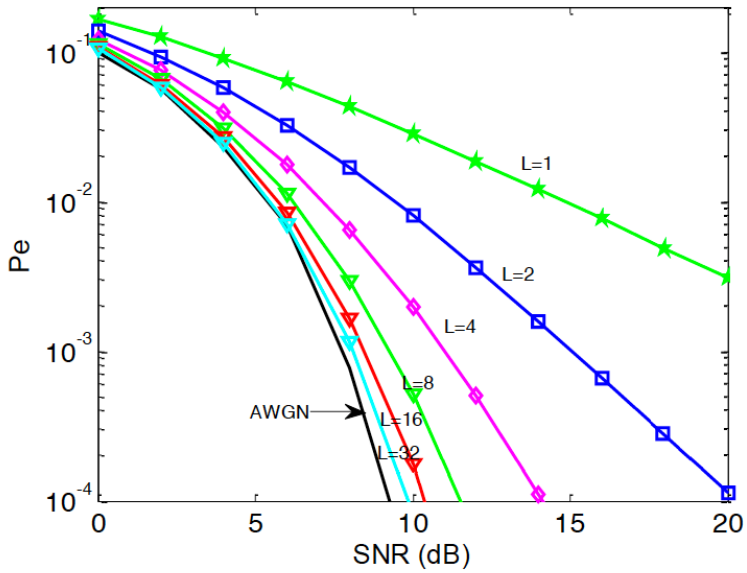

Figure 3.1: Diversity performance comparison [1].

The diversity can be achieved in time, frequency and in space [1][53]. These ways to apply diversity are described below.

Time diversity

The time diversity can be achieved when the same information is transmitted at different times and if they are separated by much more than the coherence time. Normally, time diversity is used in practice with interleaving and coding over symbols across different coherent time periods. The main disadvantage of time diversity is the decrease of the data rate, for a number of L independents paths by a factor of L.

Frequency diversity

The frequency diversity can be achieved when the same information signal is transmitted at different frequencies, where the carriers are separated by the coherence bandwidth of the channel. The main disadvantage of frequency diversity is that normally requires more bandwidth available [1].

Space diversity

As seen before, the diversity achieved by time and frequency methods became with some limitations for the wireless communications. Therefore, if we use a new dimension that is the space, where is necessary to equip the terminals with multiple antennas, we can have spatial diversity. Spatial diversity, also known as antenna diversity, consists in the transmission of information by different independent antennas spatially separated with two or more antennas to overcome the effects of multipath fading. Contrarily to time and frequency diversity, space diversity does not need an

increase of the transmitter power or an increase of the bandwidth, which is an advantage for wireless systems. Depending the number of antennas employed at the transmitter and receiver we can have transmit or receive diversity. Therefore, redundancy is achieved by the transmitted signal replicas sent and received by the multiple independent antennas [63].

3.2 Antennas Configurations

There are four types of antennas configurations depending on the number of antennas in the transmitter and in the receiver, described below.

3.2.1 SISO

The single-input single-output (SISO) configuration is the most basically case, where we only have one antenna in the transmitter and one antenna in the receiver as seen in Figure 3.2. The main advantage of this system is the simplicity that do not requires any spatial processing. However, the throughput of SISO systems depends of the channel bandwidth and SNR whereby can suffer fading effect, losses, attenuation, and as consequence the data rate is decreased [64].

Figure 3.2: SISO configuration.

3.2.2 SIMO

The single-input multiple-output (SIMO) configuration only have one antenna in the transmitter and multiple antennas in the receiver as showed in Figure 3.3. In this scheme it is possible to achieve receive diversity when the same information flows through different independent paths between the transmitter and the receiver [64].

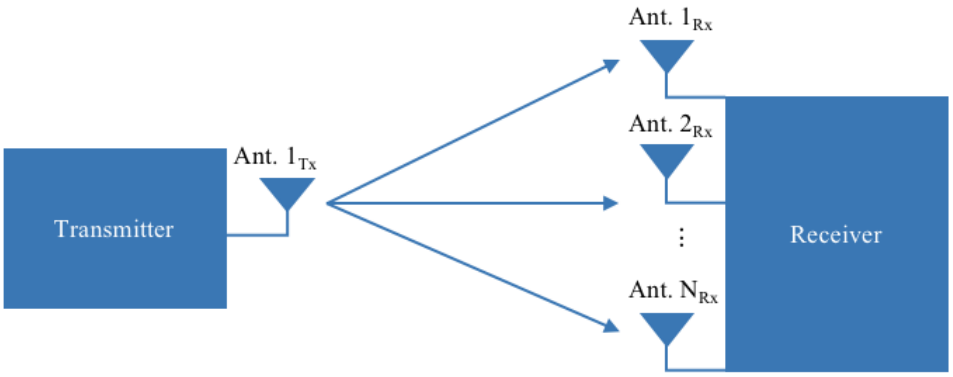

Figure 3.3: SIMO configuration.

3.2.3 MISO

The multiple-input single-output (MISO) configuration is the case with multiple antennas in the transmitter and only a single antenna in the receiver as represented in Figure 3.4. In this case it is possible to achieve transmit diversity when the information is transmitted by different antennas. [54][64].

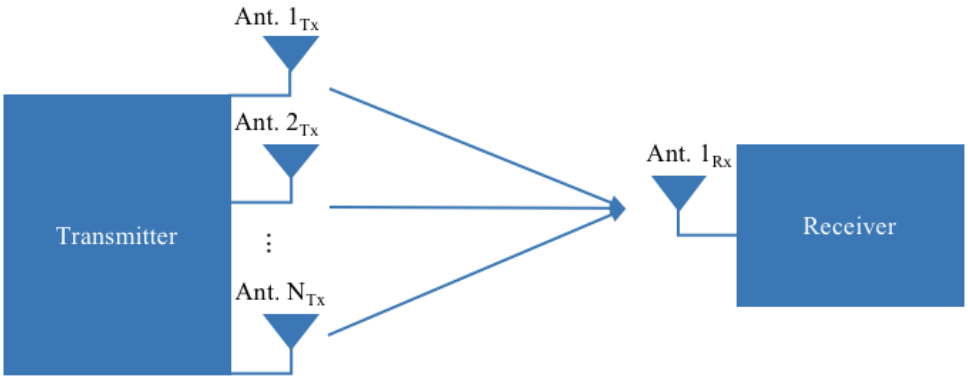

Figure 3.4: MISO configuration.

3.2.4 MIMO Communications

MISO and SIMO provides diversity and antenna gains, but do not provide multiplexing gain that is the capacity gain obtained by decomposing the MIMO channel into parallel channels and multiplexing the different data streams into these channels. MIMO systems have multiple antennas at the transmitter and at the receiver, as show in Figure 3.5, that allow an increasing of the data throughput capacity, provide additional robustness to the channel, offer an high spectral efficiency, increases the multiplexing gain and mitigate the channel fading [65][66].

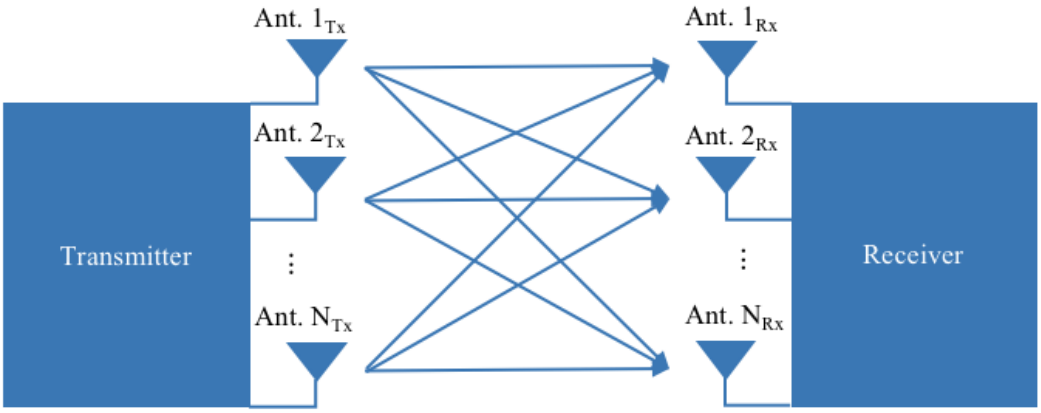

Figure 3.5: MIMO configuration.

Between the transmitter and the receiver, the signal can travel through different paths for the MIMO configuration. So, these paths can be used to provide robustness to the system by improving the SNR or the data capacity. For the conventional systems, with multiple antennas in the transmitter and receiver, it is necessary a dedicated RF chain for each antenna. For a low number of antennas this is not a big problem, but when we have a large number of antennas we need to consider this as a problem as seen in the next Chapter [64]. The main advantages of MIMO, due to the multiple antennas, are the array gain, the diversity gain and the multiplexing gain that allow to combat the fading channel and increase the data rate. Array gain and diversity gain can also be obtained in SIMO and MISO systems. The multiplexing gain can only be achieved in MIMO systems. Array gain is the improvement of SNR acquired by coherently combining the signals on multiple transmit or receive dimensions. Spatial multiplexing consists in the transmission of the different data symbols in parallel across different spatial parallel channels and space diversity is basically the improvement in the link reliability obtained by the received replicas of information through different independent paths [53].

3.3 Receive Diversity

With multiple antennas at the receiver, is possible to obtain receive diversity that can achieve diversity gain associated at the independence of the channels and antenna gain associated at the independence of the noise at each receiver [1][67]. However, to achieve these gains the received signals, from the different antennas, should be well combined. The main combining schemes are the following

1. Maximal Ratio Combining (MRC): also known as Matched Filter, in this algorithm all individual paths are co-phased and summed with weight in order to maximize the SNR.
2. Equal Gain Combination (EGC): where the signals are co-phased on each branch and then are combined with equal weights. This scheme reduces the complexity, relatively to the

MRC, due to only use equal gains and consequently, the performance is slightly lower since the antenna gain is lower.

3. Selection Combining (SC): This scheme compares and selects the instantaneous amplitude of each channel and chooses the antenna branch with the largest amplitude, ignoring the other signal antennas.

The practical performance results to the MRC and EGC are almost equal, being the MRC the better. The SC scheme is the worst, with an antenna gain much lower than MRC and EGC schemes [68].

3.4 Transmit Diversity

With multiple antennas at the transmitter side, it is possible to obtain transmit diversity. Centrally to receive diversity that simply needs the multiple receive antennas to fade independently without being necessary any specific modulation or coding schemes, the transmit diversity, depending on the CSI available, needs spatial modulation and spatial coding schemes [69].

There are two main types to achieve transmit diversity: the open loop and closed loop techniques that are described below. In the case of open loop technique is assumed that the CSI is not known at the transmitter and it is possible to implement transmit diversity with space-time coding schemes. Contrary, for the closed loop technique, the CSI is available, partial or all, at the transmitter [6].

3.4.1 Open loop

The open loop technique uses a space-time/frequency coding and do not use a CSI at transmitter side like in the closed loop technique discussed later. There are some solutions like the Space Time Block Coding (STBC), Space Frequency Block Coding (SFBC), Space-Time Trellis Code (STTC) and Layered Space-Time Codes (LSTC). Here we briefly describe the STBC/SFBC adopted by the current 4G systems.

Alamouti scheme and Tarokh codes are two examples of STBC/SFBC. Figure 3.6 shows an Alamouti encoder scheme with 2 transmit antennas and 1 receive antenna. First the bits are modulated to symbols $\begin{bmatrix} s_1 & s_2 \end{bmatrix}$ and then these symbols are transmitted. In the first time slot, the symbols s_1 and s_2 are transmitted in antenna 1 and antenna 2, respectively. At the second time slot, the symbols $-s_2^*$ and s_1^* are transmitted in antenna 1 and antenna 2, respectively. So, antenna 1 send $\begin{bmatrix} s_1 & -s_2^* \end{bmatrix}$ and antenna 2 sends $\begin{bmatrix} s_2 & s_1^* \end{bmatrix}$. The code used in antenna 1 is orthogonal to the one used in antenna 2 such as $\begin{bmatrix} s_1 & -s_2^* \end{bmatrix} \perp \begin{bmatrix} s_2 & s_1^* \end{bmatrix}$.

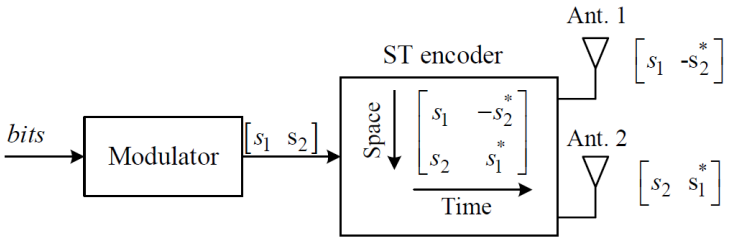

Figure 3.6: Alamouti encoder scheme 2x1 [1].

In the receiver side, represented in Figure 3.7, we have the received signal to which going to be added the noise and passes by a decoder. In the end, the estimated data symbols are demodulated obtained the bit estimates.

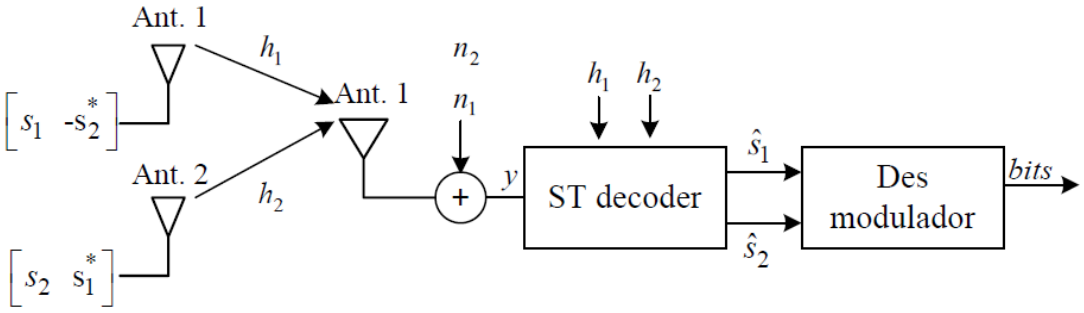

Figure 3.7: Alamouti decoder scheme 2x1 [1].

Table 3.1 show the Alamouti coding applied to instants or frequencies n and n+1.

Time/frequency	Antenna 1	Antenna 2
n	s_n	s_{n+1}
$n+1$	$-s_{n+1}^*$	s_n^*

Table 3.1: Alamouti code.

Assuming the code showed in Table 3.1, the received signal at time/frequency n and $n+1$ are

$$\begin{cases} y_n = \frac{1}{\sqrt{2}} h_{1,n} s_n + \frac{1}{\sqrt{2}} h_{2,n} s_{n+1} + n_n \\ y_{n+1} = -\frac{1}{\sqrt{2}} h_{1,n+1} s_{n+1}^* + \frac{1}{\sqrt{2}} h_{2,n+1} s_n^* + n_{n+1} \end{cases}, \tag{3.1}$$

where each symbol is multiplied by a factor of $1/\sqrt{2}$ to normalize the power per symbol to 1. The corresponding estimated signal decoding are

$$\begin{cases} \hat{s}_n = \frac{1}{\sqrt{2}} h_{1,n+1}^* y_n + \frac{1}{\sqrt{2}} h_{2,n} y_{n+1}^* \\ \hat{s}_{n+1} = \frac{1}{\sqrt{2}} h_{2,n+1}^* y_n - \frac{1}{\sqrt{2}} h_{1,n} y_{n+1}^* \end{cases}. \tag{3.2}$$

Now it is assumed the soft decision of the s_n data symbols is given by,

$$\hat{s}_n = \frac{1}{2}\left(h_{1,n+1}^* h_{1,n} + h_{2,n} h_{2,n+1}^*\right) s_n + \frac{1}{\sqrt{2}} h_{1,n+1}^* n_n + \frac{1}{\sqrt{2}} h_{2,n} n_{n+1}^*. \tag{3.3}$$

We can see that the interference caused by data symbol $n+1$ is full eliminated. Now, if we assume highly correlated channels $h_n = h_{n+1}$, the previous expression simplifies to

$$\hat{s}_n = \frac{1}{2}\left(\left|h_{1,n}\right|^2 + \left|h_{2,n}\right|^2\right) s_n + \frac{1}{\sqrt{2}} h_{1,n}^* n_n + \frac{1}{\sqrt{2}} h_{2,n} n_{n+1}^*. \tag{3.4}$$

And the corresponding SNR is given by

$$SNR = \frac{1}{2} \frac{\left(\left|h_1\right|^2 + \left|h_2\right|^2\right)}{\sigma^2}. \tag{3.5}$$

With the same logic described above, it is possible to make the same for 2 transmit antennas and 2 or more receive antennas. If we assume complex constellations, only exists orthogonal codes for 2 transmit antennas. A solution is the Quasi-Orthogonal Codes but they not achieve full diversity or the Orthogonal Codes with code rate lower than 1 but causes a bandwidth expansion. An example of Orthogonal Codes with code rate lower than 1 is the Tarokh codes that requires the same spectral efficiency of the Alamouti codes and are slightly complex [1].

3.4.2 Close loop

The closed loop transmit diversity assumes that the CSI is available at the transmitter side and apply a precoding scheme to the transmit data symbols to remove the effects of the channel like depicted in Figure 3.8. With this CSI, the receiver can adjust the phase and/or the amplitude of the antennas to improve the efficiency [70]. Depending on the half-duplex mode used, we can obtain the CSI by the following two ways

- TDD mode: The channel can be estimated at the BS in the uplink time slots and then used in the downlink slots, since we have a channel reciprocity between the DL and the UL because the carrier frequency is the same.

- FDD mode: The CSI is estimated at the UTs and then feedback from the user terminals to the BS since the carrier frequencies used for DL and UL are not the same.

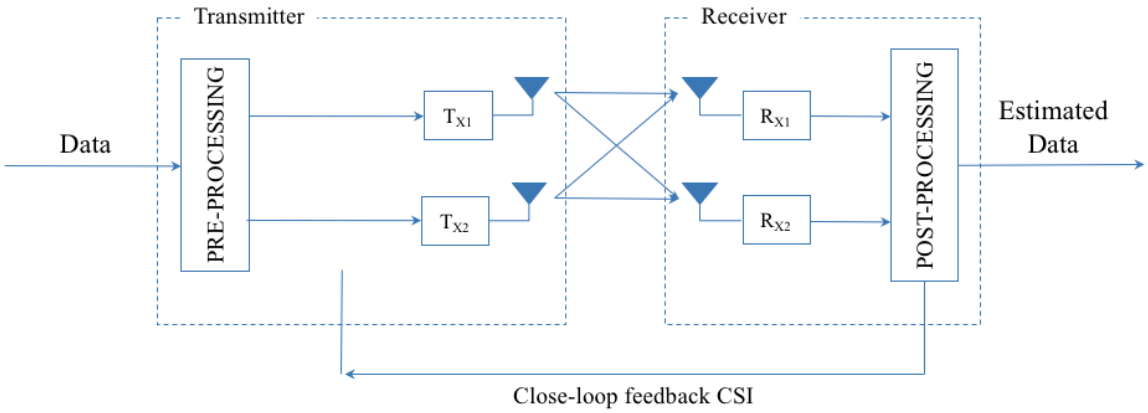

Figure 3.8: Closed Loop technique with CSI feedback.

Basically, when we know the channel at the transmitted side, all the processing done at the receiver (e.g. in the SIMO systems) can be moved to the transmitter in the MISO systems. Nonetheless, the closed loop technique can suffer some limitations such as the feedback delay that results in an outdated CSI, and the feedback channel need to be characterized by a high level of reliability [48]. Therefore, the open loop method is more appropriated for high mobility scenarios while the close loop for low mobility or indoor scenarios where the probability of the channel change between two time slots is lower.

3.5 Spatial Multiplexing

Spatial multiplexing is a transmission method for multiple antennas systems, MIMO systems that allow us to transmit parallel data streams at the same frequency and time slot. This method allows us to increase the capacity of the systems, but the complexity increases due the number of antennas with the corresponding RF chain. As seen above, SIMO and MISO do not provide multiplexing gain, also called degree-of-freedom (DoF), contrary to MIMO [71]. Spatial multiplexing, in a system with N_t transmit antennas and N_r receive antennas, offers an $\min(N_t, N_r)$ increase in the transmission rate, also known as capacity, for the same bandwidth and without additional power. Nonetheless, it is not possible to have the advantages of full diversity and multiplexing at the same time. When we transmit the same symbol information through different antennas, we improve diversity. To improve the capacity, we need to send different data streams through the different channels. An example is given in Figure 3.9, with two transmit and receive antennas without interference between channels.

In Figure 3.9 a), each symbol passes through two independent channels and these symbols are repeated. In Figure 3.9 b), each data stream goes through one channel and each channel is used for one data stream. It is clearly that is not possible to have both diversity and capacity at the same time.

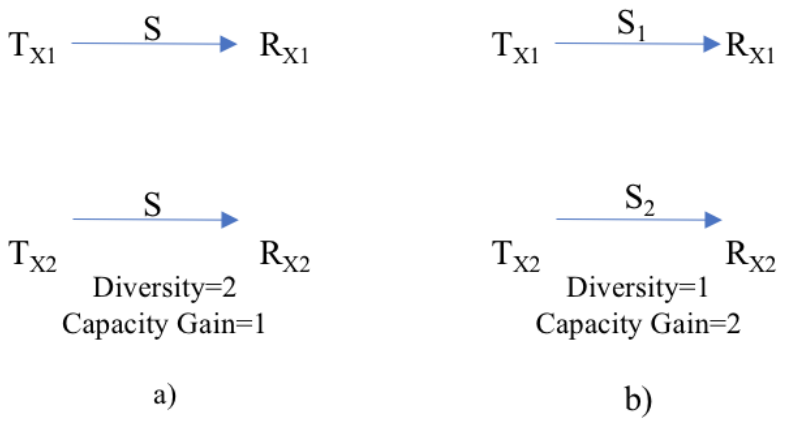

Figure 3.9: Diversity Versus Capacity Gain.

3.5.1 SU-MIMO Techniques

The Single-User MIMO (SU-MIMO) uses a single multi-antenna transmitter and a single multi-antenna receiver as shown in Figure 3.10. The signal processing techniques employed at both transmitter and receiver depends on the CSI information known at the transmitter side. Let's see the extremes cases: the CSI is fully known and not known at the transmitter.

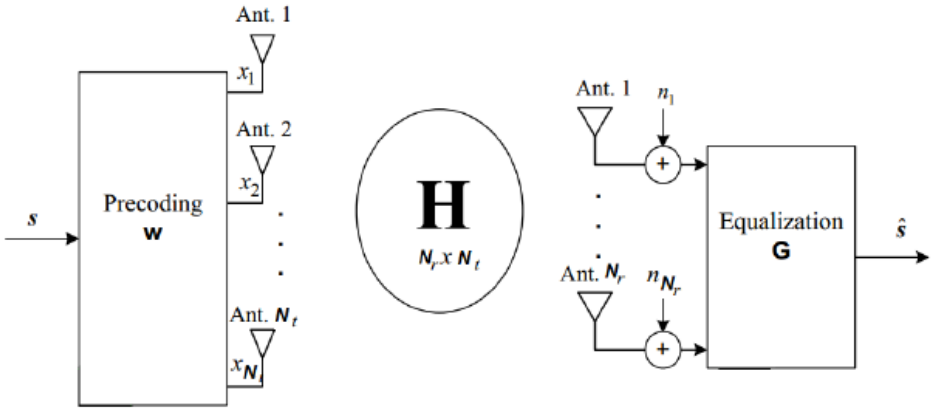

Figure 3.10: SU-MIMO system model [1].

- **Channel known at the transmitter**

  Considering the SU-MIMO system represented in Figure 3.10 with CSI available at the transmitter, the received signal is given by,

$$\mathbf{y} = \mathbf{H}\mathbf{x} + \mathbf{n}\,, \tag{3.6}$$

where $\mathbf{x} = \begin{bmatrix} x_1 & \cdots & x_{N_t} \end{bmatrix}^T$ is the transmitted signal, $\mathbf{y} = \begin{bmatrix} y_1 & \cdots & y_{N_r} \end{bmatrix}^T$ is the received signal, $\mathbf{n} = \begin{bmatrix} n_1 & \cdots & n_{N_t} \end{bmatrix}^T$ is the noise vector and $\mathbf{H} = \begin{bmatrix} h_{11} & \cdots & h_{1N_t} \\ \vdots & h_{ij} & \vdots \\ h_{N_r 1} & \cdots & h_{N_r N_t} \end{bmatrix}$ is the channel matrix with $i = 1,...,N_r$ and $j = 1,...,N_t$.

It is possible to convert the MIMO channel into a set of non-interfering parallel channels using singular value decomposition (SVD). With SVD, we get the following decomposition,

$$\mathbf{H} = \mathbf{U}\mathbf{D}\mathbf{V}^H, \tag{3.7}$$

where $\mathbf{U}$ and V are unitary matrices of size $N_r \times r$ and $N_t \times r$, with $r = rank(\mathbf{H}) \le \min(N_t, N_r)$ and $\mathbf{D} = \begin{bmatrix} \lambda_1 & 0 & 0 \\ 0 & \ddots & 0 \\ 0 & 0 & \lambda_r \end{bmatrix}$ is a diagonal matrix where the diagonal elements are non-negative real numbers with $\lambda_1,...,\lambda_r$ be the singular values of the matrix $\mathbf{H}$.

At the transmitter, we have the following precoding matrix of size $N_t \times r$,

$$\mathbf{W} = \mathbf{V}\mathbf{P}^{\frac{1}{2}}, \tag{3.8}$$

where $\mathbf{P} = \begin{bmatrix} p_1 & 0 & 0 \\ 0 & \ddots & 0 \\ 0 & 0 & p_r \end{bmatrix}^{\frac{1}{2}}$ is a square diagonal power allocation matrix of size $r \times r$.

So, the signal transmitted through the N_t antennas is,

$$\mathbf{x} = \mathbf{W}\mathbf{s}, \tag{3.9}$$

where the data vector of size $r \times 1$ is $\mathbf{s} = \begin{bmatrix} s_1 & \cdots & s_r \end{bmatrix}^T$.

At the receiver, that uses $\mathbf{U}$ matrix, the equalizer matrix is,

$$\mathbf{G} = \mathbf{U}^H, \tag{3.10}$$

Replacing $\mathbf{W}$ and $\mathbf{H}$ on the received signal we get,

$$\mathbf{y} = \mathbf{U}\mathbf{D}\mathbf{V}^H\mathbf{V}\mathbf{P}^{\frac{1}{2}}\mathbf{s} + \mathbf{n}\,. \tag{3.11}$$

So, the estimated transmitted data symbols is given by,

$$\hat{\mathbf{s}} = \mathbf{G}\mathbf{y} = \mathbf{U}^H\mathbf{U}\mathbf{D}\mathbf{V}^H\mathbf{V}\mathbf{P}^{\frac{1}{2}}\mathbf{s} + \mathbf{U}^H\mathbf{n}\,, \tag{3.12}$$

$$\hat{\mathbf{s}} = \mathbf{G}\mathbf{y} = \mathbf{D}\mathbf{P}^{\frac{1}{2}}\mathbf{s} + \tilde{\mathbf{n}}\,. \tag{3.13}$$

The soft estimate of the rth data symbol is,

$$\hat{s}_i = \lambda_i\sqrt{p_i}s_i + \tilde{n}_i \text{ with } i = 1,...,r \tag{3.14}$$

The capacity of this system is given by,

$$C = \sum_{i=1}^{r}\log_2\left(1+\frac{\lambda_i^2 p_i}{\sigma^2}\right) \; bits/s/Hz \tag{3.15}$$

So, when converting the channel MIMO into r parallel channels through SVD, it is possible to transmit r parallel free interference data symbols. To allocate the available power for the different data symbols, in order to maximize the capacity, the algorithm used is water filling (WF). Basically, in this algorithm the bad channels are discarded, and the available power is distributed by the good channels [72].

- **Channel not known at the transmitter**

Now, we consider the same system represented in Figure 3.10 but without the knowledge of the channel at the transmitter, so there is no CSI. Therefore, it is necessary a more sophisticated receiver architecture in order to separate the transmitted data symbols over the transmit antennas. The capacity of a system with channel not known at the transmitter is slightly lower comparatively to a system with channel know at the transmitter due the WF power allocation. To achieve this capacity in systems with channel not known at the transmitter, advanced architectures are applied such as the Vertical Bell Labs Space-Time Architecture (V-BLAST) and Diagonal Bell Labs Space-Time Architecture (D-BLAST).

In V-BLAST architecture independent data streams are sent by the transmit antennas and the data streams are decoded jointly as showed in Figure 3.11. The main drawback of V-BLAST is the higher complexity that grows exponentially with the number of data streams.

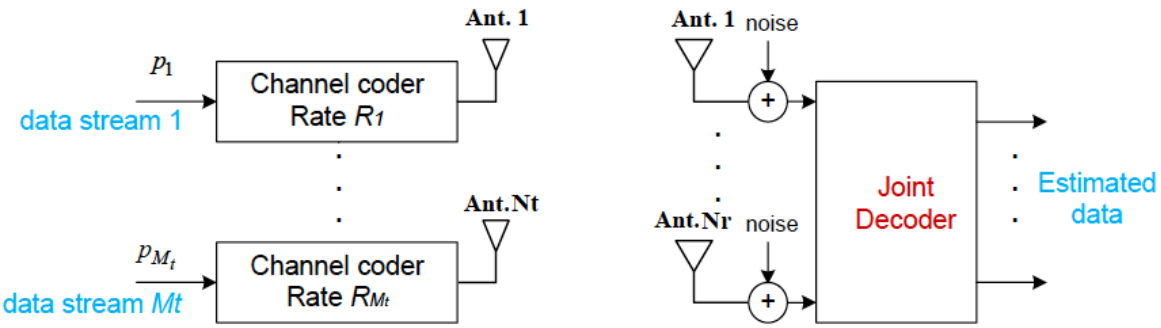

Figure 3.11: V-BLAST Scheme [1].

As a solution, we have the linear sub-optimal receiver architectures, D-BLAST, such as the zero-forcing (ZF) based equalizer, minimum mean square error (MMSE) based equalizer and interference cancellation techniques. As seen in Figure 3.12, D-BLAST architectures converts the problem of joint decoder into one of individual decoding of data streams.

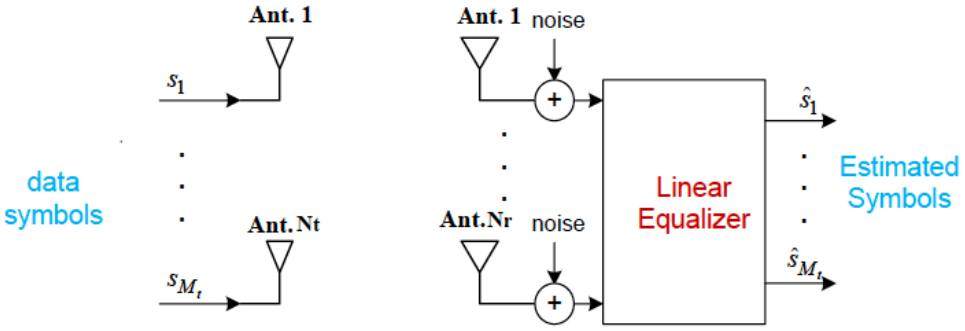

Figure 3.12: D-BLAST Scheme [1].

The ZF equalizer aim, is to design an equalizer vector for each data symbol to in order to remove the interference. A solution, only for $N_r \geq N_t$, that removes the interference is given by the pseudoinverse of matrix $\mathbf{H}$ given by,

$$\mathbf{G}_{ZF} = \left(\mathbf{H}^H\mathbf{H}\right)^{-1}\mathbf{H}^H, \tag{3.16}$$

The vector of all estimated data symbols is given by,

$$\hat{\mathbf{s}} = \mathbf{G}\mathbf{y} = \mathbf{G}\mathbf{H}\mathbf{s} + \mathbf{G}\mathbf{n}. \tag{3.17}$$

Therefore,

$$\hat{\mathbf{s}} = \left(\mathbf{H}^H\mathbf{H}\right)^{-1}\mathbf{H}^H\mathbf{H}\mathbf{s} + \left(\mathbf{H}^H\mathbf{H}\right)^{-1}\mathbf{H}^H\mathbf{n} = \mathbf{I}_{N_t}\mathbf{s} + \left(\mathbf{H}^H\mathbf{H}\right)^{-1}\mathbf{H}^H\mathbf{n}. \quad (3.18)$$

So, all the data symbols are detected without interference. The main disadvantage of ZF scheme is the noise term, $\left(\mathbf{H}^H\mathbf{H}\right)^{-1}\mathbf{H}^H\mathbf{n}$, that is amplified when the channel is in deep fading at low SNR.

A solution is the equalizer based on MMSE that minimizes the mean square error between the transmitter symbol vector $\mathbf{s}$ and its estimates $\hat{\mathbf{s}}$ at the received, given by,

$$\varepsilon = E\left[\left\|\mathbf{s} - \hat{\mathbf{s}}\right\|^2\right] = E\left[\left\|\mathbf{s} - \mathbf{G}\mathbf{y}\right\|^2\right]. \quad (3.19)$$

Thus, the MMSE equalizer, in order to reduce the above error, is given by,

$$\mathbf{G}_{MMSE} = \left(\mathbf{H}^H\mathbf{H} + \sigma^2\mathbf{I}_{N_t}\right)^{-1}\mathbf{H}^H. \quad (3.20)$$

It is possible to see if we have a high SNR in the MMSE equalizer, this tends to the ZF equalizer: $SNR \to \inf \Rightarrow \sigma^2 \to 0$.

3.5.2 MU-MIMO Techniques

We have seen the multiple transmit and receive antennas in the context of point-to-point channels, however, with spatial dimension it is also possible to separate the users that share the same frequency and time resources named as Multi-User MIMO (MU-MIMO). There are two different type: the UL where different users communicate to the receiver and the DL, where the communication is from the transmitter to the different users. Without multiple antennas is not possible to separate the users that share the same resources. The principles used in SU-MIMO seen above are similar to the ones used in MU-MIMO. The Potential advantages of MU-MIMO over SU-MIMO include robustness and the preservation of spatial multiplexing gain [12].

Figure 3.13 shows an uplink block diagram for MU-MIMO. The receiver structures used for point-to-point MIMO can also be employed for the uplink with multiple users since each UT can be seen as one antenna in the previous MIMO point-to-point system. The number of users need to be equal or lower than the number of receive antennas, i.e., $Number\ of\ \text{Rx}\ antennas \geq Number\ of\ users$. Another limitation is that the number of total transmit antennas need to be less or equal than the total number of antennas at the receiver, i.e., $Number\ of\ \text{Rx}\ antennas \geq Number\ of\ Tx\ antennas \times number\ of\ users$.

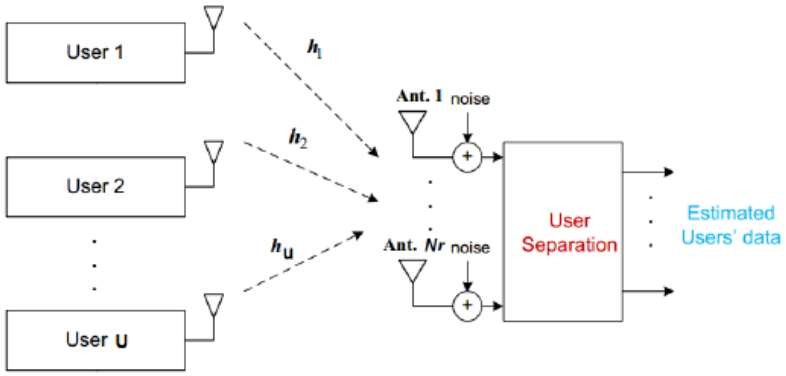

Figure 3.13: Uplink Communication [1].

Figure 3.14 shows the downlink block diagram with a precoding or beamforming to mitigate the interference that a given user can cause in other users terminals. If the transmitter does not track the channel, cannot do precoding on the DL. In the DL it is possible to use the linear equalizer ZF and MMSE filters to null the interference caused by a given user, however, the number of transmit antennas need to be equal or bigger than the number of users.

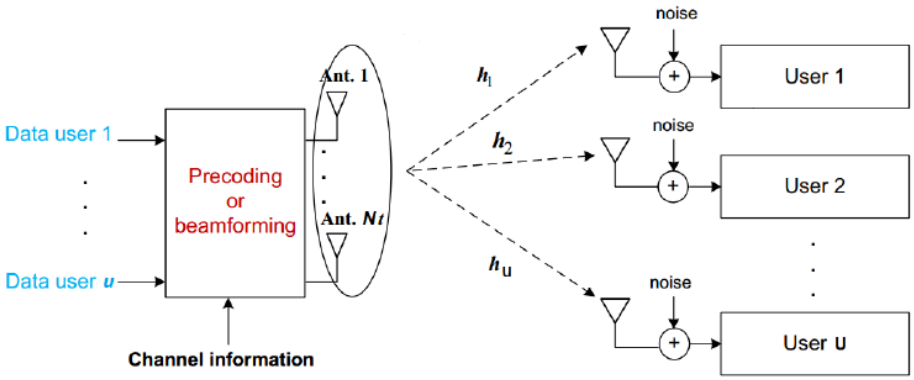

Figure 3.14: Downlink Communication [1].

3.6 Massive MIMO Systems

Massive MIMO is an emerging technology that is based in the principle that we have a high number of antennas in the terminals. Normally, conventional MIMO systems have in each BS a low number of antennas (e.g., less than 8) while mMIMO have a large number of antennas (e.g., 100 or more) per BS. While the number of antennas at the BS can be very large, the same do not occurs in the UT where the number of antennas is limited to fit into the mobile device. Another designation of mMIMO is Large Scale Antenna Systems (LSAS) [23][73]. The conventional MIMO is not reasonable for the future mobile systems because cannot achieve the SE needed and when the

frequency used between the BS and the UT are lower (sub-6GHz), the antennas need to be distributed in a large area. Otherwise, if we use high frequencies such as the mmW, the size of the antennas decreases and it is possible to have the same number of antennas in a smaller volume. Therefore, with mMIMO and high frequencies is possible to have a high number of antennas in the mobile devices [20][74]. To get a high directivity in mMIMO systems, the BS uses an antenna array via BF in order to create a beam to transfer the signal. A mMIMO multi-user beamforming communication between the BS and the users is depicted in Figure 3.15 where the increased number of antennas allows each mobile device to communicate with the BS with low interference between each other. So, we can define beamforming as the signal processing technique used for directional signal transmission or reception that allows an increase of the SNR by blocking most of the surrounded noise [75].

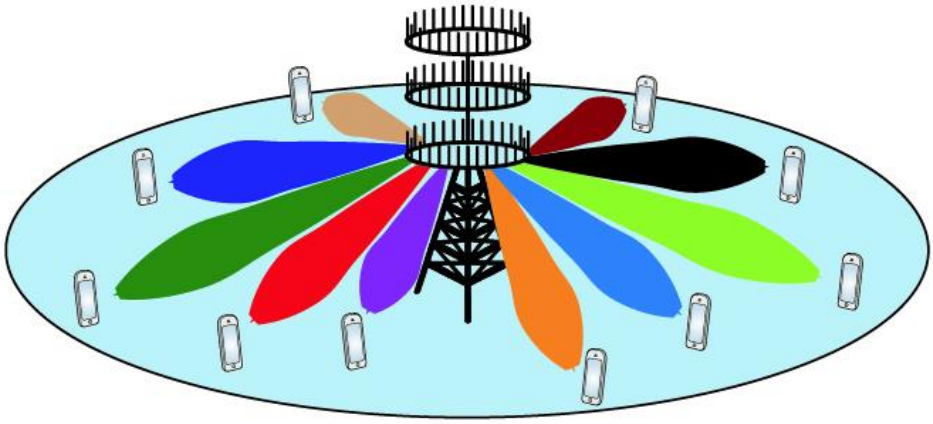

Figure 3.15: Massive MU-MIMO systems [75].

3.6.1 Massive Antennas Array

In Figure 3.16 is represented some types of massive antenna array (MAA) configurations for a BS like: linear, spherical, cylindrical, rectangular and distributed. These antennas are used depending on the considered situation, for example, a distributed MAA can be used inside a building to improve the range of the signal. The practical construction of an antenna needs some care, as the physical size limit and need to be created in order to achieve the best performance possible [76][77]. When we have a low frequency, sub 6GHz, the antennas have a big size and an example is represented in Figure 3.16 where the rectangular MAA occupies an entire building wall. This size is not reasonable and to decrease the size of antennas we need to use high frequencies, as seen in the next Chapter.

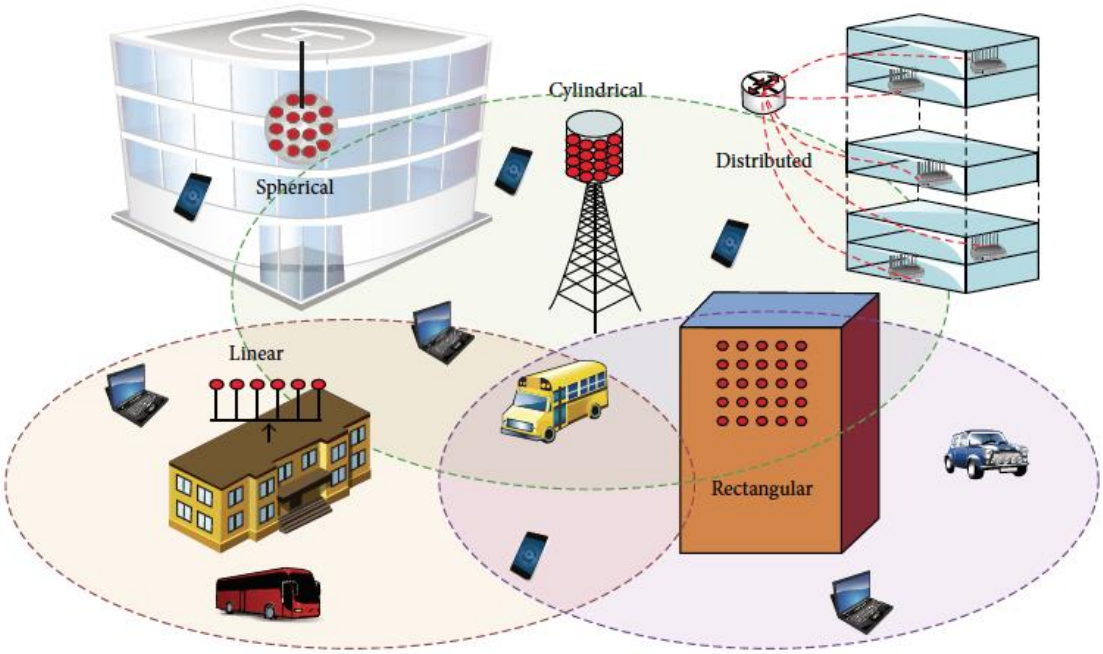

Figure 3.16: Type of antenna configurations [78].

3.6.2 Opportunities of Massive MIMO

The main potentials of mMIMO architectures can offer are:

- The aggressive spatial multiplexing and the simple linear beamforming/precoding used in mMIMO with a very large number of antennas, can increase the capacity 10 times or more and can improve both spectral and energy efficiency [79]. The energy efficiency can be achieved especially due the minimizing PA power losses by techniques that reduces the PAPR [80].
- It is expected that inexpensive and extremely low power components are used in mMIMO, in the order of milliwatts [81]. With the energy efficiency improvement, the BS of a mMIMO that consume many orders of magnitude less power, can be powered by wind or solar energy and this allow us to assemble a BS in a remote place without electricity for example. Hence, the BS will generate less electromagnetic interference [77].
- When the signal sent from a BS travels through multiple paths to arrive at the terminal, the waves resulting from these multiple paths interfere destructively each other. This fading is a challenge to build low latency wireless links and, to avoid fading dips, mMIMO has a larger number of antennas and beamforming processing. Hence, the latency is no longer limited by fading [77].

- One way to improve robustness in a system is to apply multiple antennas at the transmitter and/or the receiver. The mMIMO appears at this context with multiple antennas where it is possible to improve the multiplexing and diversity gains [77].

3.6.3 Limiting Factors of Massive MIMO

- The intercell interference, named as pilot contamination, is depicted in Figure 3.17 and can occurs in the downlink or uplink transmission. When we use the same frequency in the neighbor cell of a determined cell, happens interference between these cells. So, one way to cancel this interference is to create pilot sequences where the home cell is surrounded of cells non-contaminating that uses different frequencies comparatively to the home cell [73]. So, in Figure 3.17, the colors represent different frequencies and when the same frequency is used, is required some distance between the base stations. Note that in real applications cells geometry varies and they are not hexagonal like in the figure below. Normally, we have large cells in rural areas and small cells inside cities in order to accomplish the requirements according to the density of users. For example, in rural areas we have a low population density, so is possible a greater spacing between the BS's.

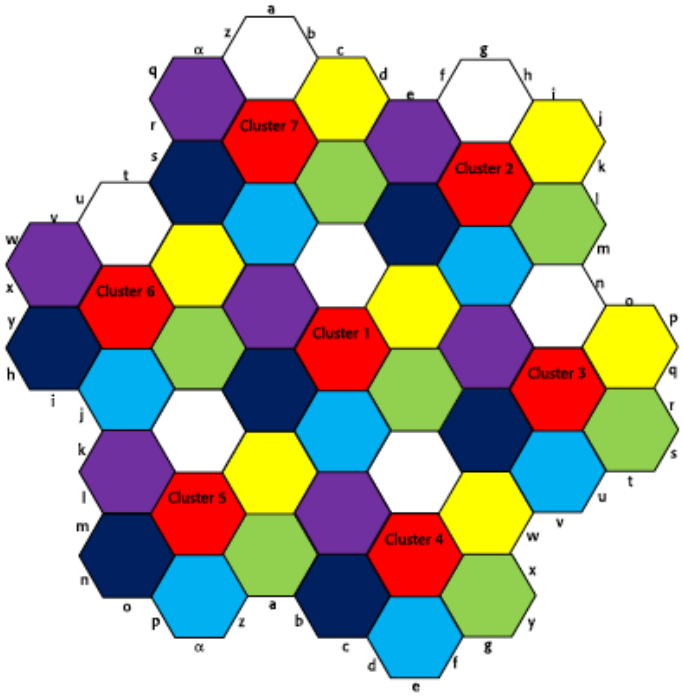

Figure 3.17: Frequency Planning with Seven Sets of Frequency [73].

- The design and construction of very large antenna arrays increase the hardware and computational costs. Massive MIMO has very compacted large antenna arrays and the space between the antennas tends to decrease. Some consequences of this space between

the antennas is the limitation of the mutual coupling effect among antenna elements and the reduction of the multiplexing gain. This effects only can be ignored when the antennas are well separated from each other but for mMIMO this is not reasonable [82]. Some other limitation such as the in-phase/quadrature imbalances in the RF chain and the failure of some antennas elements can arise in mMIMO systems [83].

- The high directivity of the beamforming at the BS is very sensitive to movement of the UT or the antenna array swaying and the antennas need to be sufficiently separated to decrease the correlation between the channels [54][78].
- In a FDD system, the requirements are proportional to the number of antennas at the BS and the CSI feedback is fundamental. For this reason, FDD is not reasonable in mMIMO systems. Therefore, TDD is the most suitable alternative to obtaining CSI due the training requirements that are independent of the number of antennas at the BS and don't need CSI feedback. For these reasons, TDD will be the most technique applied at mMIMO systems and will require further investigation in calibration methods [83].

4. Millimeter Waves Systems

Wireless communications are a way to transmit information between a transmitter and a receiver without being necessary a physical connection, which has some advantages such as the mobility, the portability and the easier connection. Electromagnetic waves are used to these communications and then, the electromagnetic spectrum needs to be efficiently used because it becomes small for the amount of applications to which it is destined. Currently, the spectrum between 300 MHz and 3 GHz is saturated with the mobile communications, so it is necessary to find another available spectrum bands for mobile communication such as the mmW band. The use of mmW was not considered in the past due to various factors such as the pathloss and penetration losses, where the propagation range decreases with the increase of the frequency [84][85].

This Chapter focuses in the characteristics of the mmW propagation channel, and highlights the main opportunities, limitations and solutions for the use of mmW. After, we present the combination of mmW systems with mMIMO systems that are two keys two achieve the high data rates for the future generations of mobile communications. Finally, some hybrid and low-resolution ADC's solutions are presented.

4.1 Electromagnetic Spectrum

The Electromagnetic spectrum can be divided into categories, like depicted in Figure 4.1, such as [86]:

- Extremely Low Frequency (ELF): 300 to 3000 Hz (λ = 1000 to 100 km)
- Very Low Frequency (VLF): 3 to 30 kHz (λ = 100 to 10 km)
- Low Frequency (LF): 30 to 300 kHz (λ = 10 to 1 km)
- Medium Frequency (MF): 300 to 3000 kHz (λ = 1000 to 100 m)
- High Frequency (HF): 3 to 30 MHz (λ = 100 to 10 m)
- Very High Frequency (VHF): 30 to 300 MHz (λ = 10 to 1 m)
- Ultra High Frequency (UHF): 300 to 3000 MHz (λ = 100 to 10 cm)
- Super High Frequency (SHF): 3 to 30 GHz (λ = 10 to 1 cm)

- Extremely High Frequency (EHF): 30 to 300 GHz (λ = 10 to 1 mm)

Through the communication, between a transmitter and a receiver, the waves propagate in earth where only the lower atmosphere layers are involved. So, the waves have three types of propagation: the ground wave where the propagation occurs in the earth surface, the sky wave where the wave propagates in space and can return by reflection in the troposphere or ionosphere, and the direct wave where the propagation occurs in the geometric horizon [1]. Note that mmW, between 30 GHz to 300 GHz, is part of the EHF group in the electromagnetic spectrum.

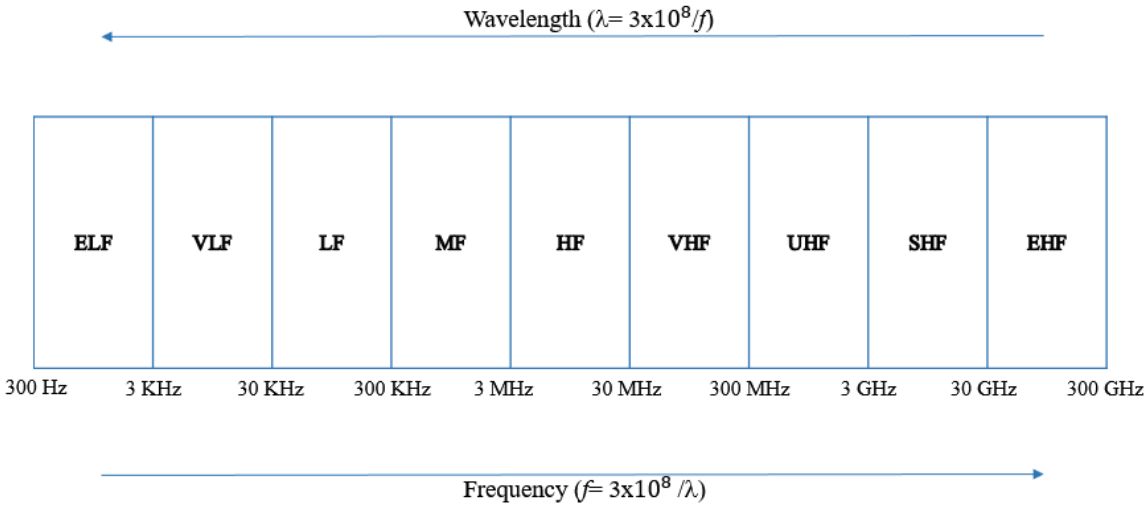

Figure 4.1: Electromagnetic Spectrum.

4.2 Millimeter Wave Spectrum Characteristics

With the emerging necessity to high data traffic demand, the mmW arrive with an enormous unlicensed bandwidth beyond the traditional licensed wireless microwave bands. The spectrum between 30 GHz to 300 GHz is underutilized and mainly unexploited whereby is a good opportunity to discover and study. This range of spectrum, situated in the EHF at the electromagnetic spectrum, is called millimeter wave due the size of the wavelengths from 1 to 10 millimeters. The mmW has a shorter wavelength in the range of millimeters once the frequency is inversely proportional to the wavelength, so we can put more antennas in the same area comparatively to the frequencies used currently. Therefore, with mmW antenna array it is possible to obtain higher gain than the current microwave communications system with the same area in the MAA [85]. It is possible to have more antennas in the same area due the combination of mmW with the complementary metal-oxide-semiconductor (CMOS) RF circuits [87].

Figure 4.2 shows the range between 3 GHz and 300 GHz and one may verify that from the 297 GHz of the total spectrum, only 252 GHz can be used for the mobile broadband. This happens

because mmW in the range of 57 GHz to 64GHz and 164 GHz to 200 GHz can experience attenuation due to the oxygen absorption and the water vapor absorption, respectively [20][21]. So, these ranges of frequencies are not appropriate to use in mobile wireless communications due the strong attenuation. In this figure we can also see that the spectrum below 3GHz is where all the current mobile communications are situated and this is not able to satisfy the demand of the next generations of mobile communications.

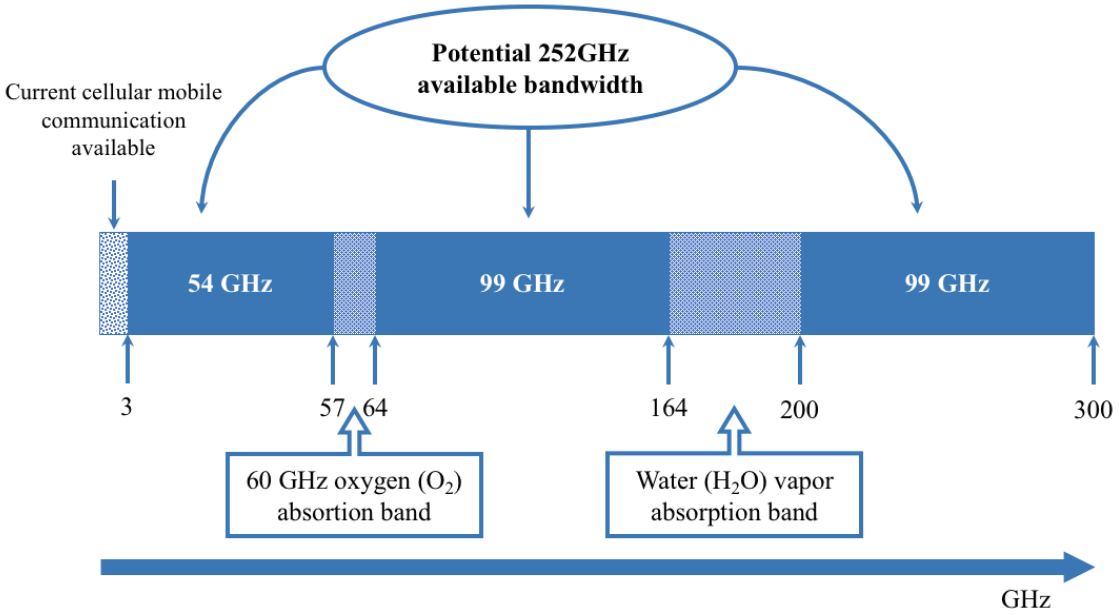

Figure 4.2: Millimeter Wave Spectrum.

4.3 Limiting Factors of Millimeter Waves systems

As seen above, the higher frequencies suffer attenuation due the water vapor absorption and the oxygen absorption. This occurs due the raindrops are roughly the same size as mmW and causes the effect called scattering of the radio signal [88]. In Figure 4.3 a) is showed the penetration loss from foliage depth and in Figure 4.3 b) is showed the rain attenuation with the frequency. For the graphics of these figures we can conclude that the loss of foliage penetration rises with the increase of the frequency and the mmW range has a significant attenuation due the various types of rain. Basically, with the increase of the quantity of rain, bigger is the attenuation for the mmW high frequencies [21][89].

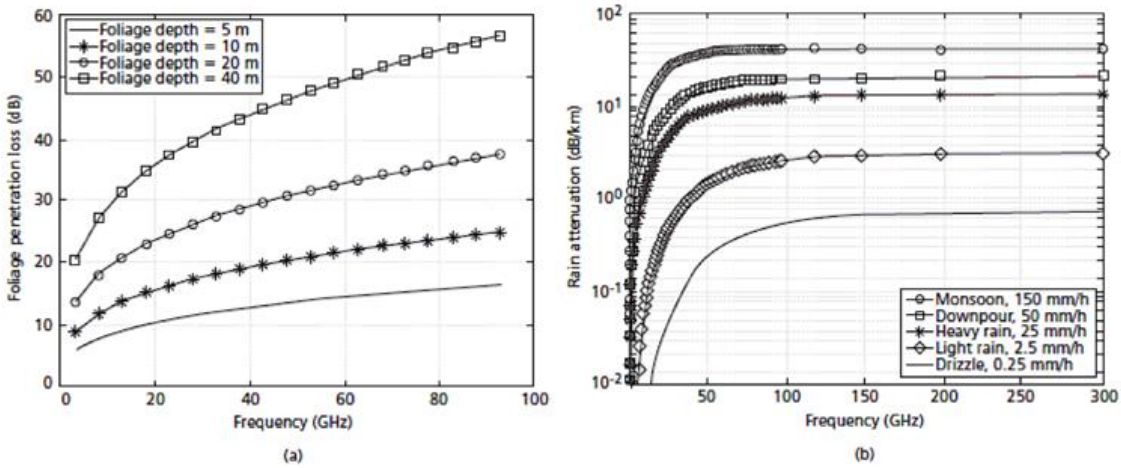

Figure 4.3: Millimeter wave characteristics: a) foliage penetration loss; b) rain attenuation [21].

Compared to the existing cellular systems, the mmW systems have a much bigger path loss in the free space. The free-space propagation depends on the frequency and propagate less well with the increase of the frequency. So, for the mmW overcome this path loss limitation, is necessary increase the number of antennas in order to increase the antenna gain. Due the high frequencies of the mmW, it is possible to put more antennas in the same area than in the current frequencies used and overcome these limitation [90].

The mmW band can experience an effect name as shadowing. At the lower frequencies is easier to cross materials, for example a wall of a building, than mmW. The high levels of attenuation for some materials for high frequencies, as seen in Table 4.1, makes difficult to use mmW specially indoors in the case of the BS is outside. If the transmitter and receiver communicate in a line of sight, do not have this problem of attenuation. Hence, the antennas need to be situated strictly indoors and outdoors in order to have a larger coverage [16][87]. In another point of view, this problem can be seen with an advantage, for example, if we want to use a protected frequency with important information in a room and make sure that frequency does not cross the walls of the room to outdoors or to the closers rooms, we can use the mmW range and some more cautions.

		ATTENUATION		
MATERIAL	Thickness (cm)	< 3 GHz	40 GHz	60 GHz
DRYWALL	2.5	5.4	-	6.0
OFFICE WHITEBOARD	1.9	0.5	-	9.6
CLEAR GLASS	0.3/0.4	6.4	2.5	3.6
MESH GLASS	0.3	7.7	-	10.2
WOOD	0.7	5.4	3.5	-
CONCRETE	10	17.7	175	-

Table 4.1: Attenuations for Different Materials [21].

The power consumption in the ADC of the multi antennas for mmW systems is another limitation. The consumption increases with the sampling rate and with the number of bits per sample. Therefore, the use of high resolution quantization and large number of antennas is an important limitation for low power and low-cost devices [87].

4.4 Millimeter Waves with Massive MIMO systems

As mentioned, massive MIMO and mmW are two key technologies that complement each other and are promising technologies for the future wireless communications [91]. With these technologies it is possible to have more antennas in the same volume due to the smaller wavelength of the mmW comparatively to the current systems that use lower frequencies and to the mMIMO systems. Hence, the terminals can have a large number of antennas [92]. With the conjugation of mmW and mMIMO, arise the opportunity to apply new efficient spatial techniques at the transmitter and/or the receiver that are different that the used currently for the systems sub-6 GHz.

It is well known that when we have a large number of antennas it is not feasible to have one dedicated RF chain per antenna and consequently a full digital BF architecture is not appropriate due to the higher costs and power consumption [23][93]. On the other hand, a system that works only in the analog domain, by employing a purely full analog BF, is not feasible due to the availability of

only quantized phase shifters and the constraints on the amplitudes of these analog phase shifters [28][94]. As result, the fully analog architecture is normally limited to a single-stream transmission [35]. To tackle these limitations, it is necessary to find a solution to overcome these limitations, such as the hybrid analog and digital BF, and the use of low-resolution ADC's. These two solutions are presented below with special focus in the hybrid architectures.

4.4.1 Hybrid Architectures

In order to overcome these problems described above, the hybrid analog/digital architectures are considered, where the number of RF chains is lower than the number of total antennas in the transmitter or receiver side. In this type of architectures, the signal processing is divided between the analog and the digital domains, therefrom the name hybrid that makes a compromise on power consumption and hardware complexity. With this hybrid architectures is possible decrease the overall complexity and performance of the system due to the number of RF chains that is smaller than the number of antennas. So, the main objective of the hybrid architectures is to reduce the hardware and signal processing complexity while providing a performance close the fully digital based systems [74].

There are several types of hybrid architectures. Two examples are the hybrid full-connected architecture and the hybrid sub-connected architecture. In the hybrid full-connected architecture each N_{RF} RF chain is connected to all antennas as depicted in Figure 4.4.

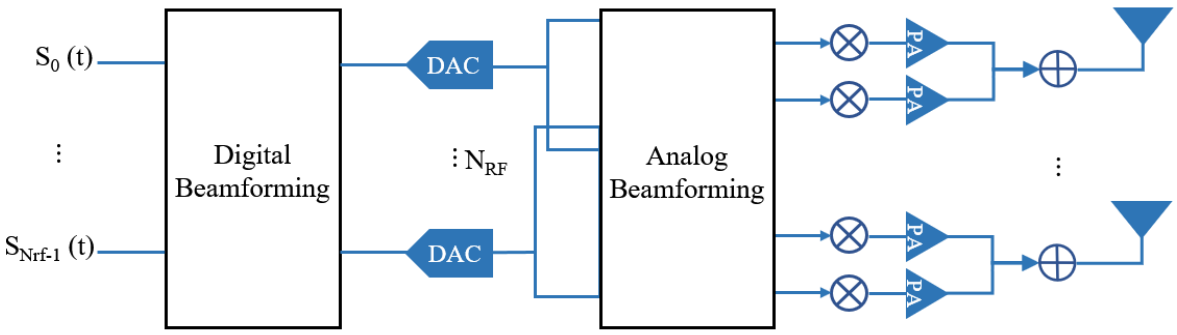

Figure 4.4: Hybrid full-connected beamforming architecture.

In the hybrid sub-connected architecture, depicted in Figure 4.5, each N_{RF} RF chain is connected only to a group of antennas and not to all antennas like the previous architecture. For the full-connected architecture we have that the number of signal processing path is $N_{tx} \times N_{RF}^2$, whereas, in the sub-connected architecture is $N_{tx} \times N_{RF}$ for a system with N_{tx} transmit antennas and N_{RF} RF

chains. Nonetheless, the full-connected architecture has a BF gain N_{RF} times greater than the sub-connected architectures. So, the hybrid sub-connected architecture is simpler and more inexpensive than the fully connected one. However, the sub-connected architecture has a lower BF gain than full-connected architecture due the RF chain connect to a set of antennas instead of all antennas [95][96].

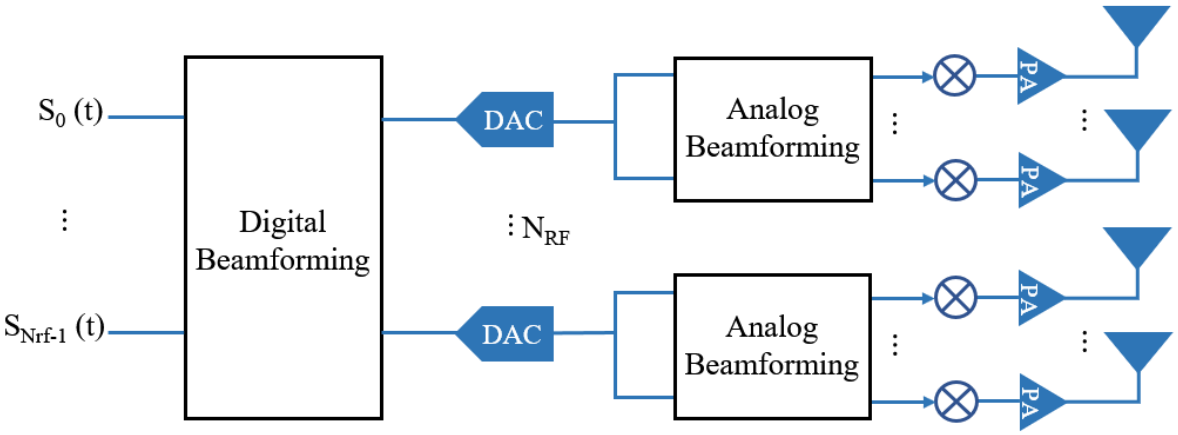

Figure 4.5: Hybrid sub-connected beamforming architecture.

There are two types of hybrid sub-connected architectures that are the fixed and the dynamic architectures. In the fixed sub-connected architecture, each RF chain are permanently connected to the same fixed subset of antennas and do not change. Contrary, the dynamic sub-connected architecture selects dynamically the subset of antennas that each RF chain connect.

Figure 4.6 illustrates the hybrid fixed sub-connected architecture and Figure 4.7 illustrate hybrid dynamic sub-connected architecture [97]. In these two figures are considered that hybrid fixed or dynamic sub-connected architecture is applied at the transmitter with N_{tx} transmit antennas.

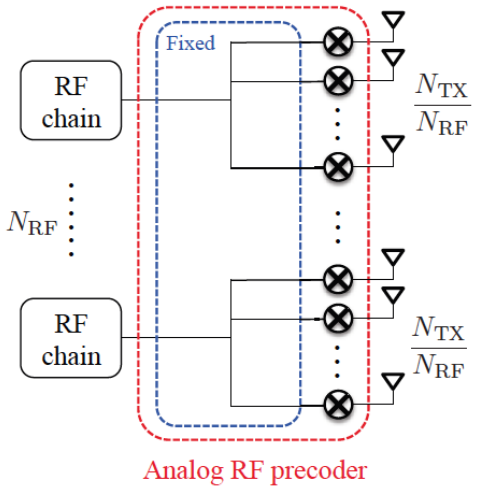

Figure 4.6: Hybrid fixed sub-connected architecture [97].

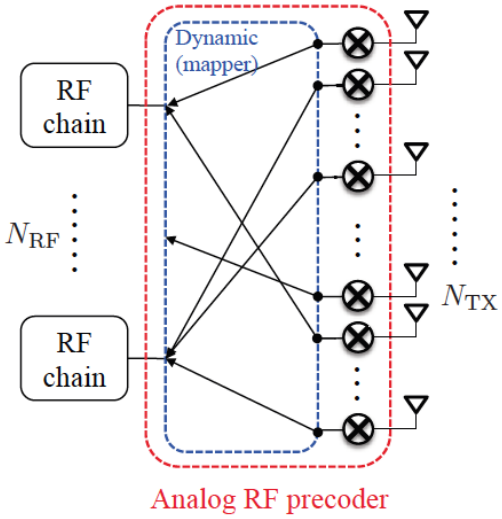

Figure 4.7: Hybrid dynamic sub-connected architecture [97].

To sum up, when the hybrid architectures are compared with full digital one, the performance of the hybrid solution is limited by the number of RF chains, but it is possible to design efficient signal processing schemes to achieve a performance close the fully digital counterpart [74][35]. Figure 4.8 compares the performance of a hybrid architecture with analog and unconstrained digital solutions. As we can see, the hybrid spectral efficiency performance is close to the achieved by the optimal unconstrained solution. Therefore, the hybrid solutions are a good alternative to the standard fully digital approach.

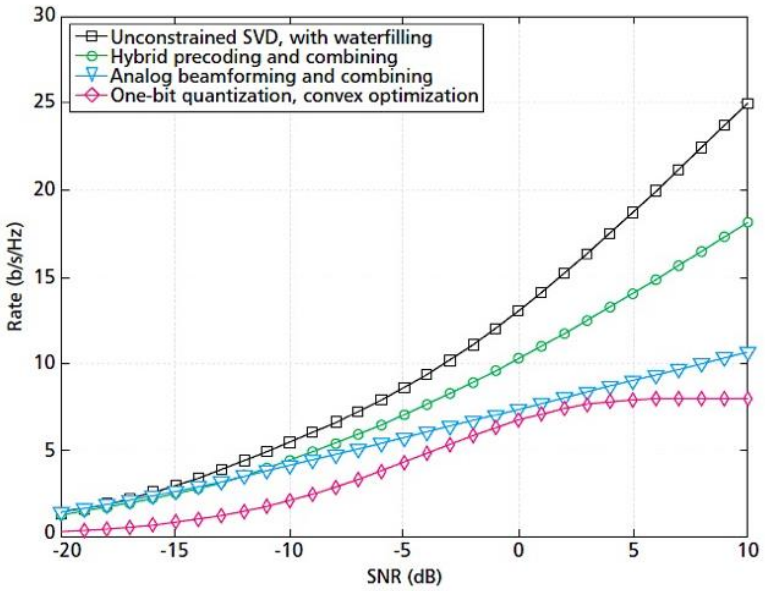

Figure 4.8: Spectral efficiency comparison of different architectures [74].

4.4.2 Low Resolution ADC's

Normally, for mmW mMIMO systems, the ADCs have 6 or more bits of resolution. However, with the increase of high data rates, the high resolution ADCs construction is very expensive and consumes much power. In order to reduce the costs and the power consumption, low resolution ADCs (1-3 bits) are a solution. Low resolution ADCs also do not require automatic gain control (AGC) that simplifies the circuit complexity. A receiver structure where 1-bit ADC is used for each in phase and quadrature baseband received signal is depicted in Figure 4.9. In this figure, we also see that each antenna has one RF chain dedicated and two 1-bit ADC's. So, the main focus of the low resolution ADCs is in the receiver [74][98].

Comparing this solution with the hybrid architecture, the low resolution ADCs is more cost efficient but needs more RF chains in the receiver and the capacity of data is limited. Nevertheless, the use of the low resolution ADC provides a cost effective and a less power consumption but this bring a limitation in the capacity of the channel [74].

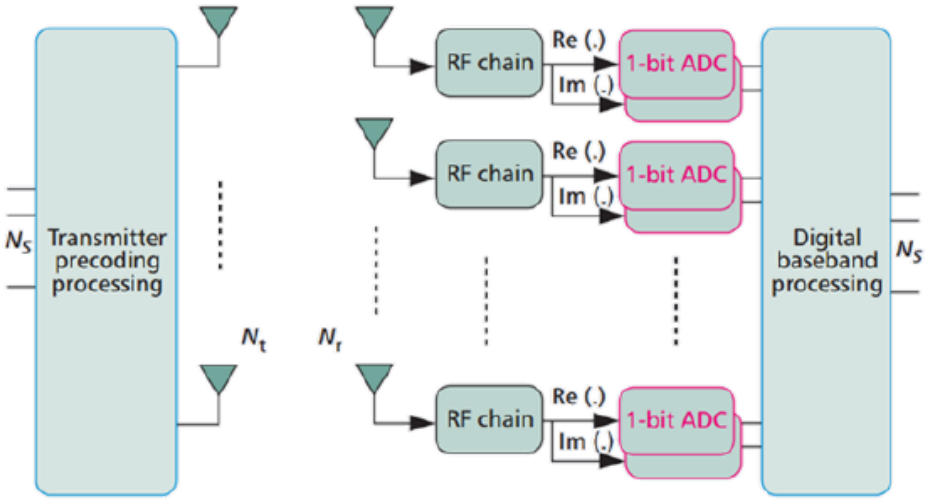

Figure 4.9: System model 1-bit ADC [74].

5. Multi-User Linear Equalizer and Precoder Scheme for Hybrid Sub-Connected Broadband Millimeter Wave Systems

Millimeter waves and massive MIMO are two promising key technologies to achieve the high demands of data rate for the future mobile communication generation. Due to hardware limitations, these systems employ hybrid analog-digital architectures. Nonetheless, most of the works developed for hybrid architectures focus on narrowband channels and is expected that millimeter waves be wideband. Moreover, it is more feasible to have a sub-connected architecture than a fully connected one, due to the hardware constraints. Therefore, the aim of this dissertation is to design a sub-connected hybrid analog-digital multi-user linear equalizer combined with an analog precoder to efficiently remove the multi-user interference. We basically extend the work proposed in [38] for full connected architecture to sub-connected one. We consider low complexity user terminals employing pure analog precoders, computed with the knowledge of a quantized version of the average angles of departure of each cluster. At the base station, the hybrid multi-user linear equalizer is optimized by using the BER as a metric over all the subcarriers. The analog domain hardware constraints together with the assumption of a flat analog equalizer over the subcarriers, considerably increase the complexity of the corresponding optimization problem. To simplify the problem at hand, the merit function is first upper bounded, and by leveraging the specific properties of the resulting problem, we show that the analog equalizer may be computed iteratively over the RF chains by assigning the users in an interleaved fashion to the RF chains. The proposed hybrid sub-connected scheme is compared with a recently proposed fully connected counterpart [38].

In this Chapter we describe the transmitter, channel and receiver system model. After we described the analog precoder employed at each UT and is derived the sub-connected hybrid analog-digital multi-user equalizer. Finally, the main performance results are presented.

5.1 System Model

In this section, we describe the transmitter, the channel model and the receiver for the considered uplink massive MIMO mmW SC-FDMA system.

5.1.1 Transmitter Model Description

We assume U UTs sharing the same radio resources, each equipped with N_{tx} transmit antennas and with a single RF chain. Figure 5.1 presents the general schematic of the *u*th user terminal. Firstly, the time domain N_c-length sequence $\left\{s_{u,t}\right\}_{t=0}^{N_c-1}$, with $\mathbb{E}[|s_{u,t}|^2]=1$, is divided into R data blocks of size $N_s = N_c/R$, where $\left\{s_{u,t}\right\}_{t=(r-1)N_s}^{rN_s-1}$ represents the *r*th data block. Then, this time domain sequence is moved to the frequency domain and the resulting sequence denominated by $\left\{c_{u,k}\right\}_{k=(r-1)N_s}^{rN_s-1}$, where $\left\{c_{u,k}\right\}_{k=(r-1)N_s}^{rN_s-1}$ is the discrete Fourier transform (DFT) of the time domain sequence $s_{u,t}$. After that, the frequency domain data are interleaved and mapped to the OFDM symbol. To simplify the formulation, we assume that $N_s = N_c$, which means that only a single N_c-length block is considered and assume the identity mapping. Therefore, the frequency domain sequence $\left\{c_{u,k}\right\}_{k=0}^{N_c-1}$ is the DFT of the full-time sequence $\left\{s_{u,t}\right\}_{t=0}^{N_c-1}$. After the CP, an analog precoder $\mathbf{f}_{a,u} \in \mathbb{C}^{N_{tx}}$ is employed. Due to the hardware constraints, we only consider analog phase shifters that force all coefficients of the precoder to equal norm, i.e., $\left|\mathbf{f}_{a,u}\right|^2 = 1/N_{tx}$ and furthermore it is assumed that they are constant over the subcarriers. So, the discrete transmit complex baseband signal $\mathbf{x}_{u,k} \in \mathbb{C}^{N_{tx}}$ of the *u*th user at subcarrier *k* can be represented as

$$\mathbf{x}_{u,k} = \mathbf{f}_{a,u} c_{u,k} \text{ , . } \tag{5.1}$$

where $c_{u,k} \in \mathbb{C}$. The design of the analog precoder coefficients will be presents in Section 5.1.4. We assume that the number of users is lower that the number of RF chains at the receiver, $U \le N_{RF}$.

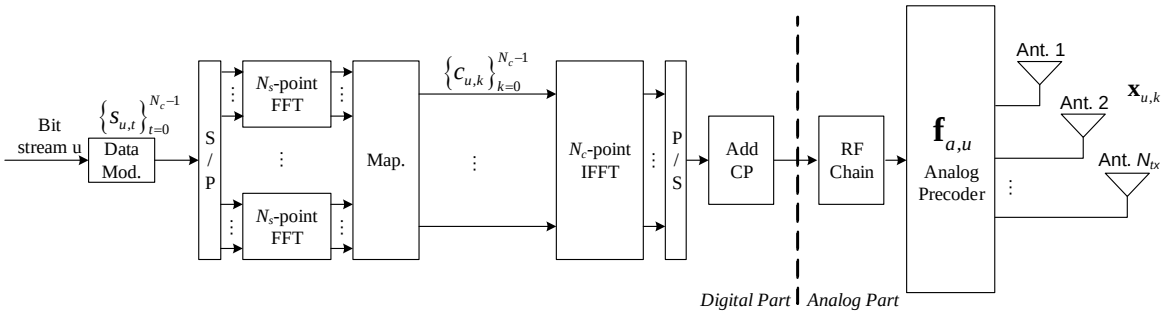

Figure 5.1: Schematic of the *u*th user terminal transmitter.

5.1.2 Channel Model Description

We assume a channel given by the sum of the contribution of N_{cl} clusters, each one contributes with N_{ray} propagation paths. The considered delay-d MIMO channel matrix of the uth user can be written as

$$\mathbf{H}_{u,d} = \sqrt{\frac{N_{tx}N_{rx}}{\rho_{PL}}} \sum_{q}^{N_{cl}} \sum_{l}^{N_{ray}} \left(\alpha_{q,l}^{u} p_{rc}\left(dT_S - \tau_q^u - \tau_{q,l}^u \right) \mathbf{a}_{tx,u}\left(\theta_q^u - \vartheta_{q,l}^u \right) \mathbf{a}_{rx,u}^H \left(\phi_q^u - \varphi_{q,l}^u \right) \right), \tag{5.2}$$

and the corresponding frequency domain channel matrix $\mathbf{H}_{u,k} \in \mathbb{C}^{N_{rx} \times N_{tx}}$ of the *u*th user at the *k*th subcarrier can be given by

$$\mathbf{H}_{u,k} = \sum_{d=0}^{D-1} \mathbf{H}_{u,d} e^{-j\frac{2\pi k}{N_c} d}, \tag{5.3}$$

where N_{rx} represents the number of receive antennas, ρ_{PL} represents the path-loss between the transmitter and the receiver, $\alpha_{q,l}^u$ is the complex path gain of the *l*th ray in the *q*th scattering cluster, and a raised-cosine filter is adopted for the pulse shaping function $p_{rc}(.)$ for T_S -spaced signaling as in [37]. The *q*th cluster has a time delay τ_q^u, angles of arrival θ_q^u, and departure ϕ_q^u. Each ray l from *q*th cluster has a relative time delay $\tau_{q,l}^u$, relative angles of arrival $\vartheta_{q,l}^u$, and departure $\varphi_{q,l}^u$. The paths delay is uniformly distributed in $[0, DT_s]$ where D is the length of the CP, and the angles follow the random distribution mentioned in [37], such that $\mathbb{E}[\|\mathbf{H}_{u,d}\|_F^2] = N_{rx}N_{tx}$. Finally, the vectors $\mathbf{a}_{rx,u}$ and $\mathbf{a}_{tx,u}$ represent the normalized receive and transmit array response vectors, respectively. For an N-element uniform linear array (ULA), the array response vector can be given by

$$\mathbf{a}_{ULA}(\theta)=\frac{1}{\sqrt{N}}\left[1,e^{jkp\sin(\theta)},...,e^{j(N-1)kp\sin(\theta)}\right]^{T}, \tag{5.4}$$

where $k=2\pi/\lambda$, λ is the wavelength, and p is the inter-element spacing. The channel matrix of the *u*th user can also be expressed as

$$\mathbf{H}_{u,k}=\mathbf{A}_{rx,u}\mathbf{\Delta}_{u,k}\mathbf{A}_{tx,u}^{H} \tag{5.5}$$

where $\mathbf{\Delta}_{u,k}$ is a diagonal matrix, with entries (q,l) that correspond to the paths gains of the lth ray in the *q*th scattering cluster. $\mathbf{A}_{tx,u}=[\mathbf{a}_{tx,u}(\theta_1^u-\vartheta_{1,1}^u),\ldots,\mathbf{a}_{tx,u}(\theta_{N_{cl}}^u-\vartheta_{N_{cl},N_{ray}}^u))]$ and $\mathbf{A}_{rx,u}=[\mathbf{a}_{rx,u}(\phi_1^u-\varphi_{1,1}^u),\ldots,\mathbf{a}_{rx,u}(\phi_{N_{cl}}^u-\varphi_{N_{cl},N_{ray}}^u))]$ hold the transmit and receive array response vectors of the *u*th user, respectively.

5.1.3 Receiver Model Description

At the receiver we consider a hybrid analog-digital sub-connected architecture, where each RF chain is connected into a group of $R=N_{rx}/N_{RF}$ antennas, where N_{RF} is the number of RF chains, as represented in Figure 5.2. We assume that the number of RF chains is lower that the number of receive antennas, $N_{RF}\le N_{rx}$.

The frequency domain received signal at the *k*th subcarrier $\mathbf{y}_k\in\mathbb{C}^{N_{rx}}$ can be written as,

$$\mathbf{y}_k=\sum_{u=1}^{U}\mathbf{H}_{u,k}\mathbf{x}_{u,k}+\mathbf{n}_k=\sum_{u=1}^{U}\mathbf{H}_{u,k}\mathbf{f}_{u,k}c_{u,k}+\mathbf{n}_k, \tag{5.6}$$

where $\mathbf{n}_k\in\mathbb{C}^{N_{rx}}$ is the zero mean Gaussian noise with variance σ_n^2. We consider a sub-connected hybrid analog-digital multi-user equalizer to efficiently separate the users, as shown in Figure 5.2. Initially, the signal is processed through phase shifters modelled by the vector $\mathbf{w}_{a,r}\in\mathbb{C}^{R}$, where all elements of $\mathbf{w}_{a,r}$ have equal norms $(|\mathbf{w}_{a,r}(n)|^2=1/N_{rx})$. The overall analog matrix $\mathbf{W}_a\in\mathbb{C}^{N_{rx}\times N_{RF}}$ that represents the connection between each subset of N_{rx}/N_{RF} antennas and the corresponding N_{RF} chain, has a block diagonal structure

$$\mathbf{W}_a=\mathrm{diag}\left[\mathbf{w}_{a,1},...,\mathbf{w}_{a,r},...,\mathbf{w}_{a,N_{RF}}\right],\ r=1,...,N_{RF}. \tag{5.7}$$

As the analog precoder, we also assume that the analog part of the equalizer is constant for all subcarriers.

After that, the CP is removed on each RF chain and the signal is moved to the frequency domain by applying the DFT. Then, the samples of each carrier pass through the digital part of the equalizer modeled by matrix $\mathbf{W}_{d,k} \in \mathbb{C}^{N_{RF} \times U}$. Therefore, the resulting signal in the end of the analog and digital processing equalizer can be written as

$$\tilde{\mathbf{c}}_k = \mathbf{W}_{d,k}^H \mathbf{W}_a^H \mathbf{H}_{eq,k} \mathbf{c}_k + \mathbf{W}_{d,k}^H \mathbf{W}_a^H \mathbf{n}_k \tag{5.8}$$

where $\mathbf{H}_{eq,k} = \begin{bmatrix} \mathbf{H}_{1,k}\mathbf{f}_{1,k} & \cdots & \mathbf{H}_{U,k}\mathbf{f}_{U,k} \end{bmatrix} \in \mathbb{C}^{N_{rx} \times U}$ represents the overall equivalent channel between the U users and the receiver, and $\mathbf{c}_k \in \mathbb{C}^U$ denotes the frequency domain transmitted signal of all users at the kth subcarrier. Finally, the equalized signals are demapped and moved to the time domain by using the inverse DFT (IDFT) obtaining the estimates $\left\{\tilde{s}_{u,t}\right\}_{t=0}^{N_c-1}$ of the uth user transmitted N_c-length data block $\left\{s_{u,t}\right\}_{t=0}^{N_c-1}$.

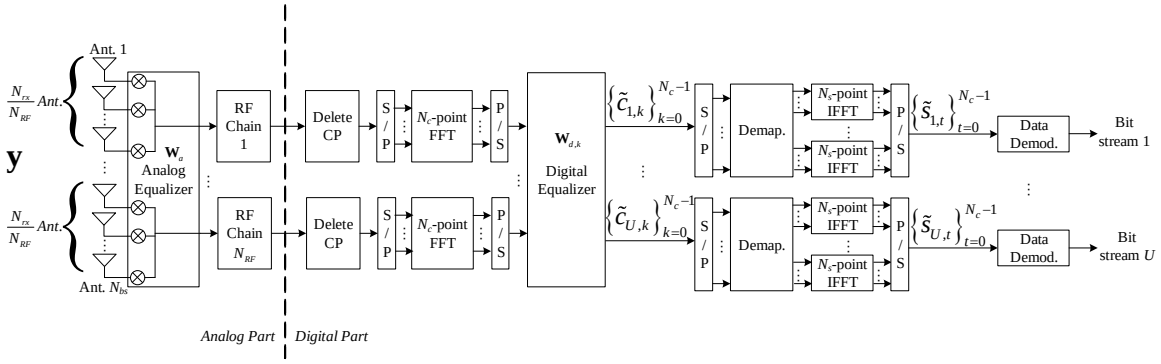

Figure 5.2: Schematic of the receiver.

5.1.4 Analog Precoder Design

In this section we design a low complexity analog precoders to be employed at the transmitters. These precoders are computed based on the knowledge of partial CSI, i.e. only a quantized version of the average AoD θ_q^u , $q = 1,...N_{cl}$ of each cluster is used. These angles estimated at the receiver are quantized as

$$\tilde{\theta}_q^u = f_Q\left(\theta_q^u\right), q = 1,...N_{cl}, u = 1,...,U, \tag{5.9}$$

and then sent to the transmitters. In this dissertation, for the sake of simplicity, we consider uniform quantizers, i.e., an uniform f_Q has 2^n levels equally spaced between clipping levels $-A_m$ and A_m.

With the knowledge of these quantized angles, user *u* should start by computing the correlation matrix $\mathbf{R}_u = \tilde{\mathbf{A}}_{tx,u}\tilde{\mathbf{A}}_{tx,u}^H$, where the overall matrix $\tilde{\mathbf{A}}_{tx,u} \in \mathbb{C}^{N_{tx}\times N_{cl}}$ is given as

$$\tilde{\mathbf{A}}_{tx,u} = [\mathbf{a}_{tx,u}(\tilde{\theta}_1^u),\ldots,\mathbf{a}_{tx,u}(\tilde{\theta}_q^u),...,\mathbf{a}_{tx,u}(\tilde{\theta}_{N_{cl}}^u)], \tag{5.10}$$

with $\mathbf{a}_{tx,u}(\tilde{\theta}_q^u)$ computed from

$$\mathbf{a}_{tx,u}(\tilde{\theta}_q^u) = \frac{1}{\sqrt{N_{tx}}}\left[1, \mathrm{e}^{jkd\sin(\tilde{\theta}_q^u)},...,\mathrm{e}^{j(N_{tx}-1)kd\sin(\tilde{\theta}_q^u)}\right], . \tag{5.11}$$

To compute the analog precoders we first need to apply the eigenvalue decomposition to the correlation matrix $\mathbf{R}_u$, i.e. $\mathbf{R}_u = \mathbf{U}_{tx,u}\mathbf{D}_{tx,u}\mathbf{V}_{tx,u}^H$. Finally, the proposed analog precoders of the *u*th user is set as

$$\mathbf{f}_{a,u}(n_{tx}) = \frac{1}{\sqrt{N_{tx}}}\mathrm{e}^{j\arg(\mathbf{U}_{tx,u}(n_{tx},1))}\ , n_{tx} = 1,..,N_{tx}, \tag{5.12}$$

where $\mathbf{U}_{tx,u}(n_{tx},1)$, $n_{tx} = 1,...,N_{tx}$ represents the largest singular value of the correlation matrix $\mathbf{R}_u$. Hence, the beam follows the best channel direction improving the transmit/receive link reliability.

5.1.5 Multi-User Equalizer Design

In this section, we design a hybrid analog-digital sub-connected equalizer for multi-user mmW mMIMO to be employed at the receiver side. A decoupled transmitter-receiver optimization problem is assumed in this dissertation, since a joint optimization problem is a very complex task. The overall analog matrix $\mathbf{W}_a$ defined in (5.7) and the digital matrix $\{\mathbf{W}_{d,k}\}_{k=0}^{N_c-1}$ are optimized by minimizing the BER, which is equivalent to minimize the MSE.

It can be shown that the digital part of the equalizer that minimizes the BER is given by

$$\mathbf{W}_{d,k} = \left(\mathbf{W}_a^H\mathbf{H}_{eq,k}\mathbf{H}_{eq,k}^H\mathbf{W}_a + \sigma_n^2\mathbf{W}_a^H\mathbf{W}_a\right)^{-1}\mathbf{W}_a^H\mathbf{H}_{eq,k}, \tag{5.13}$$

since it maximizes the overall signal-to-interference-plus-noise-ration of the *u*th at time *t*, $\mathrm{SINR}_{u,t}$, i.e., the SINR relatively to data symbol $s_{u,t}$ [38].

Let us now describe the method to compute the analog part of the considered sub-connected architecture. By using the matrix inversion lemma [99], the overall analog-digital equalizer matrix simplifies to

$$\mathbf{W}_a\mathbf{W}_{d,k} = \mathbf{W}_a\left(\mathbf{W}_a^H\mathbf{W}_a\right)^{-1}\mathbf{W}_a^H\mathbf{H}_{eq,k}\left(\mathbf{H}_{eq,k}^H\mathbf{W}_a\left(\mathbf{W}_a^H\mathbf{W}_a\right)^{-1}\mathbf{W}_a^H\mathbf{H}_{eq,k}+\sigma_n^2\mathbf{I}\right)^{-1}. \quad (5.14)$$

Assuming QPSK constellations for simplicity and without loss of generality, the average BER can be written as

$$\mathrm{BER} = \frac{1}{N_c U}\sum_{t=0}^{N_c-1}\sum_{u=1}^{U}\mathcal{Q}\left(\sqrt{2\mathrm{SINR}_{u,t}}\right), \quad (5.15)$$

where $\mathcal{Q}$ represents the well-known Q-function and with the $\mathrm{SINR}_{u,t}$ given by

$$\mathrm{SINR}_{u,t}\left[\mathbf{W}_a\right] = \left(\frac{\sigma_n^2}{N_c}\sum_{k=0}^{N_c-1}\left[\left(\mathbf{H}_{eq,k}^H\mathbf{W}_a\left(\mathbf{W}_a^H\mathbf{W}_a\right)^{-1}\mathbf{W}_a^H\mathbf{H}_{eq,k}+\sigma_n^2\mathbf{I}\right)^{-1}\right]_{u,u}\right)^{-1}-1, \quad (5.16)$$

where $\left[\mathbf{A}\right]_{n,n}$ represents the entry of the *u*th row and column of matrix $\mathbf{A}$. From (5.16) we see that $\mathrm{SINR}_{u,t}$ is independent of the time index. So, we can simplify (5.15) as,

$$\mathrm{BER} = \frac{1}{U}\sum_{u=1}^{U}\mathcal{Q}\left(\sqrt{2\mathrm{SINR}_u\left[\mathbf{W}_a\right]}\right), \quad (5.17)$$

with $\mathrm{SINR}_u = \mathrm{SINR}_{u,1} = \mathrm{SINR}_{u,2} = \ldots = \mathrm{SINR}_{u,\mathrm{N}_c}$.

The optimization problem to compute the analog part of the equalizer may be mathematically formulated as

$$\left(\mathbf{W}_a\right)_{\mathrm{opt}} = \arg\min_{\mathbf{W}_a}\ \mathrm{BER}\left[\mathbf{W}_a\right],\ \text{s.t. } \mathbf{W}_a \in \mathcal{W}_a\ , \quad (5.18)$$

where $\mathcal{W}_a = \left\{\mathbf{W}_a : \mathbf{W}_a = \mathrm{diag}\left[\mathbf{w}_{a,1},...,\mathbf{w}_{a,r},...,\mathbf{w}_{a,N_{RF}}\right], |\mathbf{w}_{a,r}(n)|^2 = 1/N_{rx}\right\}$ denotes the feasible set for the analog equalizer. Due to the non-convex nature of the merit function and the constraint imposed in (5.18), it is difficult or even impossible to obtain an analytical solution to the optimization problem at hand. Moreover, as we are considering a multi-user scenario, the resulting average BER is a weighted function of the average BER for each user, making it even harder to obtain a solution to the aforementioned problem. Hence, instead of an exact solution to (5.18) we will derive, in the following, an algorithm to obtain an approximate solution to the previous optimization problem.

Using the exponential upper bound of the Q-function $(\mathcal{Q}(x) \le (1/2)e^{-x^2/2})$, we obtain $\mathcal{Q}(x) \le (1/2)(1+x^2/2)^{-1}$, and as a consequence we have

$$\text{BER} \le \frac{1}{2U}\sum_{u=1}^{U}\frac{1}{1+\text{SINR}_u}. \tag{5.19}$$

Replacing (5.16) in (5.19) and after some mathematical manipulations we obtain,

$$\text{BER} \le \frac{\sigma_n^2}{2UN_c}\sum_{u=1}^{U}\sum_{k=0}^{N_c-1}\left[\mathbf{H}_{eq,k}^H\mathbf{W}_a\left(\mathbf{W}_a^H\mathbf{W}_a\right)^{-1}\mathbf{W}_a^H\mathbf{H}_{eq,k}+\sigma_n^2\mathbf{I}\right]_{u.u}^{-1}, \tag{5.20}$$

and then an approximate solution to the optimization problem (5.18) may be obtained from the following simplified optimization problem,

$$\mathbf{W}_a = \arg\min_{\mathbf{W}_a}\sum_{u=1}^{U}\sum_{k=0}^{N_c-1}\left(\mathbf{h}_{eq,u,k}^H\mathbf{W}_a\left(\mathbf{W}_a^H\mathbf{W}_a\right)^{-1}\mathbf{W}_a^H\mathbf{h}_{eq,u,k}+\sigma_n^2\right)^{-1},\ \text{s.t. } \mathbf{W}_a\in\mathcal{W}_a, \tag{5.21}$$

where $\mathbf{h}_{eq,u,k}\in\mathbb{C}^{N_{rx}}$ represents the equivalent channel of user *u*. To solve it, we propose to iteratively compute matrix $\mathbf{W}_a$ column by column, which in practice corresponds to iteratively add RF chains to the receiver. Let matrix $\mathbf{W}_a^{(i)}$ and vector $\mathbf{w}_a^{(i)}$ denote the first i columns and column i of matrix $\mathbf{W}_a$, respectively, we can define $\mathbf{W}_a^{(i)}=[\mathbf{W}_a^{(i-1)},\mathbf{w}_a^{(i)}]$. The aim is to compute $\mathbf{w}_a^{(i)}$ iteratively instead to compute the overall matrix $\mathbf{W}_a$ at once, and thus the optimization problem can be modified as

$$\left(\mathbf{w}_a^{(i)}\right)_{\text{opt}} = \arg\min_{\mathbf{w}_a^{(i)}}\sum_{u=1}^{U}\sum_{k=0}^{N_c-1}\left(\mathbf{h}_{eq,u,k}^H\mathbf{W}_a^{(i)}\left(\left(\mathbf{W}_a^{(i)}\right)^H\mathbf{W}_a^{(i)}\right)^{-1}\left(\mathbf{W}_a^{(i)}\right)^H\mathbf{h}_{eq,u,k}+\sigma_n^2\right)^{-1},\quad \text{s.t. } \mathbf{W}_a\in\mathcal{W}_a. \tag{5.22}$$

To further simplify the optimization problem we associate a given user, denoted by u_i, to iteration i. We propose to do this association using the following mapping between users and iterations $u_i = i \bmod U$, i.e., the U users are interleaved along the iterations. For example, for $N_{RF}=4$ and $U=2$, we have $[u_1,u_2,u_3,u_4]=[1,2,1,2]$. With this assumption (5.22) simplifies to

$$\mathbf{w}_a^{(i)} = \arg\min_{\mathbf{w}_a^{(i)}}\sum_{k=0}^{N_c-1}\left(\mathbf{h}_{eq,u_i,k}^H\mathbf{W}_a^{(i)}\left(\left(\mathbf{W}_a^{(i)}\right)^H\mathbf{W}_a^{(i)}\right)^{-1}\left(\mathbf{W}_a^{(i)}\right)^H\mathbf{h}_{eq,u_i,k}+\sigma_n^2\right)^{-1},\quad \text{s.t. } \mathbf{W}_a\in\mathcal{W}_a. \tag{5.23}$$

From the definition of $\mathbf{W}_a^{(i)}$ and the Gram-Schmidt orthogonalization follows $\mathbf{W}_a^{(i)}(\mathbf{W}_a^{(i)^H}\mathbf{W}_a^{(i)})^{-1/2}=[\mathbf{U}^{i-1},\mathbf{P}^{(i-1)}\mathbf{w}_a^{(i)}]$ [37], where $\mathbf{P}^{(i-1)}=\mathbf{I}-\mathbf{U}^{(i-1)}\mathbf{U}^{(i-1)^H}$, and $\mathbf{U}^{(i-1)}=\mathbf{W}_a^{(i-1)}(\mathbf{W}_a^{(i-1)^H}\mathbf{W}_a^{(i-1)})^{-1/2}$. Therefore, the optimization problem (5.22) can be approximated by

$$\mathbf{w}_a^{(i)} = \arg \min_{\mathbf{w}_a^{(i)}} \left(\sum_{k=0}^{N_c-1} \left(\mathbf{h}_{eq,u_i,k}^H \mathbf{P}^{(i-1)} \mathbf{w}_a^{(i)} \mathbf{w}_a^{(i)^H} \mathbf{P}^{(i-1)^H} \mathbf{h}_{eq,u_i,k} + \alpha_{u_i,k}^{(i)} + \sigma_n^2 \right)^{-1} \right), \quad \text{s.t. } \mathbf{w}_a^{(i)} \in \mathcal{W}_{a,u_i}. \tag{5.24}$$

where $\mathcal{W}_{a,u_i}$ represents the column *i* of the elements of set $\mathcal{W}_a$ and $\alpha_{u_i,k}^{(i)} = \mathbf{h}_{eq,u_i,k}^H \mathbf{U}^{(i-1)} \mathbf{U}^{(i-1)^H} \mathbf{h}_{eq,u_i,k}$. In spite of the previous simplifications, the optimization problem is still non-convex and hard to solve due to the constraint $\mathbf{w}_a^{(i)} \in \mathcal{W}_{a,u_i}$. Therefore, to further simplify it, we replace the set $\mathcal{W}_{a,u_i}$ by the codebook $\mathcal{F}_{a,u_i} = \mathbf{D}_{u_i} \mathbf{A}_{rx,u_i}$, where $\mathbf{D}_{u_i}$ is a block diagonal matrix where all blocks are zero except u_i, which is equal to the identity matrix, i.e., the elements of the codebook are the normalized receiver array response vectors, which leads to the simpler optimization problem

$$\mathbf{w}_a^{(i)} = \arg \min \sum_{k=0}^{N_c-1} \left(\mathbf{w}_a^{(i)^H} \mathbf{P}^{(i-1)^H} \mathbf{h}_{eq,u_i,k} \mathbf{h}_{eq,u_i,k}^H \mathbf{P}^{(i-1)} \mathbf{w}_a^{(i)} + \alpha_{u_i,k}^{(i)} + \sigma_n^2 \right)^{-1}, \quad \text{s.t. } \mathbf{w}_a^{(i)} \in \mathcal{F}_{a,u_i}. \tag{5.25}$$

The procedure to obtain the analog part of the equalizer matrix is presented in Table 5.1. It can be summarized as follows, firstly we start with user 1, $\mathbf{U}^{(0)} = 0$ (line 1) and compute the projection matrix $\mathbf{P}^{(1)}$ (line 4). After that, we compute the merit function of the optimization problem (5.25) for each element of the codebook $\mathcal{F}_{a,u_1}$ (lines 5-9). Vector $\mathbf{w}_a^{(1)}$ is set to be equal to the element of codebook $\mathcal{F}_{a,u_1}$ with the lowest value (lines 10-11). Then, the column vector $\mathbf{P}^{(0)} \mathbf{w}_a^{(1)}$ is added to matrix $\mathbf{U}^{(0)}$ to form $\mathbf{U}^{(1)}$ (line 12). With $\mathbf{U}^{(1)}$, the same procedure may be repeated for the other users according to the mapping between users and iterations defined by $u_i = i \bmod U$.

To compute the optimization problem of (5.25), we need to compute the correlation matrix $\alpha_{u_i,k}^{(i)} + \mathbf{w}_a^{(i)^H} \mathbf{P}^{(i-1)^H} \mathbf{h}_{eq,u_i,k} \mathbf{h}_{eq,u_i,k}^H \mathbf{P}^{(i-1)} \mathbf{w}_a^{(i)}$ for all the elements of the selected codebook $\mathcal{F}_{a,u_1}$, which may be accomplished with the following expression

$$\mathbf{r}_{i,k} = \alpha_{u_i,k}^{(i)} + \text{diag}\left(\mathbf{A}_{rx,u_i}^H \mathbf{D}_{u_i} \mathbf{P}^{(i-1)^H} \mathbf{h}_{eq,u_i,k} \mathbf{h}_{eq,u_i,k}^H \mathbf{P}^{(i-1)} \mathbf{D}_{u_i} \mathbf{A}_{rx,u_i} \right). \tag{5.26}$$

Notice that $\mathbf{P}^{(i)} \mathbf{P}^{(i)} = \mathbf{P}^{(i)}$ since $\mathbf{P}^{(i)}$ is an idempotent matrix. Nonetheless, as the Gram-Schmidt procedure may lead to a loss of orthogonality among vectors [100], we use a Gram-Schmidt algorithm with reorthogonalization that amounts to applying two times the projection matrix $\mathbf{P}^{(i)}$ or using $(\mathbf{P}^{(i)})^2$ instead of $\mathbf{P}^{(i)}$.

Algorithm 1: The proposed analog-digital multi-user linear equalizer algorithm for sub-connected architecture

Inputs: $N_{rx}, N_{RF}, N_c, \mathbf{H}_{eq}$

Analog Part of the equalizer

1: $\mathbf{U}^{(0)} = 0$

2: **for** i = 1 to N_{RF} **do**

3: $u_i = i \bmod U$

4: $\mathbf{P}^{(i-1)} = \left(\mathbf{I} - \mathbf{U}^{(i-1)}\mathbf{U}^{(i-1)^H}\right)^2$

5: $\mathbf{f}^{(i)} = 0$

6: **for** k = 1 to N_c **do**

7: $\mathbf{r}_{i,k} = \alpha_{u_i,k}^{(i)} + \text{diag}\left(\mathbf{A}_{rx,u_i}^H \mathbf{D}_{u_i} \mathbf{P}^{(i-1)^H} \mathbf{h}_{eq,u_i,k} \mathbf{h}_{eq,u_i,k}^H \mathbf{P}^{(i-1)} \mathbf{D}_{u_i} \mathbf{A}_{rx,u_i}\right)$

8: $\mathbf{f}^{(i)} = \mathbf{f}^{(i)} + (\mathbf{r}_{i,k} + \sigma_n^2)^{-1}$

9: **end for**

10: $(q,l) = \arg\min \mathbf{f}^{(i)}$

11: $\mathbf{w}_a^{(i)} = \mathbf{P}^{(i-1)} \mathbf{a}_{rx,u_i}(\phi_q^{u_i} - \varphi_{q,l}^{u_i})$

12: $\mathbf{U}^{(i)} = \left[\mathbf{U}^{(i-1)}, \mathbf{P}^{(i-1)}\mathbf{w}_a^{(i)} / \left\|\mathbf{w}_a^{(i)}\right\|\right]$

13: $\mathbf{W}_a^{(i)} = [\mathbf{W}_a^{(i-1)}, \mathbf{w}_a^{(i)}]$

14: **end for**

Digital part of the equalizer

$\mathbf{W}_{d,k} = \left(\mathbf{W}_a^H \mathbf{H}_{eq,k} \mathbf{H}_{eq,k}^H \mathbf{W}_a + \sigma_n^2 \mathbf{W}_a^H \mathbf{W}_a\right)^{-1} \mathbf{W}_a^H \mathbf{H}_{eq,k}.$

return: $\mathbf{W}_{d,k}$, $\mathbf{W}_a$

Table 5.1: Proposed hybrid multi-user equalizer algorithm for sub-connected architecture

5.2 Performance Results

In this section, we evaluate the performance of the proposed multi-user linear equalizer and precoder scheme designed for hybrid sub-connected broadband mmW Systems.

The carrier frequency was set to 72 GHz and for each user is considered a clustered wideband channel model, discussed previously, with five clusters $N_{cl}=5$, all with the same average power, such that $\mathrm{E}\left[\|\mathbf{H}_{u,d}\|_F^2\right]=N_{rx}N_{tx}$, and each one contributes with $N_{ray}=3$ propagation path. The path delays are uniformly distributed in the CP interval. We consider a ULA with antenna element spacing set to half-wavelength, but it should be emphasized that the schemes proposed in this dissertation can be applied to any antennas arrays. The azimuth angles of departure and arrival have a Laplacian distribution as in [35] and is considered an angle spread of 10^{o} for both the transmitter and receiver. It is assumed QPSK modulation, a perfect synchronization and CSI know at the receiver side. At the transmitter, only a quantized version of the average angle of departure of each cluster is known. We assume $N_c=64$ subcarriers, and the CP is set to be a quarter of the number of subcarriers, such that $D=N_c/4=16$. The BER is considered the performance metric, presented as a function of E_b/N_0, where E_b is the average bit energy and N_0 is the one-sided noise power spectral density. We consider that the average E_b/N_0 is identical for all the users *u* and is given by $E_b/N_0=\sigma_u^2/(2\sigma_n^2)$.

We consider that each transmitter has a single RF chain and is equipped with $N_{tx}=8$ antennas. At the receiver side, is assumed a sub-connected architecture where each RF chain is connected to a group of $R=N_{rx}/N_{RF}$ antennas, with $N_{rx}=16$ antennas. The results are compared with fully connected counterpart recently proposed in [38].

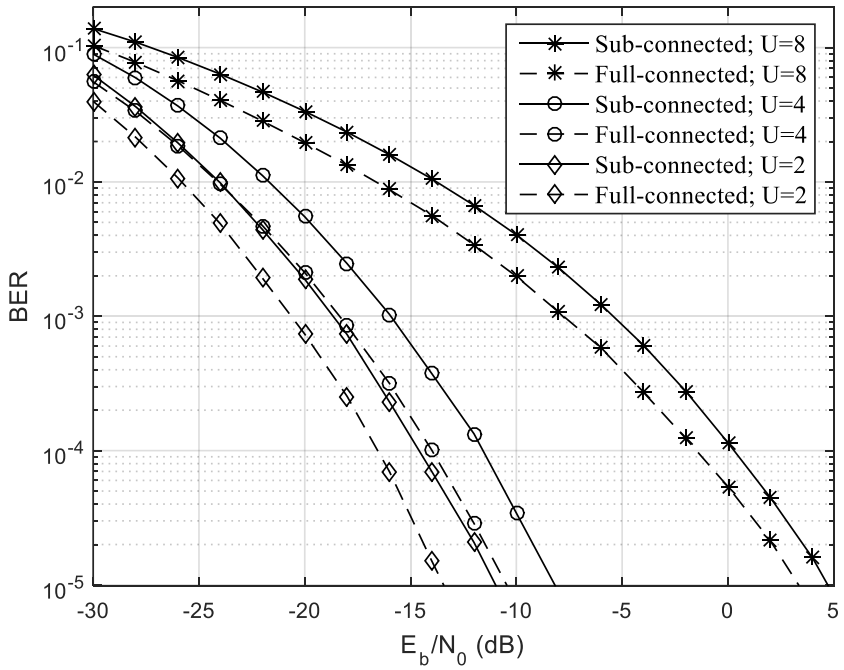

Figure 5.3: Performance of the proposed hybrid sub-connected schemes for $U\in\{2,4,8\}$.

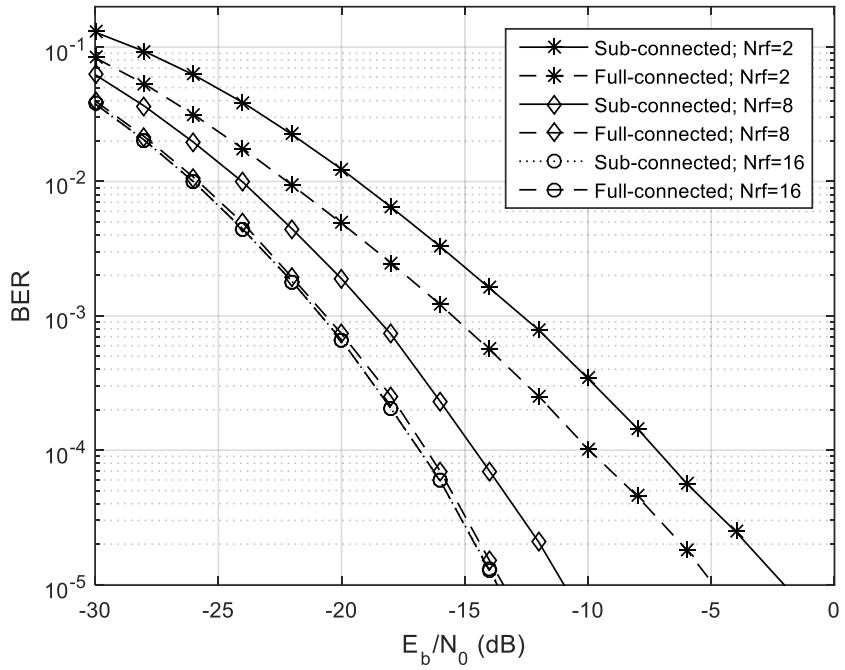

Figure 5.4: Performance of the proposed hybrid sub-connected schemes for $N_{RF} \in \{2,8,16\}$ and $U = 2$.

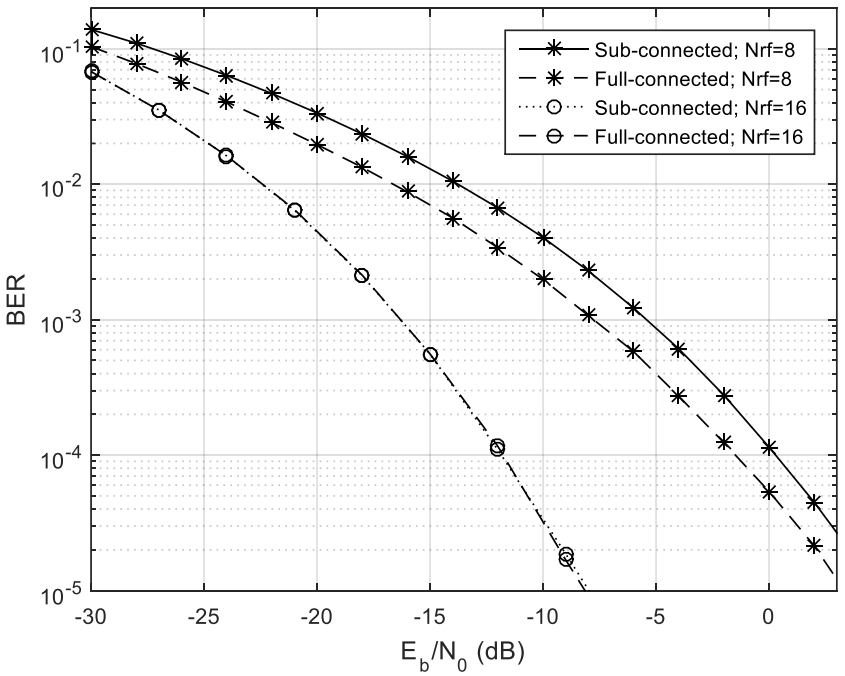

Figure 5.5: Performance of the proposed hybrid sub-connected schemes for $N_{RF} \in \{8,16\}$ and $U = 8$.

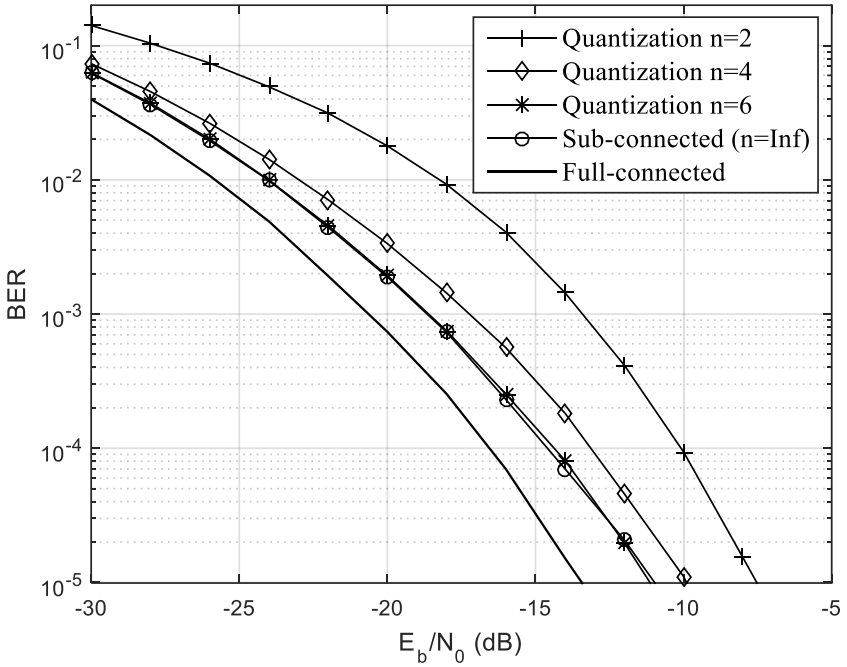

Figure 5.6: Performance of the proposed hybrid sub-connected schemes for different number of quantization bits of the average AoD, $U = 2$.

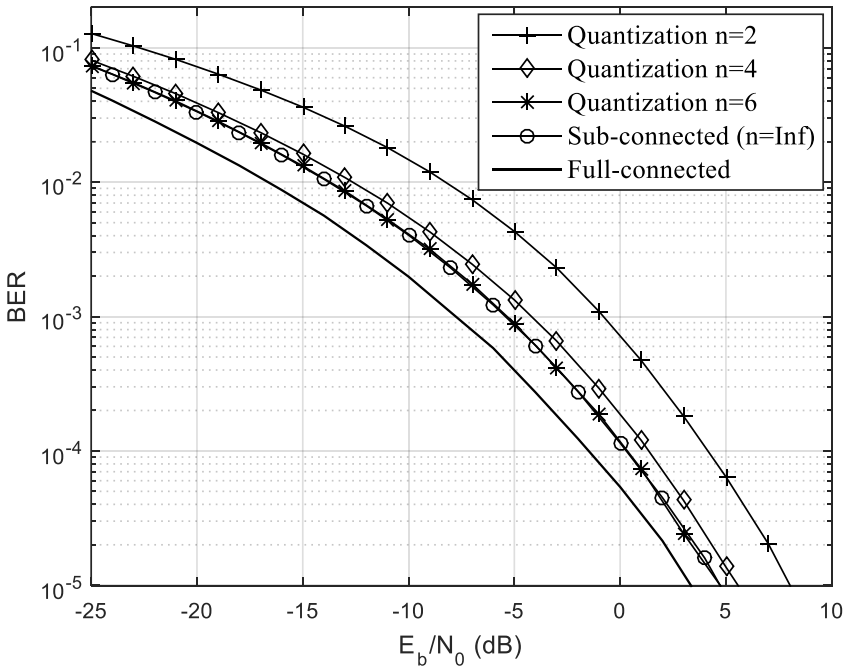

Figure 5.7: Performance of the proposed hybrid sub-connected schemes for different number of quantization bits of the average AoD, $U = 8$.

Figure 5.3 depicts the results for the proposed hybrid sub-connected multi-user equalizer with the analog precoder for 2, 4 and 8 users. In this figure it is assumed perfect knowledge of the average AoD of each cluster. It is also assumed 8 RF chains which means that each one is connected to 2 antennas. As it can be seen the performance of both sub and fully connected improves as the number of users decreases as expected, since the multi-user equalizer has to deals with less interference and the available degrees of freedom can be used to provide more diversity. We can also observe a performance penalty of the sub-connected approach against fully connected one of approximately 2 dB, irrespectively to the number of users, at a target BER of 10^{-3}. This is because the number of connections of the fully-connected architecture is larger than the number of connections for the sub-connected architecture and, as expected, the result for the fully-connected one is better than the sub-connected architecture. The worst performance, for both fully and sub connected approaches, is obtained for full load case, i.e., when the number of user equals to the number of RF chains $N_{RF} = U$.

In Figure 5.4 and Figure 5.5 we present results to different number of RF chains, for 2 and 8 users, respectively. If the number of antennas (R) connected to each RF chain is reduced, we verify that the penalty for fully digital approach decreases. We can observe in Figure 5.4 a penalty of approximately 3 dB, 2 dB and 0 dB for ($R = 4, N_{RF} = 2$), ($R = 2, N_{RF} = 8$) and ($R = 1, N_{RF} = 16$), respectively (BER of 10^{-3}). This happens because reducing the number of antennas connected to each RF chain the degrees of freedom of the sub-connected architecture increases since the number of RF increases and the gap between the sub and fully connected approaches decreases. For the extreme case of $R = 1$ (one RF chain per antenna) the curve obtained for the sub-connected approximately overlaps the one obtained for the fully connected.

In Figure 5.6 and Figure 5.7, we evaluate the impact of imperfect knowledge of the average AoD at the transmitter side. To compute the analog precoders we assume the knowledge of only a quantized version of the average AoD of each cluster, as discussed in previously. We present results for $n = [2, 4, 6]$ quantization bits. Figure 5.6 and Figure 5.7 depicts the results for 2 and 8 users, respectively. As expected, increasing the number of quantization bits improves the performance of the proposed sub-connected scheme and tends to the one achieved for perfect knowledge of the average AoD ($n = \infty$) for both cases $U = 2, 8$. When the number of bits in the quantizer is lower, the performance is worse comparatively to the perfect curve. In Figure 5.6 we can observe a performance penalty, for BER of 10^{-3}, of approximately 5 dB, 1.5 dB and 0 dB, for *n*=2, 4 and 6, respectively. This means that a very limited number of bits for the quantization of the average AoD of each cluster is enough to get a performance close to the perfect case. Since the mmW channels are usually sparse the amount of information needed to be feedback from the BS to the UTs is small.

6. Conclusions and Future Work

In this Chapter we present the main conclusions of this work and provide some insights for future work.

6.1 Conclusions

In this master dissertation, we start by presenting, in Chapter 1, the evolution of the wireless communication systems over the years since the analog communications until the digital era, that allow the high data rates needed to the high demand of the users. In this Chapter 1 we also described the next generation, 5G, which is expected that allows a very high data rates with a low latency.

In Chapter 2 we introduced single and multicarrier systems. We saw that it is possible to obtain a high spectral gain with the OFDM, however, this technique has a high PAPR. After it were described the OFDMA that is an extension of OFDM to multi-user communication systems but also have a high PAPR. Then, SC-FDMA was also described and we saw that this technique offers a low PAPR. In the end of this Chapter it was presented a technique that can be an option for the future wireless communications, CE-OFDM since the PAPR is zero.

Then, it was introduced the concept of the multiple antennas, at the transmitter and receiver, in Chapter 3. We start by presenting the diversity concept and the antennas configurations where we saw that it is possible to obtain diversity and multiplexing with multiple antennas. After, was introduced the spatial multiplexing for single and multi-users. In the end of Chapter 3 it was described the massive MIMO technology with its advantages and disadvantages.

In Chapter 4 we started by presenting the millimeter waves spectrum followed by its opportunities and limitations. After, we presented the conjugation of the millimeters waves systems with the massive MIMO technology that allow us to put more antennas in the same volume than the frequency used currently. With the conjugation of these two keys technologies it is possible to achieve the high demand for high data rates necessary for the next generations of mobile communications. In the end of this Chapter 4 we saw hybrid and low-resolution ADC's architectures.

In this dissertation we proposed, in Chapter 5, an analog precoder combined with an efficient hybrid analog-digital multi-user equalizer for sub-connected mmW massive MIMO SC-FDMA systems. At the UT, we proposed a low complexity pure analog precoder that requires the knowledge of a quantized version of the average AoD of each cluster. At the BS, a hybrid analog-digital multi-user equalizer was developed for a sub-connected architecture. It was assumed that the analog part is constant over all subcarriers, while the digital part is computed on a per subcarrier basis. We considered an MMSE-based equalizer for the digital part, and the analog part is optimized using the average bit-error-rate of all subcarriers as a metric. In order to simplify the optimization problem at hand, the merit function was first upper bounded and then, due to the specific properties of the resulting problem, we showed that the analog part of the hybrid equalizer may be computed iteratively over the RF chains by assigning the users in an interleaved fashion to the RF chains. The main conclusion includes:

- The numerical results showed that the proposed broadband hybrid multi-user linear equalizer is quite efficient at removing the multi-user interference;
- The performance of the proposed system tends to the one achieved by the fully connected counterpart as the number of RF chains increases;
- Only a few number of quantization bits of the average AoD of each cluster is enough to obtain a performance close to the perfect case;
- The small performance gap between the proposed sub-connected approach and the fully connected one, together with the lower complexity make it a very interesting choice for practical systems.

6.2 Future Work

Some suggestions for future work is presented in this section. In the proposed sub-connected hybrid multi-user equalizer we considered, at the analog part, a fixed sub-connected architecture and it would be interesting to evaluate the performance with a dynamic sub-connected architecture where the RF chains connect dynamically to the set of antennas. In the UTs, it was assumed a single RF chain for all the antennas. It would be interesting to design a UT with more than one RF chain and consequently send more than one data stream per time slot. In the same way that we apply a (fixed or dynamic) sub-connected architecture in the BS, it would be interesting to apply this concept at the UT.

Bibliography

[1] A. Silva, A. Gameiro, Comunicações Sem Fios (Wireless Communications), DETI, University of Aveiro, 2016.

[2] The Evolution of Mobile Technologies: 1G – 2G - 3G - 4G LTE [Available online at] https://www.qualcomm.com/media/documents/files/theevolution-of-mobile-technologies-1g-to-2g-to-3g-to-4g-lte.pdf [Accessed] 20/05/18.

[3] D. Tse, and P. Viswanathan, *Fundamentals of Wireless Communications*, Cambridge University Press, 2005.

[4] M. L. Roberts, M. A. Temple, R. F. Mills, and R. A. Raines, "Evolution of The Air Interface of Cellular Communications Systems Toward 4G Realization", *IEEE Commun. Surveys & Tutorials*, vol. 8, no. 1, pp. 2-23, 2006.

[5] B. Anil Kumar, and P. Trinatha Rao, "Overview of Advances in Communication Technologies", in *2015 13th Int. Conf. on Electromagnetic Interference and Compatibility (INCEMIC)*, Visakhapatnam, India, 2015.

[6] Mohinder Jankiraman, *Space-Time Codes and MIMO Systems*, Universal Personal Communications Series, Artech House, 2004.

[7] GSM Bands information by country (April 19, 2018) [Available online at] https://www.worldtimezone.com/gsm.html [Accessed] 07/05/2018.

[8] S. Chia, T. Gill, L. Ibbetson, D. Lister, A. Pollard, R. Irmer, D. Almodovar, N. Holmes, and S. Pike, "3G Evolution", *IEEE Microwave Magazine*, vol. 9, no. 4, pp. 52-63, 2008.

[9] W. Stallings, *Wireless Communications and Networks, Second Edition*, Pearson Prentice Hall, 2005.

[10] WiMAX Technology [Available online at] http://www.recenttechinventions.com/wpcontent/uploads/2012/10/wimaximage.png [Accessed] 08/05/2018

[11] Global Mobile Statistics [Available online at] http://www.5gamericas.org/en/resources/statistics/statistics-global/ [Accessed] 08/05/2018.

[12] S. Sesia, I. Toufik, and M. Baker, *LTE the UMTS Long Term Evaluation: From Theory to Practice*, Jonh Wiley & Sons, 2009.

[13] P. Chan, E. Lo, R. Wang, E. Au, V. Lau, R. Cheng, W. Mow, R. Murch, and K. Letaief, "The Evolution Path of 4G Networks: FDD or TDD?", *IEEE Communications Magazine*, vol. 44, no. 12, pp. 42-50, 2006.

[14] P. Demestichas, A. Georgakopoulos, D. Karvounas, K. Tsagkaris, V. Stavroulaki, J. Lu, C. Xiong, and J. Yao, "5G on the Horizon: Key Challenges for the Radio-Access Network," *IEEE Vehic. Tech. Mag.*, vol. 8, no. 3, pp. 47-53, 2013.

[15] E. Hossain, M. Rasti, H. Tabassum, and A. Abdelnasser, "Evolution toward 5G multi-tier cellular wireless networks: An interference management perspective," *IEEE Wireless Commun.*, vol. 21, no. 3, pp. 118-127, 2014.

[16] W. Roh, J. Seol, J. Park, B. Lee, J. Lee, Y. Kim, J. Cho, K. Cheun, and F. Aryanfar, "Millimeter-Wave Beamforming as an Enabling Technology for 5G Cellular Communications: Theoretical Feasibility and Prototype Results," *IEEE Commun. Mag.*, vol. 52, no. 2, pp. 106-113, 2014.

[17] T. Bogale and L. Le, “Massive MIMO and mmWave for 5G wireless HetNet: potential benefits and challenges,” *IEEE Vehic. Tech. Mag.*, vol. 11, no. 1, pp. 64-75, 2016.

[18] P. Gandotra, R. Jha, and S. Jain, “Green Communication in Next Generation Cellular Networks: A Survey”, *IEEE Access.*, vol.5, pp.11727-11758, 2017.

[19] M. Aydemir, and K. Cengiz, “Emerging infrastructure and technology challenges in 5G wireless networks,”in 2017 *2nd Intern. Multidisciplinary Conf. on Computer and Energy Science (SpliTech),*Split, Croatia, 2017.

[20] A. Swindlehurts, E. Ayanoglu, P. Heydari, and F. Capolino “Millimeter-Wave Massive MIMO: The Next Wireless Revolution?,” *IEEE Commun. Mag.*, vol. 52, no. 9, pp. 56-62, 2014.

[21] Z. Pi, and F. Khan, “An Introduction to Millimeter-Wave Mobile Broadband Systems,” *IEEE Communications Mag.*, vol. 49, no. 6, pp. 101-107, 2011.

[22] K. Prasad, E. Hossain, and V. Bhargava, “Energy Efficiency in Massive MIMO-Based 5G Networks: Opportunities and Challenges,” *IEEE Wireless Commun.*, vol. 24, no. 3, pp. 86-94, 2017.

[23] S. Han, C. Lin I, C. Rowell, Z. Xu, S. Wang, and Z. Pan, “Large Scale Antenna System with Hybrid Digital and Analog Beamforming Structure,” in *IEEE International Conference on Communications Workshops*, Sydney, Australia, 2014.

[24] Conceitos Básicos de 5G [Available online at] https://www.rohde-schwarz.com/br/solucoes/comunicacoes-sem-fio/5g/conceitos-basicos-de-5g/conceitos-basicos-de-5g_229439.html [Accessed] 08/05/2018.

[25] The Mobile Economy 2018 [Available online at] https://www.gsma.com/mobileeconomy/wp-content/uploads/2018/02/The-Mobile-Economy-Global-2018.pdf [Accessed] 08/05/2018.

[26] T. Vu, C. Liu, M. Bennis, M. Debbah, M. Latva-aho, and C. Hong, "Ultra-Reliable and Low Latency Communication in mmWave-Enabled Massive MIMO Networks," *IEEE Commun. Lett.*, vol. 21, no. 9, pp. 2041-2044, 2017.

[27] W. Tan, M. Matthaiou, S. Jin, and X. Li, “Spectral Efficiency of DFT-Based Processing Hybrid Architectures in Massive MIMO,” *IEEE Wireless Commun. Lett.*, vol. 6, no. 5, pp. 586-589, 2017.

[28] A. Alkhateeb, O. Ayach, G. Leus, and R. Heath, “Channel estimation and hybrid precoding for millimeter wave cellular Systems,” *IEEE J. Sel. Topics in Signal Process.*, vol. 8, no. 5, pp. 831-846, 2014.

[29] O. Ayach, S. Rajagopal, S. Surra, Z. Pi, and R. Heath, “Spatially sparse precoding in millimeter wave MIMO systems,” *IEEE Trans. Wireless Commun.*, vol. 13, no. 3, pp. 1499-1513, 2014.

[30] X. Gao, L. Dai, C. Yuen, and Z. Wang, “Turbo-like beamforming based on Tabu search algorithm for millimeter-wave massive MIMO systems,” *IEEE Trans. Veh. Technol.*, vol. 65, no. 7, pp. 5731-5737, 2016.

[31] W. Ni, X. Dong and W. S. Lu, "Near-optimal hybrid processing for massive MIMO systems via matrix decomposition," *IEEE Trans. on Signal Process.*, vol. 65, no. 15, pp. 3922-3933, 2017.

[32] A. Alkhateeb, G. Leus, and R. Heath, “Limited feedback hybrid precoding formulti-user millimeter wave systems,” *IEEE Trans. on Wireless Commun.*, vol. 14, no. 11, pp. 6481–6494, 2015.

[33] F. Sohrabi and W. Yu, "Hybrid digital and analog beamforming design for large-scale antenna Arrays," *IEEE J. of Sel. Topics in Signal Process.*, vol. 10, no. 3, pp. 501-513, April 2016.

[34] D. Nguyen, L. Le, T. Le-Ngoc, and R. Heath, "Hybrid MMSE precoding and combining designs for mmWave multiuser systems," *IEEE Access*, vol. 5, pp. 19167-19181, 2017.

[35] R. Magueta, D. Castanheira, A. Silva, R. Dinis, and A. Gameiro, “Hybrid Iterative Space-Time Equalization for Multi-User mmW Massive MIMO Systems”, *IEEE Transactions on Commun.*, vol. 65, no. 2, pp. 608-620, 2017.

[36] Z. Wang, M. Li, X. Tian, and Q. Liu, "Iterative hybrid precoder and combiner design for mmWave multiuser MIMO systems," *IEEE Commun. Lett.*, vol. 21, no. 7, pp. 1581-1584, 2017.

[37] A. Alkhateeb, and R. W. Heath, "Frequency selective hybrid precoding for limited feedback millimeter wave systems", *IEEE Trans. Commun.*, vol. 64, no. 5, pp. 1801-1818, 2016.

[38] D. Castanheira, G. Barb, G. Anjos, A. Silva, and A. Gameiro, "A new hybrid multi-user linear equalizer scheme for broadband millimeter wave systems", Accepted to *IEEE Trans. Commun.*, July 2018.

[39] S. He, C. Qi, Y.Wu, and Y. Huang, "Energy-efficient transceiver design for hybrid sub-array architecture MIMO systems," *IEEE Access*, vol. 4, pp. 9895-9905, 2016.

[40] N. Li, Z. Wei, H. Yang, X. Zhang, and D. Yang, "Hybrid precoding for mmWave massive MIMO systems with partially connected structure," *IEEE Access*, vol. 5, pp. 15142-15151, 2017.

[41] X. Gao, L. Dai, S. Han, C.-L. I, and R. Heath, "Energy-efficient hybrid analog and digital precoding for mmWave MIMO systems with large antenna arrays," *IEEE J. Sel. Areas Commun.*, vol. 34, no. 4, pp. 998-1009, 2016.

[42] A. Li, and C.Masouros, "Hybrid analog-digital millimeter-wave MU-MIMO transmission with virtual path selection," *IEEE Commun. Lett.*, vol. 21, no. 2, pp. 438-441, 2017.

[43] R. Magueta, V. Mendes, D. Castanheira, A. Silva, R. Dinis, and A. Gameiro, "Iterative Multiuser Equalization for Subconnected Hybrid mmWave Massive MIMO Architecture," *Wireless Commun. and Mobile Computing*, vol. 2017, pp. 1-13, 2017.

[44] C. Hu, and J. Zhang, "Hybrid precoding design for adaptive subconnected structures in millimeter-wave MIMO systems," *IEEE Systems Journal*, vol. PP, no. 99, pp. 1-10, 2018.

[45] F. Sohrabi, and W. Yu, "Hybrid analog and digital beamforming for mmWave OFDM large-scale antenna arrays," *IEEE J. Sel. Areas Commun.*, vol. 35, no. 7, pp. 1432-1443, 2017.

[46] H. Holma, and A. Toskala, *LTE for UMTS - OFDMA and SC-FDMA Based Radio Access*, John Wiley & Sons, LTD, 2009.

[47] Concepts of OFDM [Available online at] http://rfmw.em.keysight.com/wireless/helpfiles/89600b/webhelp/subsystems/wlan-ofdm/content/ofdm_basicprinciplesoverview.htm [Accessed] 16/05/2018.

[48] N. Marchetti, M. Rahman, S. Kumar, R. Prasad, *New Directions in Wireless Communications Research*, Tarokh, Vahid (Ed.), 2009.

[49] D. Dalwadi, and H. Soni, "A Novel Channel Estimation Technique of MIMO-OFDM System Based on Extended Kalman Filter," in *4th International Conference on Electronics and Commun. Systems*, Coimbatore, India, 2017.

[50] M. Iqbal, M. Iqbal, I. Rasheed, and A. Sandhu, "4G evolution and multiplexing techniques with solution to implementation challenges," in *2012 International Conference on Cyber-Enabled Distributed Computing and Knowledge Discovery*, Sanya, China, 2012.

[51] G. Kaur, and S. Garg, "Difference between two Subcarrier Mapping Techniques IOFDMA and LOFDMA," *International Journal of Enhanced Research in Science Technology & Engineering*, vol. 4, no. 2, pp. 29-33, 2015.

[52] D. Castanheira, A. Silva, R. Dinis, and A. Gameiro, "Efficient Transmitter and Receiver Designs for SC-FDMA Based Heterogeneous Networks," *IEEE Transactions on Communications*, vol. 63, no. 7, pp. 2500-2510, 2015.

[53] P. Serralheiro, Master thesis: *Implementação de um Sistema de Comunicações Móveis para o Uplink*, DETI, University of Aveiro, 2011.

[54] G. Barb, Master thesis: *Técnicas Lineares de Equalização para Sistemas Híbridos de Comunicação na Banda das Ondas Milimétricas*, DETI, University of Aveiro, 2017.

[55] M. Rumney, *3GPP LTE: Introducing single-carrier FDMA*, Agilent Technologies, 2008.

[56] Y. Guo, H. Yang, and Y. Zhang, "Tracking reference signal design for phase noise compensation for SC-FDMA waveform," in *2017 IEEE 17th International Conference on Communication Technology (ICCT)*, Chengdu, China, 2017.

[57] Y. Tsai, G. Zhang, and J. Pan, "Orthogonal Frequency Division Multiplexing with Phase Modulation and Constant Envelope Design," in *MILCOM 2005 - 2005 IEEE Military Commun. Conf.*, Atlantic City, USA, 2005.

[58] K. Rabie, E. Alsusa, A. Familua, and L. Cheng, "Constant envelope OFDM transmission over impulsive noise power-line communication channels," in *2015 IEEE International Symposium on Power Line Commun. and Its Applications (ISPLC)*, Austin, USA, 2015.

[59] S. Thompson, J. Proakis, J. Zeidler, and M. Geile, "Constant Envelope OFDM in Multipath Rayleigh Fading Channels," in *MILCOM 2006 - 2006 IEEE Military Commun. conf.*, Washington, USA, 2006.

[60] R. Magueta, D. Castanheira, A. Silva, R. Dinis, and A. Gameiro, "Iterative space-frequency equalizer for CE-OFDM mmW based systems," in *2016 IEEE Symposium on Computers and Commun. (ISCC)*, Messina, Italy, 2016.

[61] S. Thompson, A. Ahmed, J. Proakis, J. Zeidler, and M. Geile, "Constant Envelope OFDM," *IEEE Transactions on Communications*, vol. 56, no. 8, pp. 1300-1312, 2008.

[62] D. Castanheira, A. Silva, and A. Gameiro, "Minimum Codebook Size to Achieve Maximal Diversity Order for RVQ-Based MIMO Systems," *IEEE Communications Letters*, vol. 18, no. 8, pp. 1463-1466, 2014.

[63] Y. Huang, and K. Boyle, *Antennas: from theory to practice*, Jonh Wiley & Sons, 2008.

[64] K. Sengar, N. Rani, A. Singhal, D. Sharma, S. Verma, and T. Singh, "Study and capacity evaluation of SISO, MISO and MIMO RF wireless Communication Systems", *International Journal of Engineering Trends and Technology (IJETT)*, vol. 9, no. 9, pp. 436-440, 2014.

[65] A. Moco, H. Lima, A. Silva, and A. Gameiro, "Multiple antenna relay-assisted schemes for the uplink OFDM based systems," in *2009 6th International Symposium on Wireless Communication Systems*, Tuscany, Italy, 2009.

[66] E. Castañeda, A. Silva, A. Gameiro, and M. Kountouris, "An Overview on Resource Allocation Techniques for Multi-User MIMO Systems," *IEEE Commun. Surveys & Tutorials*, vol. 19. no. 1, pp. 239-284, 2017.

[67] E. Dahlman, S. Parkvall, and J. Skold, 4G: LTE/LTE-Advanced for Mobile Broadband second edition, Elsevier, 2014.

[68] A. Goldsmith, *Wireless Communications*, Cambridge University Press, 2005.

[69] D. Palomar, Ph. D. Thesis, *A Unified Framework for Communications through MIMO Channels*, Universitat Politècnica de Catalunya, 2003.

[70] Transmit diversity [Available online at] www.comlab.hut.fi/opetus/238/lecture6_ch6.pdf [Accessed] 22/05/2018.

[71] R. Magueta, D. Castanheira, A. Silva, R. Dinis, and A. Gameiro, "Two-stage space-time receiver structure for multiuser hybrid mmW massive MIMO systems," in *2016 IEEE Conference on Standards for Communications and Networking (CSCN)*, Berlin, Germany, 2016.

[72] B. Gu, M. Dong, Z. Liu, C. Zhang, and Y. Tanaka, "Water-filling power allocation algorithm for joint utility optimization in femtocell networks,"in *2017 IEEE Global Comm. Conf. (GLOBECOM)*, Singapore, Singapore.

[73] Thomas L. Marzetta, "Massive MIMO: An Introduction", *Bell Labs Technical Journal*, vol.20, pp.11-22, 2015.

[74] A. Alkhateeb, J. Mo, N. Prelcic, and R. Heath Jr, "MIMO Precoding and Combining Solutions for Millimeter-Wave Systems", *IEEE Commun. Mag.*, vol.52, no.12, pp.122-131, 2014.

[75] Massive MIMO Communications Systems [Available online at] http://www.commsys.isy.liu.se/en/research/projects/CENIIT-Radio-Resource-Management [Accessed] 24/05/2018.

[76] K. Zheng, L. Zhao, J. Mei, B. Shao, W. Xiang, and L. Hanzo, "Survey of Large-Scale MIMO Systems", *IEEE Journals & Mag.*, vol.17, no.3, pp.1738-1760, 2015.

[77] E. Larsson, O. Edfors, F. Tufvesson, and T. Marzetta, “Massive MIMO for Next Generation Wireless Systems”, *IEEE Commun. Mag.*, vol.52, no.2, pp.186-195, 2014.

[78] K. Zheng, S. Ou, and X. Yin, “Massive MIMO Channel Models: A Survey,” *International Journal of Antennas and Propagation*, vol. 2014, Article ID 848071, pp. 1-10, 2014.

[79] N. Adnan, I. Rafiqul, and A. Alam, "Massive MIMO for Fifth Generation (5G): Opportunities and Challenges," in *2016 International Conf. on Computer and Commun. Engineering (ICCCE)*, Kuala Lumpur, Malaysia, 2016.

[80] K. Prasad, E. Hossain, and V. Bhargava, “Energy Efficiency in Massive MIMO-Based 5G Networks: Opportunities and Challenges,” *IEEE Wireless Commun.*, vol. 24, no.3, pp. 86-94, 2017.

[81] F. Rusek, D. Persson, B. Lau, E. Larsson, T. Marzetta, O. Edfors, and F. Tufvesson, “Scaling up MIMO: Opportunities and challenges with very large arrays,” *IEEE Signal Process. Mag.*, vol. 30, no.1, pp. 40-46, Jan. 2013.

[82] L. Lu, G. Li, A. Swindlehurst, A. Ashikhmin, and R. Zhang, "An Overview of Massive MIMO: Benefits and Challenges," *IEEE Journal of Selected Topics in Signal Processing*, vol. 8, no. 5, pp. 742-758, 2014.

[83] R. Lamare, "Massive MIMO systems: Signal processing challenges and future trends," *URSI Radio Science Bulletin*, vol. 2013, no. 347, pp. 8-20, 2013.

[84] Schwartz, M. (2004). *Mobile Wireless Communications. Cambridge*, Cambridge University Press.

[85] J. Zhang, X. Ge, Q. Li, M. Guizani, and Y. Zhang, "5G Millimeter-Wave Antenna Array: Design and Challenges," *IEEE Wireless Commun.*, vol. 24, no. 2, pp. 106-112, 2017.

[86] A. Salcedo, and E. Martinez, "Analysis of the electromagnetic spectrum under the Extremely Low Frequency band: frequency sub-bands classification", in *2017 International Conference on Mechatronics Electronics and Automotive Engineering (ICMEAE)*, Cuernavaca, Mexico, 2017.

[87] S. Rangan, T. Rappaport, and E. Erkip, “Millimeter-Wave Cellular Wireless Networks: Potentials and Challenges”, *Proceedings of the IEEE*, vol. 102, no. 3, pp. 366-385, 2014.

[88] M. Giordani, A. Zanella, and M. Zorzi, "Millimeter wave communication in vehicular networks: Challenges and Opportunities," in *2017 6th International Conf. on Modern Circuits and Systems Tech. (MOCAST)*, Thessaloniki, Greece, 2017.

[89] F. Al-Ogaili, and R. Shubair, "Millimeter-Wave Mobile Communications for 5G: Challenges and Opportunities", in *2016 IEEE International Symposium on Antennas and Propagation (APSURSI)*, Fajardo, Puerto Rico, 2016.

[90] A. Li, and C. Masouros, "Hybrid precoding and combining design for millimeter-wave multi-user MIMO based on SVD," in *2017 IEEE International Conference on Communications (ICC)*, Paris, France, 2017.

[91] R. Magueta, D. Castanheira, A. Silva, R. Dinis, and A. Gameiro, "Nonlinear Equalizer for Multi-User Hybrid mmW Massive MIMO Systems," in *2017 IEEE 85th Vehicular Technology Conference (VTC Spring)*, Sydney, Australia, 2017.

[92] E. Yaacoub, M. Husseini, and H. Ghaziri, "An overview of research topics and challenges for 5G massive MIMO antennas," in *2016 IEEE Middle East Conference on Antennas and Propagation (MECAP)*, Beirut, Lebanon, 2016.

[93] A. Rozé, M. Crussière, M. Hélard, and C. Langlais, “Comparison between a hybrid digital and analog beamforming system and a fully digital massive MIMO system with adaptive beamsteering receivers in millimeter-wave transmissions,” in *Intern. Symp. on Wireless Commun. Systems*, Poznan, Poland, 2016.

[94] D. Castanheira, P. Lopes, A. Silva, and A. Gameiro, "Hybrid Beamforming Designs for Massive MIMO Millimeter-Wave Heterogeneous Systems," *IEEE Access*, vol. 5, pp. 21806-21817, 2017.

[95] S. Han, Chih-Lin I, Z. Xu, and C. Rowell, “Large-Scale Antenna Systems with Hybrid Analog and Digital Beamforming for Millimeter Wave 5G”, *IEEE Commun. Magazine*, vol.53, no.1, pp.186-194, 2015.

[96] I. Ahmed, H. Khammari, A. Shahid, A. Musa, K. Kim, E. Poorter, and I. Moerman, “A survey on Hybrid Beamforming Techniques in 5G: Architecture and System Model Perspectives,” *IEEE Comm. Surveys & Tutorials (Early Acceess)*, pp. 1-40, 2018.

[97] S. Park, A. Alkhateeb, and R. Heath Jr., “Dynamic Subarray Architecture for Wideband Hybrid Precoding in Millimeter Wave Massive MIMO Systems,” *IEEE Transactions on Commun.*, vol. 16, no. 5, pp. 2907-2920, 2017.

[98] P. Dong, H. Zhang, W. Xu, and X. You, "Efficient Low-Resolution ADC Relaying for Multiuser Massive MIMO System," *IEEE Trans. on Vehic. Tech.*, vol. 66, no. 12, pp. 11039-11056, 2017.

[99] D. Palomar and Y. Jiang, *MIMO transceiver design via majorization theory*, Boston: Now, 2007.

[100] L. Giraud, J. Langou and M. Rozloznik, “The loss of orthogonality in the Gram-Schmidt orthogonalization process,” *Comput. Math. Appl.*, vol. 50, no. 7, pp. 1069-1075, 2005.